The Messenger

No. 177 – Quarter 3 | 2019

Distributed Peer Review
M87 Event Horizon Telescope Results
The PHANGS Surveys
Total Solar Eclipse Over La Silla

ESO, the European Southern Observatory, is the foremost intergovernmental astronomy organisation in Europe. It is supported by 16 Member States: Austria, Belgium, the Czech Republic, Denmark, France, Finland, Germany, Ireland, Italy, the Netherlands, Poland, Portugal, Spain, Sweden, Switzerland and the United Kingdom, along with the host country of Chile and with Australia as a Strategic Partner. ESO's programme is focussed on the design, construction and operation of powerful ground-based observing facilities. ESO operates three observatories in Chile: at La Silla, at Paranal, site of the Very Large Telescope, and at Llano de Chajnantor. ESO is the European partner in the Atacama Large Millimeter/submillimeter Array (ALMA). Currently ESO is engaged in the construction of the Extremely Large Telescope.

The Messenger is published, in hardcopy and electronic form, four times a year. ESO produces and distributes a wide variety of media connected to its activities. For further information, including postal subscription to The Messenger, contact the ESO Department of Communication at:

ESO Headquarters
Karl-Schwarzschild-Straße 2
85748 Garching bei München, Germany
Phone +498932006-0
information@eso.org

The Messenger
Editor: Gaitee A. J. Hussain
Layout, Typesetting, Graphics:
Jutta Boxheimer, Mafalda Martins,
Lorenzo Benassi
Design, Production: Jutta Boxheimer
Proofreading: Peter Grimley,
Caroline Reid
www.eso.org/messenger/

Printed by FIBO Druck- und Verlags GmbH
Fichtenstraße 8, 82061 Neuried, Germany

ISSN 0722-6691

Contents

Front cover: A series of exposures showing the trajectory of the Sun over roughly two and a half hours. The total solar eclipse resulted in almost two minutes of totality at 20:39 UT. Credit: ESO/P. Horálek

DOI: 10.18727/0722-6691/5147

The Distributed Peer Review Experiment

Ferdinando Patat[1]
Wolfgang Kerzendorf[2,3,4]
Dominic Bordelon[1]
Glen Van de Ven[5]
Tyler Pritchard[2]

[1] ESO
[2] Center for Cosmology and Particle Physics, New York University, USA
[3] Department of Physics and Astronomy, Michigan State University, USA
[4] Department of Computational Mathematics, Science and Engineering, Michigan State University, USA
[5] Department of Astrophysics, University of Vienna, Austria

All large, ground- and space-based astronomical facilities serving wide communities face a similar problem: in many cases the number of applications they receive in response to each call exceeds 1000. This poses a serious challenge to running an effective selection process under the classic peer-review paradigm, in which the proposals are assigned to pre-allocated panels with fixed compositions. Although, in principle, one could increase the size of the time allocation committee, this creates logistic and financial problems which place a practical limit on its maximum size, making this solution unviable beyond a certain volume of applications. For this reason, alternative solutions must be sought. One of these is the so-called Distributed Peer Review (DPR) in which, by submitting a proposal, the Principal Investigators (PIs) agree both to act as reviewers and to have their proposal reviewed by their peers. In this article we report the results of a DPR experiment run by ESO in Period 103, in parallel with the regular review by the Observing Programmes Committee (OPC).

Introduction

Following the start of VLT operations in 1998, the number of applications to use ESO telescopes has been steadily growing, exceeding 1100 proposals in Period 84. After this peak, the number of submissions per semester stabilised at around 900 (Patat et al., 2017). Despite the significant growth of the user community, which has made ESO one of the largest astronomical facilities in the world, the way telescope time applications are reviewed has remained substantially the same since 1993. Barring the necessary increase in the number of reviewers, the procedure has changed in the details, but not in its substance. Following steady growth in the numbers of submissions, the current review load is about 70 proposals per panel member and up to 100 for OPC-proper members (the latter serve on a second panel which reviews the recommendations across all science categories). These numbers have reached critical levels, requiring a re-evaluation of the procedures and an examination of the effectiveness of peer review.

The pressure on the peer review process has been the subject of a study by the ESO OPC Working Group (Brinks et al., 2012) and the Time Allocation Working Group (TAWG; Patat, 2018a). Both studies identified the excessive number of proposals per referee as the most urgent problem that ESO needs to tackle. Not only does the workload severely affect the referees (also increasing the rejection rate during the recruitment phase), but it can also have an impact on the quality of the reviews and the feedback provided to the applicants, with potentially serious consequences. The feedback has been repeatedly and consistently identified as a major problem by the OPC and the Users Committee, and via direct communications from numerous individual users. Problems with the peer review could ultimately affect the scientific productivity and impact of the Organisation itself. A number of recommendations have been proposed by the working groups, some of which are interdependent.

As a first step, since Period 102 ESO has decreased the number of referees (from six to three) who review a proposal ahead of the OPC meeting. Triage is then applied using the three pre-OPC meeting grades, with about the lowest 30% of proposals being rejected. At the meeting all non-conflicted panel members are then asked to discuss and grade only the surviving proposals. While this measure has successfully reduced the workload of the panel members, it has become cumbersome to manage in practice. For example, late dropouts during the review process can reduce the number of pre-meeting reviews per proposal, making the triage procedure less robust. While this change was relatively easy to implement, experience gained during Periods 102 and 103 suggests that the negative consequences outweigh the benefits. It is clear that further and more drastic and structured actions need to be taken; these include a move to an annual cycle and the deployment of a fast track channel (FTC; see Patat, 2018a).

By construction, the FTC requires a short duty cycle during which referees are continuously on duty. The most suitable mechanism for reviewing the proposals is a Distributed Peer Review (DPR), one of the most innovative schemes through which the load on referees can be alleviated (Merrifield & Saari, 2009). This concept has been successfully applied to the Fast Turnaround channel deployed at the Gemini Telescope, which has processed over 1000 proposals in this way since 2015. The Gemini Observatory has published a report (Andersen et al., 2019) and updates are continuously provided on its webpages[1].

Depending on the fraction of total telescope time that is allocated via the FTC, this channel may also serve to decrease the load on the OPC, which would then focus only on proposals with larger time requests. ESO has conducted a systematic study aimed at better evaluating the application of DPR to its programmes. In Period 103, in parallel with the regular OPC cycle, a DPR experiment was run involving a subset of submitted proposals. This article presents a brief description of the experiment setup and summarises an analysis of several statistical indicators. More details can be found in Kerzendorf et al. (2019).

Distributed Peer Review and the DPR Experiment

Different measures to alleviate the load on the reviewers have been and are being considered by various facilities. These include drastic solutions, like the one deployed by the National Science Foundation (NSF, USA) to limit the number of applications (Mervis, 2014a). The

Distributed Peer Review (DPR) concept is simple; in submitting a proposal the PI agrees to review *n* proposals submitted by peers, and to have her/his proposal/s reviewed by *n* peers. Also, if s/he submits *m* proposals, s/he accepts to review $n \times m$ proposals, hence essentially limiting the number of submissions through a self-regulating mechanism. Following this idea, the Gemini Observatory deployed the DPR for its Fast Turnaround channel (Andersen et al., 2019), which is capped to 10% of the total time. The NSF also explored this possibility with a pilot study in 2013, in which each PI was asked to review seven proposals submitted by peers (Ardabili & Liu, 2013; Mervis, 2014b). The NSF pilot was based on 131 applications submitted by volunteers within the Civil, Mechanical and Manufacturing Innovation Division, but the outcome is unknown as no report on the study was published. Interestingly, a similar pilot experiment was carried out in 2016 by the National Institute of Food and Agriculture[2]; in this case too the results were not published. Despite the general acceptance that followed the deployment of this channel at the Gemini Observatory, to the best of our knowledge the Fast Turnaround channel is the only example of DPR being employed by a large-scale astronomical facility.

In the specific case of ESO, the TAWG tasked to address these issues has produced a set of recommendations. The core aim is to reduce the number of applications per reviewer, which has been identified as an urgent action that ESO needs to take (Patat, 2018a). The deployment of DPR falls within the recommendations. As a first step, and after consulting the advisory bodies, ESO decided to run a test during the ESO Period 103 in parallel to the regular OPC review. The experiment was designed in line with the implementation at Gemini, enhancing the process by means of Natural Language Processing (NLP) and Machine Learning (a different method of using NLP for proposal reviews can be found in Strolger et al., 2017).

The DPR experiment was announced in the Call for Proposals for Period 103, released on 30 August 2018. A total of 172 PIs — representing 23% of all distinct PIs in that semester — volunteered to participate in the experiment. This implied that each would review eight proposals submitted by peers and have their proposal refereed by the same number of peers. The participants were given two weeks to complete their reviews and were informed that the outcome of the DPR would have no effect on the fate of their proposals. By the deadline (22 October 2018) 167 (97.1%) had completed their task. In a real implementation the five PIs who did not meet the deadline would have had their proposals automatically rejected. In this experiment however, their proposals were kept in the sample, but the PIs did not receive the final feedback. Additionally, the participating PIs were asked to fill in a web-based questionnaire covering various aspects of the experiment. A total of 140 (83.8% of the DPR sample, 19% of the total PI sample of P103) returned the completed form.

The proposal distribution was performed using two channels, which we will call OPC Emulate (OE) and DeepThought (DT). In both cases the reviewers were assigned eight proposals each. For the OE channel, 60 volunteers were selected at random and assigned, on the basis of the category of the proposal each submitted, to the four scientific categories: A (Cosmology), B (Galaxy Structure and Evolution), C (Planets, Star Formation and Interstellar Medium) and D (Stellar Evolution). The underlying (and reasonable) assumption is that a scientist submitting a proposal for a given category is an expert in that same area. This emulates the case of the real OPC, in which a person only receives proposals within her/his area of expertise.

For the remaining 112 volunteers selected for the DT channel, the process was as follows. For each scientist, a knowledge vector was built based on their publications, which were downloaded from the public SAO/NASA Astrophysics Data System database (ADS) and processed by a machine learning algorithm (Kerzendorf, 2017). The same approach was used for the proposals and applied to their scientific rationale. The match between the referee expertise and the area covered by the proposal was then quantified through the "cosine distance", which is directly related to the angle formed by the two hyper-vectors; a null cosine signals a complete mismatch (orthogonal knowledge vectors), while a unit cosine indicates a case of perfect match (parallel knowledge vectors). For the purposes of the statistical analysis, each DT referee received four proposals with the largest similarity, two proposals with median similarity, and two proposals with the lowest similarity.

The participants were not aware of the distribution mechanism just described. They were just provided with a simple web-based interface giving them access to the eight assigned proposals and allowing them to review, grade and comment on the applications. Before accessing the proposals, the referees were asked to sign a non-disclosure agreement, very similar to that signed by the OPC and Panel members.

During the review phase, the participants were also asked to declare any scientific/personal conflicts, while institutional conflicts were automatically taken into account by the distribution software, based on the affiliations recorded in the User Portal database. For each proposal, the referees had to fill in a comment (with a minimum length of 80 characters), and also provide a self-evaluation of their expertise level (high/medium/low) for each proposal assigned to them.

Once the review process was completed, the grades of the various referees were combined using a simple average (similar to the regular OPC process), and a final ranking list was compiled. The PIs were then provided with the quartile rank and the individual, unedited anonymous comments. Finally, they were asked to provide feedback on the experiment via a web-based form; this included a request to express the usefulness of each comment they received on their proposal.

General statistics and demographics

Although, in principle, each proposal should have been reviewed by eight scientists and each scientist should have reviewed eight proposals, because of the scientific/personal conflicts declared during the refereeing process (and to a much smaller extent because five participants did not complete the process),

both these numbers were on average smaller than eight. The number of reviewers N_r ranged from 4 to 8, with an average of 7.3; in 95% of the cases the number was $N_r \geq 6$. The number of proposals N_p varied from 5 to 8, with an average of 7.6, and $N_r \geq 6$ in 98% of cases. The DPR produced a total of 4055 distinct grade pairs, to be compared with the maximum number of pairs $172 \times 8 \times 7/2 = 4816$ (see below for more details) one would obtain in the case of no conflicts and no dropouts.

The F/M gender distribution of the DPR participants (32/68) and the scientific seniority distribution derived from the DPR questionnaire (see Figure 1) reflect the underlying PI population of ESO users (Patat, 2016). Since participation in the experiment was on a completely voluntary basis, we cannot exclude the presence of self-selection biases. For instance, one could argue that researchers who already had a positive opinion of the DPR concept would be more willing to participate than opponents, hence introducing systematics into the final analysis. On the other hand, if the community were strongly against the paradigm, one would expect a similar effect. In general, although we cannot guarantee that there are no specific attributes that lead the participants to self-selection, the demographics indicate that, if they exist, they are well hidden.

An important aspect regarding the demographics of the experiment concerns the fraction of junior scientists. Since, as a rule, the regular panel members serving on the OPC are required to have a minimum seniority level (typically starting with scientists at their second postdoc onward), this establishes a significant difference between the two pools of reviewers. In the case of the OPC, the distribution is heavily skewed towards senior members (88%), with a small fraction of postdocs (12%) and no students (Patat, 2016), while the postdoc and student reviewers reach about 18% in the case of the DPR sample (Figure 1).

Most DPR participants were relatively experienced in submitting proposals (Figure 2), although almost 60% of them had never served on a time allocation commitee before (Figure 3). Although

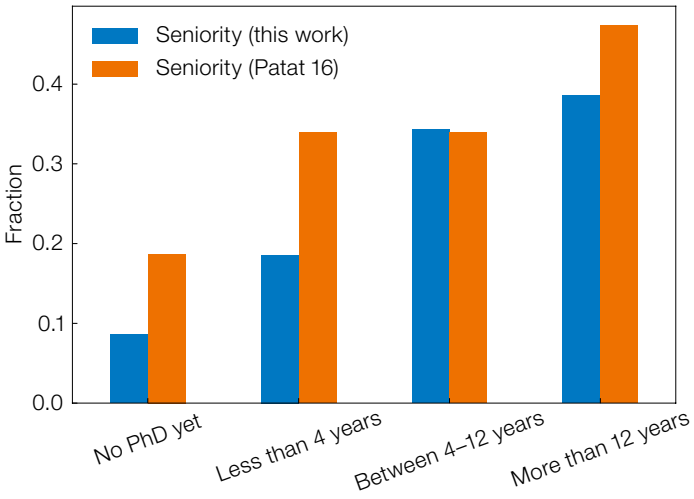

Figure 1. Scientific seniority distribution of the DPR sample (blue) and the OPC sample (orange). From Patat (2016).

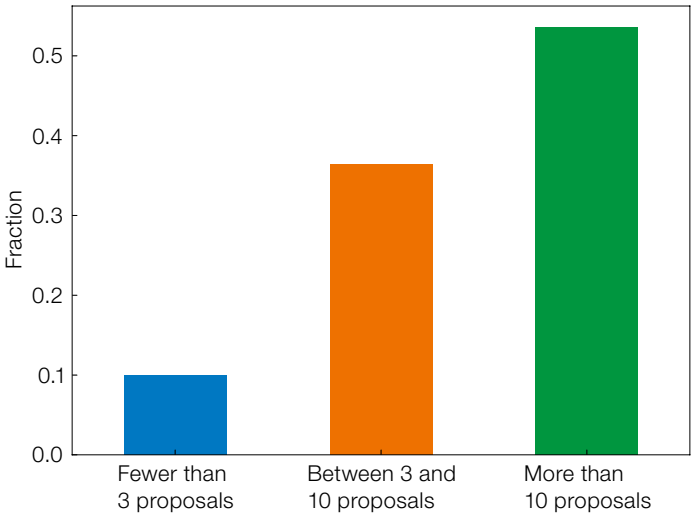

Figure 2. Distribution of the number of proposals submitted to ESO by the DPR participants.

there are published studies that indicate reviewers who self-report higher levels of expertise tend to be less generous in assigning the top grades (Gallo et al., 2016), the differences seen between the grade distributions of senior and junior DPR participants are not statistically significant.

Referee-Proposal matching

In the regular OPC process, the panel members are recruited to cover the widest possible range of astrophysical areas. Each of the selected reviewers is asked to declare her/his expertise by providing sub-categories from the same list used by the applicants to categorise their proposal. While the PI is allowed to indicate one single proposal sub-category (within a given scientific category), the panel members are requested to identify three sub-categories, ranking them in order of expertise. This information is then used to compose review panels in such a way that the expertise coverage within each of them is as broad as possible. This is required by any schema in which physical panels exist, which is in turn a constraint stemming from the fact that the panels have to meet face-to-face and discuss the same set of proposals. This introduces a certain rigidity, which is also related to the relatively small number of available reviewers.

Since DPR has the advantage of involving a much larger number of reviewers, it allows a significantly more flexible and

more objective approach in which, for each proposal, an ad hoc, optimised panel can be formed. A key ingredient in this approach is the proposal-referee matching, which should work without the need for human supervision, especially when the turnaround has to be fast.

For this purpose, the DT algorithm used in the DPR experiment was designed to predict what we call domain expertise, which in this context can be considered to be the objective ability of a given scientist to review a given proposal. Before we discuss its reliability, we examine how referees assessed their own ability to review each proposal assigned to them. As anticipated in the introduction, during the refereeing process each participant was asked to express their self-perceived expertise level for each of the assigned proposals, resulting in about 1200 evaluations. The distribution of participants' self-evaluated ability to review the assigned proposals is presented in Figure 4, where we have used different colours for the different classes of scientific seniority. As expected, junior scientists tend to perceive themselves as experts less often than senior scientists do. Also, they often indicate that they have limited knowledge of a given field. We take this is an indication that the self-evaluated ability of a referee to review the assigned proposals is a useful proxy of the more objective (albeit more abstract) concept of domain knowledge.

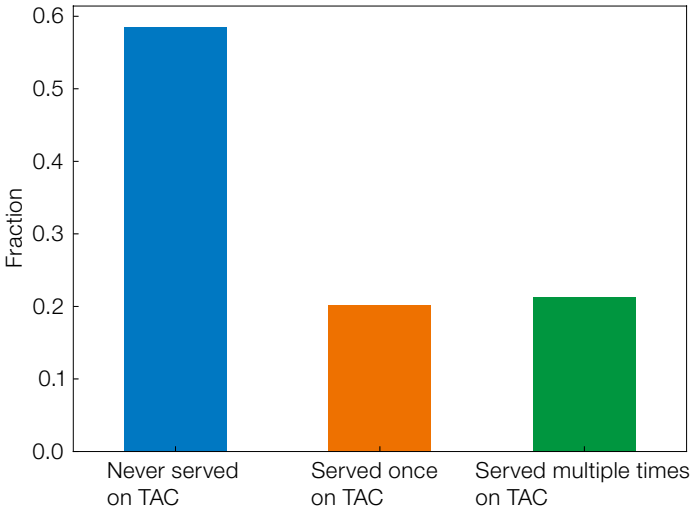

Figure 3. Distribution of expertise in serving on Time Allocation Committees (TAC) for the DPR participants.

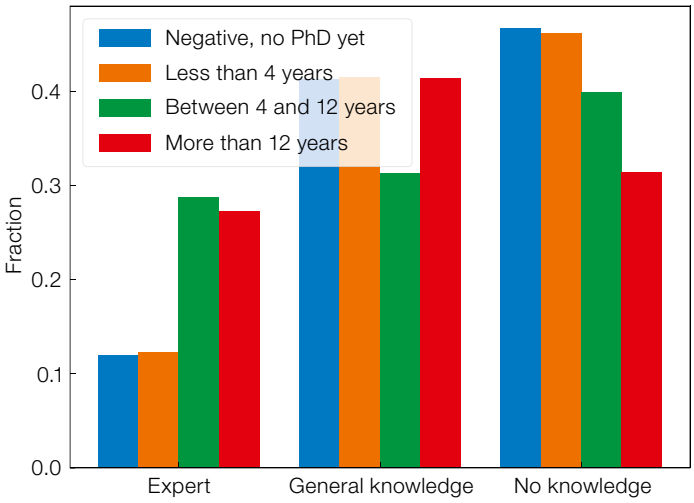

Figure 4. Distribution of self-reported domain knowledge for the different scientific seniority of the DPR participants.

The data collected in the DPR experiment enable an additional analysis of a possible gender dependence on the above self-evaluation. This has been reported, for instance, by Huang (2013), who concluded that females tend to under-predict their performance in certain STEM fields. Our data suggest that, at least for postgraduates in the domain of astrophysics, there is no statistically significant gender difference.

Since the DT is designed to predict the expertise of a referee with respect to a given proposal, the first question one should ask is how reliable the algorithm is. Obviously, there is no absolute reference; the DT is one possible objective estimate of this quality. Therefore, as a first exploratory test, one can check the DT results against the self-evaluation of expertise, which can be considered as a reasonable first approximation to the underlying domain knowledge. From a statistical point of view, this is equivalent to computing the Bayesian conditional probability P (self-reported | DT) of having a certain self-reported expertise level, given the DT-inferred level. In simpler words, one checks how the self-reported and DT-inferred levels correlate. The result is presented in Figure 5, which shows an encouragingly high correlation. For instance, the probability that the DT considers a match as the worst which the referee believes is the best, is less then 1%. At the other extreme, it is very likely (78%) that if the DT estimates the match is poor, the referee is of the same opinion. The agreement on the best matches is at the level of 50%, while for 81% of the best DT matches, the referees perceive them to be the top and intermediate classes. As shown in Figure 5, the correlation in the intermediate cases becomes fuzzier. With the available data it is impossible to tell which of the two estimators is responsible for the observed noise. If on the one hand we can argue that the DT approach has obvious limitations (which is certainly true), on the other hand the self-reported levels are affected by a significant level of uncertainty, as they are related to subjective perceptions rather than to objective criteria.

Another aspect is the importance of proper proposal-referee matching. Our direct experience, accumulated over many years of managing the review process at ESO, shows that, in addition to the obvious problem related to excessively large numbers of proposals, panel

members report a general uneasiness when dealing with proposals in areas in which they feel they are not experts. For a more quantitative assessment, DPR participants were asked to express their level of confidence, using a four-point scale, when asked to evaluate those cases; the corresponding distribution is presented in Figure 6. In about 60% of the cases, the reviewers were not comfortable with this situation. This implies that better matching of expertise gives the reviewers a better experience, an aspect which should not be underestimated.

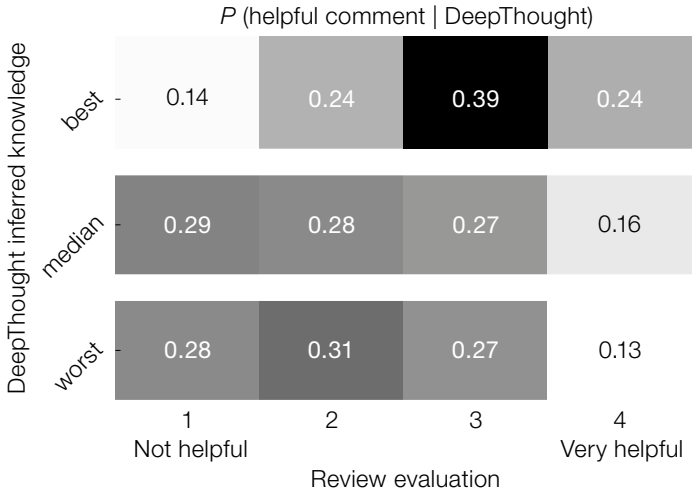

Figure 5. Conditional probability for the various combinations of self-reported and DT-inferred knowledge level.

Feedback quality

In the classical review concept, the feedback provided by the panel to the PI is supposed to reflect the consensus opinion. This paradigm has at least two obvious limitations: (a) proposals that are triaged out (i.e., the bottom ~ 30%) are not discussed, and the feedback is based on the opinion of the primary referee; (b) for proposals that are discussed during the face-to-face meeting the primary referee tries to capture the main points of the discussion and produces a single comment. There is simply not enough time for the panel members to review all the feedback and to make sure it reflects all the aspects of the discussion. In the current implementation at ESO, the comments are formally supervised by panel chairs, who are responsible for the integrity of the feedback (particularly as it relates to the language used). The net effect, possibly coupled with a sub-optimal matching between proposal and referee, is a high level of dissatisfaction in the community, which is consistently reported by the Users Committee; the dissatisfaction reported is about 30% for all of ESO and exceeds 50% for ALMA[3].

Since the TAWG recommended the use of DPR for a FTC, no attempt was made to produce consensus feedback and/or to edit/check individual comments, which were distributed to the PIs in their original form. The purpose of this implementation was two-fold: (a) to get feedback on the concept itself, and (b) to detect possible problems (for example, inappropriate language) generated by the unedited/unfiltered text.

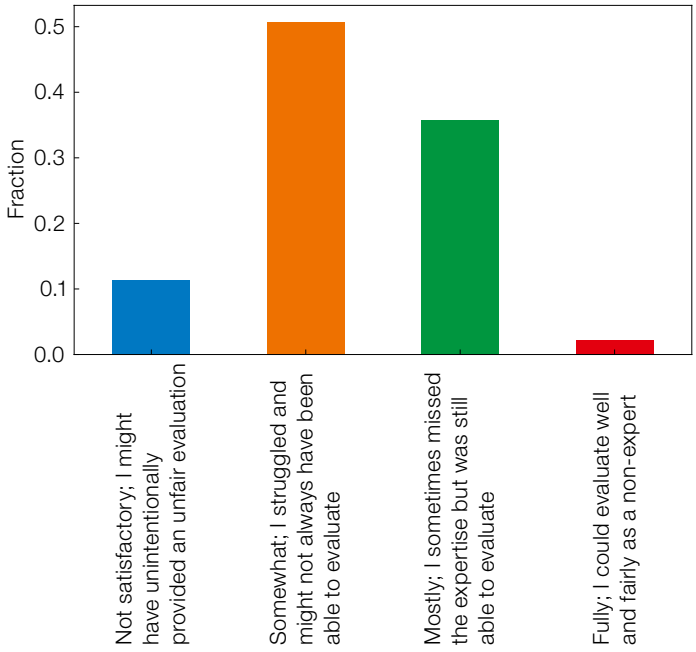

Figure 6. Distribution of the answers to the question: "How satisfactorily were you able to evaluate the proposals for which you were not an expert?".

The participants were asked to rate each of the comments they received for their proposal, based on its helpfulness. It is important to stress that they were not asked whether the comments were good or bad, or whether they liked them or not, but whether they were useful for improving the quality of their proposal. The general response was very satisfactory, as shown in Figure 7, with more than 60% of the comments judged as being useful, and about 5% not useful. One of the questions also concerned the comparison with the edited OPC comments received by the PIs in previous semesters (99% of the sub-sample that responded). In about 40% of the cases the DPR was reported to have provided better comments, while the fraction of comments with quality similar to, or better than the OPC reaches about 85%.

The analysis of comment helpfulness as a function of the reviewer's expertise (either self-reported or DT-inferred) shows that the dependence is mild in the central regions; the experts very rarely gave unhelpful comments and, conversely, non-experts rarely gave very helpful comments. A similar analysis as a function of

the reviewer's scientific seniority reveals a flat distribution (within the noise), with one remarkable exception: graduate students seem to be unable to provide very useful comments. This may signal a training issue, which can probably be addressed by exposing the students to schemes like the DPR. Finally, no statistically significant difference is seen between the helpfulness of comments written by female and male referees.

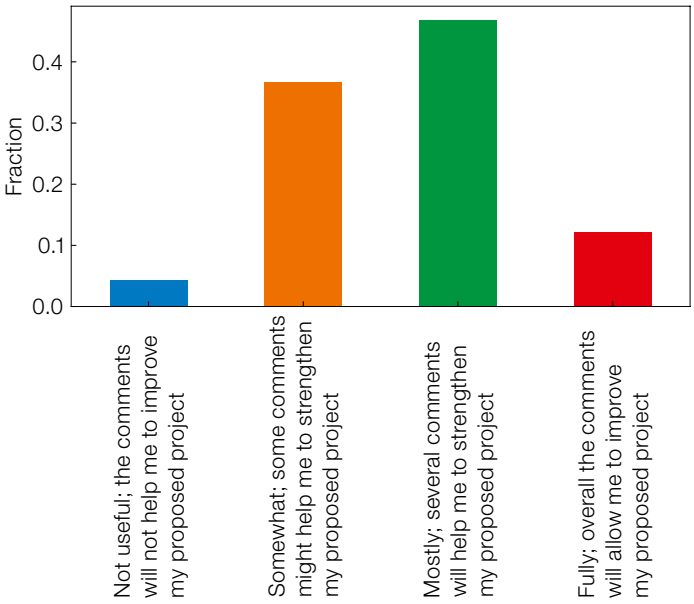

Figure 7. Distribution of the "helpfulness" ratings of the referee comments for the entire DPR sample.

A brief primer on subjectivity

Before we proceed with the comparison between the final OPC and DPR outcomes, a digression on the subjectivity inherent in the process is necessary. Although it is common knowledge that two different panels reviewing the same set of proposals would provide different rankings (and this is often used to compare time allocation committees to roulette), quantitative statements are very rare. This matter is addressed in great detail in an extensive study based on about 15 000 ESO proposals (Patat, 2018b; hereafter P18). The interested reader is referred to the paper for a thorough discussion, while here we will focus only on the concepts relevant to the present discussion.

One way of quantitatively describing the reproducibility of a review process is the correlation between the grades attributed to the same set of applications by two distinct bodies. These bodies can be composed of a single individual or of several members. We will be talking about referee–referee (r–r) and panel–panel (p–p) correlations. In the first instance, one simply considers all the distinct grade pairs attributed by referee #1 and referee #2 to the same set of proposals, placing them in a diagram in which the grades are used as coordinates, so that each single grade pair is represented by a point. One can then repeat the process for all possible referee pairs, plotting all the corresponding points on the r–r plane. Since the same proposal is graded by many reviewers, each single proposal is represented on the r–r plane by a cloud of points.

In the simplifying assumption that each proposal is seen by N_r referees, the number of distinct grade pairs n_p for each proposal is $n_p = N_r\,(N_r–1)/2$. For instance, in the case of the DPR experiment, with typically $N_r = 7$, the above combinatorics formula yields 21 distinct pairs per proposal. Of course, the same operation can be repeated for all N_p proposals in the sample, which will populate the diagram with $N_p = 172$ clouds of points. In the case of the DPR experiment, this would yield 172 × 21 = 3612 points. In an ideal situation, all the clouds would be very small in size (meaning that all referees would provide very similar grades for the given proposal), and so the points would

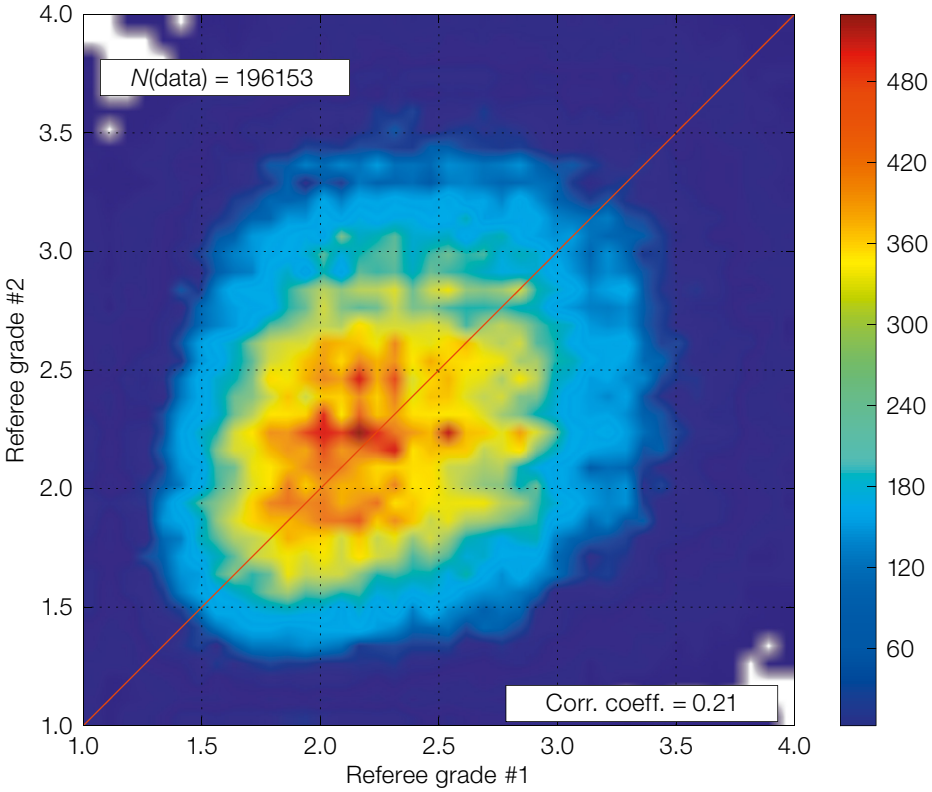

Figure 8 (below). Pre-meeting OPC referee–referee correlation. In this density diagram each point represents a pair of grades attributed to the same proposal by two distinct referees. The data are from the P18 sample.

be distributed very close to the straight-line $y = x$ on the r–r plane.

To illustrate what one is to expect in real life, we have constructed the r–r plane for the pre-meeting OPC P18 sample, from which we derived almost 200 000 grade pairs accumulated over 16 ESO cycles. The resulting diagram is presented in Figure 8. It is important to note that for a perfectly stochastic process, the points would be distributed within a circular area, with some radial, typically Gaussian, distribution. The fact that the real distribution is elongated along the diagonal direction signals that the process is not aleatory. This qualitative conclusion can be made more quantitative by computing the Pearson linear correlation coefficient, which ranges from –1 (complete anti-correlation) to 1 (complete correlation) and is null for complete uncorrelation. The value derived for the sample is 0.21. Given the very large number of points, this is a very robust estimate which can be reliably taken as a low correlation. For the same reason, however, this value reveals that there is a statistically significant signal indicating that the process is not completely aleatory. If on the one hand this may sound discouraging, it helps to put things in the correct context, as it characterises the subjectivity of the process in a more quantitative and objective way, as opposed to the common statements which are normally based on pure anecdotal evidence.

A different way of measuring the repeatability of the process, which we will use extensively in the next section, is the quartile agreement fraction (P18). The concept is as follows. When the same set of proposals is reviewed by two different bodies #1 and #2, one can compile the rankings for the two distinct reviews based on their distinct grades. The rankings are then used to derive a merit classification within the classical quartile scheme. For instance, the top 25% of proposals are ranked in the first quartile of the distribution of grades.

Once this is done, one can compute the fraction of applications ranked in the first quartile by review #1 which are also graded in the same quartile by review #2. For a complete agreement the fraction is 1, while a null value would signal a complete disagreement. The average agreement is expected to be 0.25 in case a fully stochastic process, i.e., when there is no correlation between the two bodies. The concept can be extended to all quartiles, including cross-quartile values, and the quartile agreement matrix (QAM) can be constructed. In statistical terms, the generic element M_{ij} of the QAM is the conditional probability that a proposal ranked in the i-th quartile by referee #1 is ranked in the j-th quartile by referee #2.

The application of this concept to the P18 pre-meeting sample shows that, on average, the ranking lists produced by two distinct referees have about 33% of the proposals in common in their first and last quartiles. In the central quartiles the intersection is compatible with a purely random selection (25%). This extends to the mixed cases ($i \neq j$), with the exception of the extreme quartiles; the fraction of proposals ranked in the first quartile by referee #1 and in the fourth quartile by referee #2 is ~ 17%, which deviates in a statistically significant way from the random value. As in the case of the r–r correlation introduced above, the r–r agreement fraction gives a quantitative estimate of the high level of subjectivity that characterises the process, providing a precise indication of what one should expect.

The reason why the applications are usually evaluated by more than one reviewer is to reduce the inherent "noise" which, as we have just seen, is quite substantial. For this purpose, the grades attributed by different referees to the same proposal (typically grouped in panels) are aggregated to form one single figure of merit. In the ESO implementation (and this is a common recipe), this is achieved simply taking the average, with no weights and/or rejection. The effect of increasing the number of reviews is diffusely discussed in P18; here it suffices to say that for $N_r = 3$ the first quartile agreement fraction grows to 43% and 30% in the first and second quartiles, respectively.

Armed with these terms of reference we can now discuss the results of the DPR experiment.

Comparing the OPC and DPR outcomes

The first test we apply to the DPR data concerns the subjectivity level characterising the typical participant. For this purpose, we have computed the average r–r QAM that we introduced in the previous section. Because of the DPR setup, the ranking list for each referee includes at most eight proposals, so each quartile contains no more than two proposals. Also, at variance with the classical panel scheme, the number of proposals in common between two reviewers is typically very small. As a direct comparison between ranks is not possible, we use a bootstrap approach. Very briefly, for each of the 172 proposals we randomly extract one grade pair and form two ranking lists, which are used to compute the quartile agreement fractions. The process is repeated a large number of times and the average values and standard deviations are derived for each of the QAM elements. The result is presented in Table 1. A direct comparison with the values derived from the P18 sample reveals that the two results are statistically indistinguishable. No meaningful difference is seen in the QAMs computed for the OE and DT sub-samples.

In a further test, we have investigated the possible dependence on the scientific seniority level introduced above. Of the 167 reviewers, 136 provided this information, which we used to sub-divide the reviewers into two classes: junior (groups 0 and 1) and senior (groups 2 and 3). These classes roughly correspond to PhD students plus junior postdocs (37), and advanced postdocs plus senior scientists (99), respectively. We then computed the r–r QAM for the two classes; the first quartile terms are 0.22 and 0.32, respectively. At face value this indicates a larger agreement between senior reviewers. However, the small size of the

Table 1. Bootstrapped r–r Quartile Agreement Matrix for the DPR experiment.

Referee #1 quartile	Referee #2 quartile 1	2	3	4
1	0.33	0.26	0.24	0.18
2	0.26	0.26	0.25	0.23
3	0.24	0.25	0.25	0.26
4	0.18	0.23	0.26	0.34

junior class produces a significant scatter, so the difference may not be significant.

One can extend the above bootstrapping procedure to subsets with a number of referees $N_r > 1$. The case of $N_r = 3$ is particularly interesting as this is directly comparable to the results presented in P18. The procedure is as follows: we first make a selection of the proposals having at least 6 reviews (164); for each of these we randomly select two distinct (i.e., non-intersecting) subsets of $N_r = 3$ grades each, from which two average grades are derived; the subsequent steps are identical to the r–r procedure, and lead to what we will call the p–p QAM.

The first-quartile agreement turns out to be 41%, while for the second and third quartiles this is 30%. The top-bottom quartile agreement is 10%. These values are very similar to those presented in P18 for the OPC process for $N_r = 3$ subpanels. As for the r–r case, the OE and DT sub-samples yield statistically indistinguishable values. The conclusion is that, in terms of self-consistency, the DPR review behaves in the same way as the pre-meeting OPC process.

We now come to what is perhaps one of the most interesting aspects. As anticipated, the proposals used in the DPR experiment were also subject to the regular OPC review. This enables the comparison between the outcomes of the two selections, with the caveats outlined above about their inherent differences.

For a first test we used a bootstrap procedure in which, for each proposal included in the DPR, we randomly extracted one evaluation from the DPR (typically one out of 7) and one from the OPC (one out of 3), forming two ranking lists from which a r–r QAM was computed. The operation was repeated a large number of times and the average and standard deviation matrices were constructed. This approach provides a direct indication of the DPR-OPC agreement at the r–r level and overcomes the problem that the two reviews have a different number of evaluations per proposal (see below). The result is presented in Table 2. The typical standard deviation of single realisations from the average is 0.06.

Table 2. Average DPR–OPC (pre-meeting) r–r Quartile Agreement Matrix.

DPR referee quartile	OPC referee quartile 1	2	3	4
1	0.31	0.26	0.24	0.18
2	0.24	0.27	0.25	0.24
3	0.24	0.23	0.26	0.26
4	0.20	0.23	0.25	0.31

This matrix is very similar to that derived within the DPR reviews (see Table 1), possibly indicating a DPR–OPC r–r agreement slightly lower than the corresponding DPR–DPR. A check performed on the two sub-samples for the junior and senior DPR reviewers (according to the classification described above) has given statistically indistinguishable results.

As explained in the introduction, the proposals were reviewed by $N_r = 3$ OPC referees in the pre-meeting phase. This constitutes a significant difference, in that the DPR ranking is typically based on ~ 7 grades, whereas the pre-meeting OPC ranking rests on 3 grades only. With this caveat in mind, one can nevertheless compute the QAM for the two overall ranking lists. The result is presented in Table 3. At face value, about 37% of the proposals ranked in the 1st quartile by the DPR were ranked in the same quartile by the OPC, with a similar fraction for the bottom quartile. When looking at these values, one needs to consider that this is only one realisation, which is affected by large scatter, as can be deduced from the comparatively large fluctuations in the QAM. These are evident when compared to, for instance, the average values obtained from the bootstrapping procedures described above. The numerical simulations show that the standard deviation of a single realisation is ~ 0.1.

Using the model presented in P18, one can predict that, on average, the top and bottom quartile agreement between the DPR and the pre-meeting OPC should be around 0.5 (see Kerzendorf, 2019 for more detail). The observed value (0.37) differs at the 1.3-σ level from the average value. For the central quartiles the difference is at the ~ 1.5-σ level. Therefore, although lower than expected on average, the observed DPR–OPC agreement is statistically consistent with that expected from the statistical description

Table 3. DPR–OPC (pre-meeting) p–p Quartile Agreement Matrix.

DPR quartile	OPC (pre-meeting) quartile 1	2	3	4
1	0.37	0.26	0.28	0.09
2	0.28	0.16	0.28	0.28
3	0.16	0.40	0.19	0.26
4	0.19	0.19	0.26	0.37

of the pre-meeting OPC process (P18). Note that, given the large noise inherent in the process, a much larger data set (or more realisations of the experiment) would be required to reach a sufficiently high statistical significance and to make robust claims about possible systematic deviations.

The fact that in the real OPC process there is a face-to-face meeting constitutes the most pronounced difference between the two review schemes. In the meeting, the opinions of single reviewers are changed during the discussion, so that grades assigned by individual referees are not completely independent from each other (as opposed to in the pre-meeting phase, in which any significant correlation should depend only on the intrinsic merits of the proposal). The effects of the meeting can be quantified in terms of the quartile agreement fractions between the pre- and post-meeting outcomes, as outlined in Patat (in preparation; hereafter called P19). Based on the P18 sample, P19 concludes that the change is significant; on average, only 75% of the proposals ranked in the top quartile before the meeting remain in the top quartile after the discussion (about 20% are demoted to the second quartile, and 5% to the third quartile). P19 characterises this effect by introducing the Quartile Migration Matrix (QMM). For the specific case of Period 103, the QMM is reported in Table 4 for the subset of the DPR experiment. Of the initial 172 proposals included in the DPR sample, 36 were triaged out in the OPC process and are therefore not considered.

As anticipated, the effect is very marked; the meeting does have a strong effect on the final outcome. In light of these facts, we can finally inspect the QAM between the DPR and the final outcome of the OPC process. This is presented in Table 5. With the only possible exception of $M_{4,4}$, which indicates a relatively

Table 4. OPC Quartile Migration Matrix for the DPR sub-sample (N = 136).

OPC pre-meeting quartile	OPC post-meeting quartile 1	2	3	4
1	0.56	0.32	0.12	0.00
2	0.32	0.32	0.29	0.06
3	0.12	0.26	0.38	0.24
4	0.00	0.09	0.21	0.71

Table 5. DPR–OPC (post-meeting) Quartile Agreement Fraction.

DPR quartile	OPC post-meeting quartile 1	2	3	4
1	0.26	0.38	0.24	0.12
2	0.24	0.35	0.24	0.18
3	0.32	0.12	0.29	0.26
4	0.19	0.15	0.24	0.44

marked agreement for the proposals in the bottom quartile, the two reviews appear to be almost completely uncorrelated. By means of simple Monte-Carlo calculations one can show that for two fully aleatory panels, the standard deviation of a single realisation around the average value (0.25) is 0.10. We conclude the majority of the $M_{i,j}$ elements in Table 5 are consistent with a stochastic process at the 1-σ level.

The main conclusion of this analysis is that, while the pre-meeting agreement is consistent, with the DPR and OPC reviewers behaving in a very similar way (in terms of r–r and p–p agreements), the face-to-face meeting has the effect of significantly increasing the discrepancy between the two processes. However, we caution that the sample is relatively small, and therefore the results are significantly affected by noise.

That the DPR–OPC agreement is smaller than the internal DPR–DPR agreement is not unexpected, as there are intrinsic differences between the two setups, the largest one being the absence of a face-to-face meeting, which is potentially the weakest aspect of the DPR. However, it remains unclear whether panel discussions lead to the selection of better science. In this respect, it is important to note that several studies have shown that panel meetings can increase the differences between two panels with respect to the pre-meeting agreement. In other words, while the meeting increases the internal consensus by polarising different opinions within the panels, it does not lead to a better panel-panel agreement (see Obrecht et al., 2007 and references therein). One would expect the discussions to bring judgment closer to identifying the best science; however, these studies indicate that a face-to-face meeting does not necessarily make the process better.

Conclusions and outlook

Gemini has already implemented a variant of this mechanism successfully over the past few years for their Fast Turnaround (Andersen et al., 2019). The approach presented here enhances this process, using better review-proposal matching based on natural language processing. The next logical step is to expand this experiment and distribute a fraction of observing time using DPR at more facilities. More than 95% of the participants suggest an implementation of such a scheme for some part of the ESO proposal types, with 75% support for the short programmes (time requests < 20 hours). Fewer than 5% of the responses were against implementing DPR for any of the programme types. In particular, about 70% of the responses are in favour of deploying DPR for the Fast Track Channel, while only about 15% are against it (the remaining 15% is indifferent). We take this as a clear indication of support.

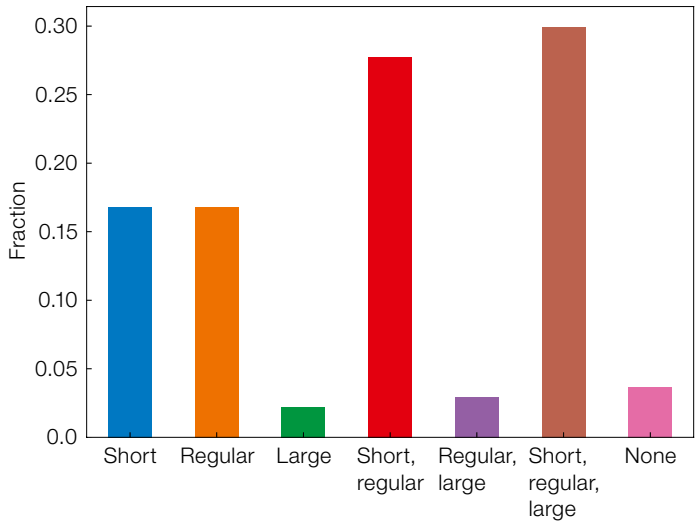

Figure 9. Distribution of the answers to the question: "For which types of proposals do you think distributed peer review would be beneficial?" in the DPR survey.

One of the objections that is typically made to the DPR concept is that, by distributing the proposals to a larger number of unselected scientists, it increases the chances of information leakage and plagiarism. In the specific case of the DPR experiment, the proposals were distributed to 172 reviewers, while in the OPC process the applications were seen by 78 individuals. However, while in the OPC implementation each reviewer has access to all proposals assigned within her/his panel (typically 70–80), the DPR reviewer sees a factor of ~ 10 fewer proposals. Therefore, under the reasonable hypothesis that the fraction of "malevolent" scientists is the same in both review bodies (which are selected from the same community), one would actually expect that the DPR is less prone to confidentiality issues on average. To get a direct opinion from DPR participants, the questionnaire contained an explicit question about this aspect. The distribution of the responses is shown in Figure 10. Excluding the "no strong opinion" cases, 66% of the users declared themselves to be equally or more confident in the DPR process, resulting in about a third of the users placing more trust in the classical scheme.

Another concern that is often heard when discussing DPR is the possible presence of biases. Again, the specific question put to the participants regarding this point does not support this concern; 74% of the respondents believe DPR is equally or more robust against biases (Figure 11).

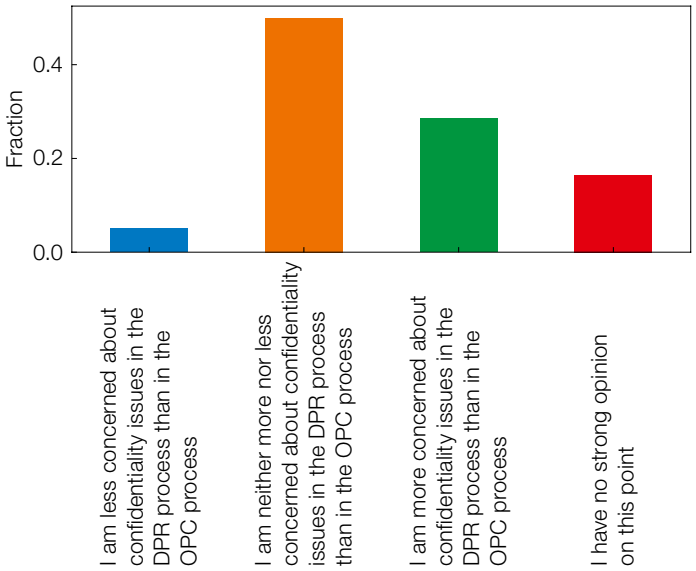

Figure 10. Distribution of answers to a question about how secure the participants felt about confidentiality issues.

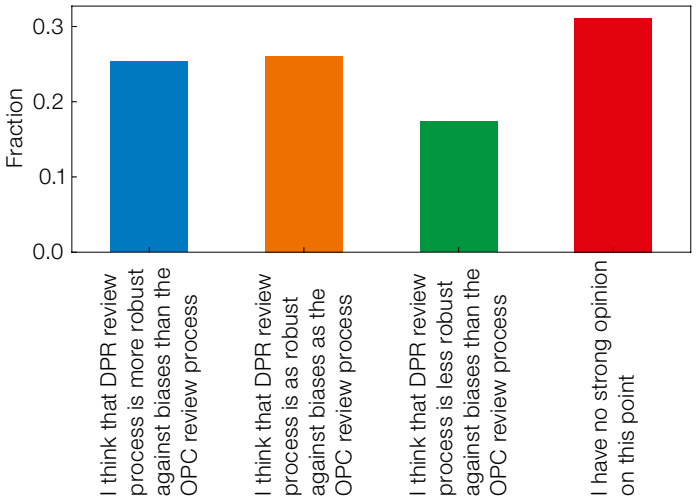

Figure 11. Distribution of answers to a question about the robustness of the process against biases.

The main conclusions drawn from the DPR experiment can be summarised as follows:

– The DeepThought-enhanced DPR experiment was very well received by the participants.
– The mechanism allows an optimal referee-proposal matching.
– The DPR process is as subjective as the OPC process.
– The participants do not see the confidentiality and bias issues as being more severe than in the classical scheme.
– ESO should consider deploying DPR for regular proposals below a certain time request, while leaving the classical review for larger time requests.

To these aspects, which come directly from the data, other positive facts can be added. DPR allows a much larger statistical basis enabling robust outlier rejection (the number of proposals per referee can be easily brought to 10–12) and it removes possible biases generated by panel member nominations. The larger pool of scientists allows much better coverage in terms of proposal expertise matching, and the smaller number of proposals per reviewer allows more careful work and more useful feedback.

Another aspect of the DeepThought approach to proposal-referee matching is that it can be semi-automated; it also gives an objective criterion to assign a particular expertise, eliminating biases in self-reporting. DPR implicitly removes the concept of panel, which adds rigidity to the process. For instance, it maximises the overlap in evaluations, which is a typical issue in pre-allocated panels. The lack of a face-to-face meeting prevents strong personal opinions from having a pivotal influence on the process. Also, DPR involves a larger part of the community, increasing its democratic breadth and exposing all applicants to the typical quality of the proposals. This allows them to better understand if their request is not allocated time by placing it in a wider context, which will help to improve their proposal-writing skills, training the members of the community without additional effort.

We acknowledge that the lack of a meeting does not allow the exchange of opinions and the possibility of asking and answering questions to/from the peers. Despite the fact that its effectiveness remains to be demonstrated and quantified (see above), it is clear that the social, educational and networking aspects of the face-to-face meeting should not be undervalued. In this respect, we note that the resources freed by the DPR approach can be used by the organisations for education and community networking (training on proposal writing, fostering collaborations, etc.).

In April and May 2019, results of the DPR experiment were presented to the ESO governing bodies most closely concerned with the Peer Review process (i.e., the Scientific Technical Committee, the Users Committee and the Observing Programmes Committee). The ensuing discussions have resulted in a wealth of useful feedback that is being discussed internally. We would like to conclude by pointing out that these kinds of studies are crucial if we are to progress from a situation in which the classical peer review process is adopted notwithstanding its limitations simply due to the lack of better alternatives. As scientists, we firmly believe in experiments, including those that address the selection of the experiments themselves.

Acknowledgements

The authors wish to express their gratitude to the 167 volunteers who participated in the DPR experiment, for their work and enthusiasm. The authors are also grateful to Markus Kissler-Patig for passionately promoting the DPR experiment following his experience at Gemini; to ESO's Director General Xavier Barcons and ESO's Director for Science Rob Ivison for their support; and to Hinrich Schütze for several suggestions on the NLP process.

Links

[1] Gemini Observatory Fast Turnaround Observing Mode webpage: http://www.gemini.edu/sciops/observing-gemini/proposal-routes-and-observing-modes/fast-turnaround

[2] Distributed Peer Review Pilot in Foundational Program: https://nifa.usda.gov/resource/distributed-peer-review-pilot-foundational-program

[3] Report from ESO Users Committee No. 42 (2018): https://www.eso.org/public/about-eso/committees/uc/uc-42nd/UCreport2018.pdf

References

Andersen, M. et al. 2019, AAS, 233, 455.03
Ardabili, P. N. & Liu, M. 2013, CoRR, arxiv:1307.6528
Brinks, E. et al. 2012, The Messenger, 150, 20
Gallo, S. A., Sullivan, J. H. & Glisson, S. R. 2016, PLoS ONE, 11, e0165147
Huang, C. 2013, European Journal of Psychology of Education, 28, 1
Kerzendorf, W. E. 2017, Journal of Astrophysics and Astronomy, arxiv:1705.05840
Kerzendorf, W. E. et al. 2019, submitted to Nature Astronomy
Merrifield, M. R. & Saari, D. G. 2009, Astronomy and Geophysics, 50, 4.16
Mervis, J. 2014a, Science, 344, 1328
Mervis, J. 2014b, Science, 345, 248
Obrecht, M., Tibelius, K. & D'Aloisio, G. 2007, Research Evaluation, 16 (2), 79
Patat, F. 2016, The Messenger, 165, 2
Patat, F. et al. 2017, The Messenger, 169, 5
Patat, F. 2018a, The Messenger, 173, 7
Patat, F. 2018b, PASP, 130, 084501
Strolger, L.-G. et al. 2017, AJ, 153, 181

ESO/G. Hüdepohl (atacamaphoto.com)

Snowfall at Paranal is a rare phenomenon that serves to utterly transform the surroundings of the VLT/I into an otherworldly landscape.

DOI: 10.18727/0722-6691/5148

On the Telluric Correction of KMOS Spectra

Lodovico Coccato[1]
Wolfram Freudling[1]
Alain Smette[1]
Eleonora Sani[1]
Jose A. Escartin[1,2]
Yves Jung[1]
Gurvan Bazin[1]

[1] ESO
[2] Max-Planck-Institut für extraterrestrische Physik, Garching, Germany

The presence of strong absorption lines in the atmospheric transmission spectrum affects spectroscopic observations, in particular those in the near- and mid-infrared. Therefore, there is the need to correct scientific observations for this effect, a process known as telluric correction. The use of a detailed model of the atmospheric transmission spectrum brings several advantages over the method of empirically deriving corrections using observations of a telluric standard star. In this paper, we discuss and compare the two methods applied to *K*-band Multi-Object Spectrograph (KMOS) observations and show the improvements in the quality of the final products obtained by implementing the modelling technique offered by the ESO molecfit sky tool.

Correction for atmospheric transmission in spectroscopic data

Ground-based spectroscopic observations are strongly affected by the Earth's atmosphere. In particular, spectra of objects taken in the near- and mid-infrared wavelength ranges are characterised by a forest of absorption lines, called telluric absorptions. These features are caused by (mainly water and OH) molecules present in the atmosphere that absorb the light from astrophysical sources. The standard way to correct for this effect is to acquire a spectrum of a bright and featureless star close in time and airmass to the scientific target, and compare it either with its model or, if available, with a spectrum taken from space. This empirical strategy, however, has some drawbacks. First, it requires additional (expensive) telescope time. Second it can be complicated to separate atmospheric and instrumental effects, (for example, the instrument response) if a large wavelength range of stellar continuum is absorbed by blended absorption lines. Last but not least, the noise and imperfections in the data reduction of these stars are inevitably propagated to scientific spectra.

Alternatively, one can model the atmosphere, generate its transmission spectrum and apply it to observations. The model itself can be obtained by fitting well-defined telluric lines to the spectrum of either a standard star or a sufficiently bright science target. In general, a model depends on four components: (a) a radiative transfer model; (b) a set of parameters that determines the absorption and transmission properties of individual molecules; (c) atmospheric profiles of temperature, humidity, and volume mixing ratio for the molecules involved; and (d) instrumental parameters such as spectral resolution. This model-dependent approach has several advantages over the empirical method. First, no additional noise or sources of error coming from the standard star observations and reduction are propagated to the science spectra. Second, it allows additional components to be taken into account, such as the amount of precipitable water vapour from external sources and inaccurate wavelength calibrations, and differences between the observations of the standard star and the science target (for example, airmass and spectral resolution). On the other hand, using a model of the atmosphere for the telluric correction risks the introduction of systematics because of limitations in the modelling. In practice, the artefacts caused by such systematics are outweighed by the improvements made in the corrections.

The model approach has been developed in a software package named molecfit (Kausch et al., 2013; Smette et al., 2015). Molecfit uses (a) the Line-by-line Radiative Transfer Model[1] (LBLRTM) algorithm (Clough, Iacono & Moncet, 2005) to compute the radiative transfer model, (b) the high-resolution transmission molecular absorption (HITRAN) database[2] for the molecular parameters, (c) Global Data Assimilation System[3] (GDAS) and ESA Michelson Interferometer for Passive Atmospheric Sounding[4] (MIPAS) atmospheric profiles for temperature, humidity, water vapour and other molecules, and (d) analytic functions or user-provided files for the instrumental spectral resolution. The fit to the telluric absorption lines in the observed spectra provides the integrated column density of individual molecules. Future versions will further improve the quality of the model by including real-time measurement of precipitable water vapour and other molecules along the line of sight of the exposures.

In the following, we describe the improvements in the quality of KMOS (Sharples et al., 2013) spectra obtained with the model approach using molecfit with respect to the empirical method. Data were reduced using the KMOS pipeline (Davies et al., 2013). In the model approach, the atmospheric model was obtained by fitting a number of predefined telluric lines on a standard star spectrum observed close in time to the scientific data (i.e., the same standard star that was used in the empirical method). The telluric correction over the full wavelength range was then computed accounting for the differences in airmass and spectral resolution between the scientific spectrum to correct and the standard star. As a test-bench for comparison, we processed one month of KMOS data and compared the results obtained with these two different telluric correction strategies.

Benefits of the molecfit strategy for KMOS observations

As described previously, because the molecfit correction is based on a model, it does not add noise to the final products or defects such as uncorrected cosmic rays that are embedded in the standard star spectrum. Figure 1 shows a comparison between the mean signal-to-noise per pixel of the datacubes obtained by correcting the telluric absorption directly with a standard star (i.e., the empirical method) and by modelling the atmospheric absorptions with molecfit. The signal-to-noise is measured in a wavelength region that is free of sky or telluric lines, and therefore is an indication of the noise added by the telluric correction. As expected, the data corrected with

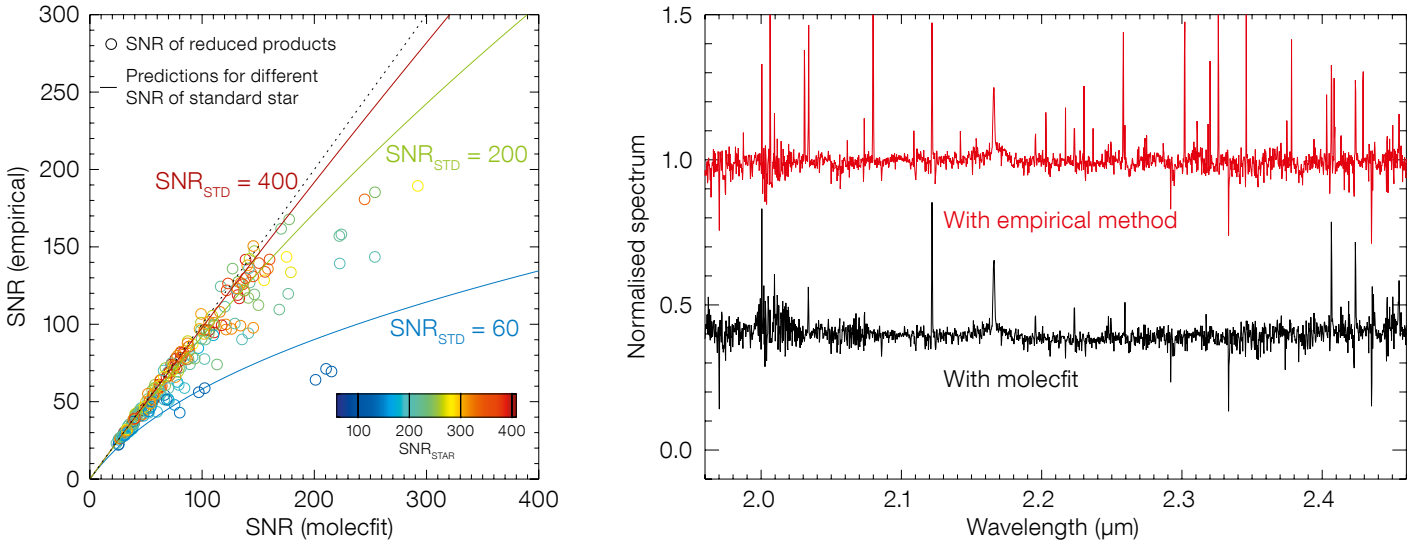

Figure 1. Left panel: Comparison between the signal-to-noise ratio (per pixel) of the final KMOS datacubes obtained with the empirical corrections and the method with molecfit on-standard model for the telluric correction. The colour of the symbols is proportional to the signal-to-noise of the telluric star used in the data reduction; predicted trends for several values of the signal-to-noise of the telluric standard are shown. The dashed black line shows the 1:1 relation. Right panel: Example of spectra corrected with the empirical corrections (in red) and with the model approach with molecfit (in black) for the dataset KMOS.2018-10-23T07:35:07.185.

molecfit contain less noise; the effect is much more visible for bright objects which have signal-to-noise ratios close to those of the telluric standard stars. No major improvement is expected for objects with signal-to-noise < 50, because the noise in the telluric standard is negligible with respect to the total noise in the data. Even with the model approach there are systematic artefacts in the reduced spectrum that are due to residuals in the sky subtraction or cosmic ray cleaning. However, with the empirical approach the number of artefacts is higher; these additional artefacts are not due to the sky subtraction in the science spectra (in fact, the same procedure as in the model approach is used). Some of these are inherited from imperfections in the reduction of the standard star while others are due to the limitations of the empirical method in dealing with differences between the observations of the science and the telluric star (see Figures 2 and 3).

One of the limitations of the empirical telluric correction method is that the telluric star and the science target are observed at different airmasses. The KMOS night calibration plan is designed to minimise such differences; for example, a telluric standard is observed every two hours at airmasses close to the scientific targets observed during the night. However, differences up to ~ 0.4 in airmass are unavoidable owing to observational constraints, in particular during observations in visitor mode during which the requirements for the observation of the telluric standard stars are relaxed. The consequence is that some telluric lines are over- or under-corrected by up to or over 10%, because the column density of the molecules, and therefore the atmospheric transmission, is linked to the airmass. The empirical approach offered by the KMOS pipeline does not account for such airmass differences, whereas the model approach does. Figure 2 shows the change in intensity in the telluric line at 1.27 μm for a difference in airmass of $\Delta z = 0.34$, and its effects on the corrected science spectrum; accounting for this difference overestimates the absorption feature at 1.27 μm by ~ 10%. The bottom panel of Figure 2 shows a systematic artefact at 1.27 μm, which is due to there being no correction for the difference in airmass between science and standard star observations.

Another limitation of the empirical method is that taking a telluric calibration in each of the 24 arms is time consuming. Therefore, the large majority of programmes observe a telluric standard star in only 3 out of the 24 arms available in KMOS, i.e., one per detector. However, the spectral resolutions of the various arms are different, therefore the absorption features in atmospheric transmission will have different shapes in different arms. This means that the observed shape of the absorption lines in telluric correction determined for a star observed with one arm does not fully match the shape of the telluric lines of a scientific spectrum obtained with another arm. This issue can be taken into account in the model approach, by including a set of static calibrations that reproduce the wavelength dependency of the instrumental spectral resolution for each arm and instrument configuration. These calibrations are included in the KMOS pipeline distribution and allow one to compute the telluric correction for each arm with the exact shape of the absorption lines, regardless of which arm the telluric standard was observed with. Figure 3 compares the effects of taking and not taking into account the spectral resolution during the modelling in the final KMOS products. The shape of the absorption features can differ by 10% or more, leading to artificial features in the final corrected spectrum.

Molecfit implementation in the KMOS instrument pipeline

The original molecfit software interface does not support the use of KMOS data

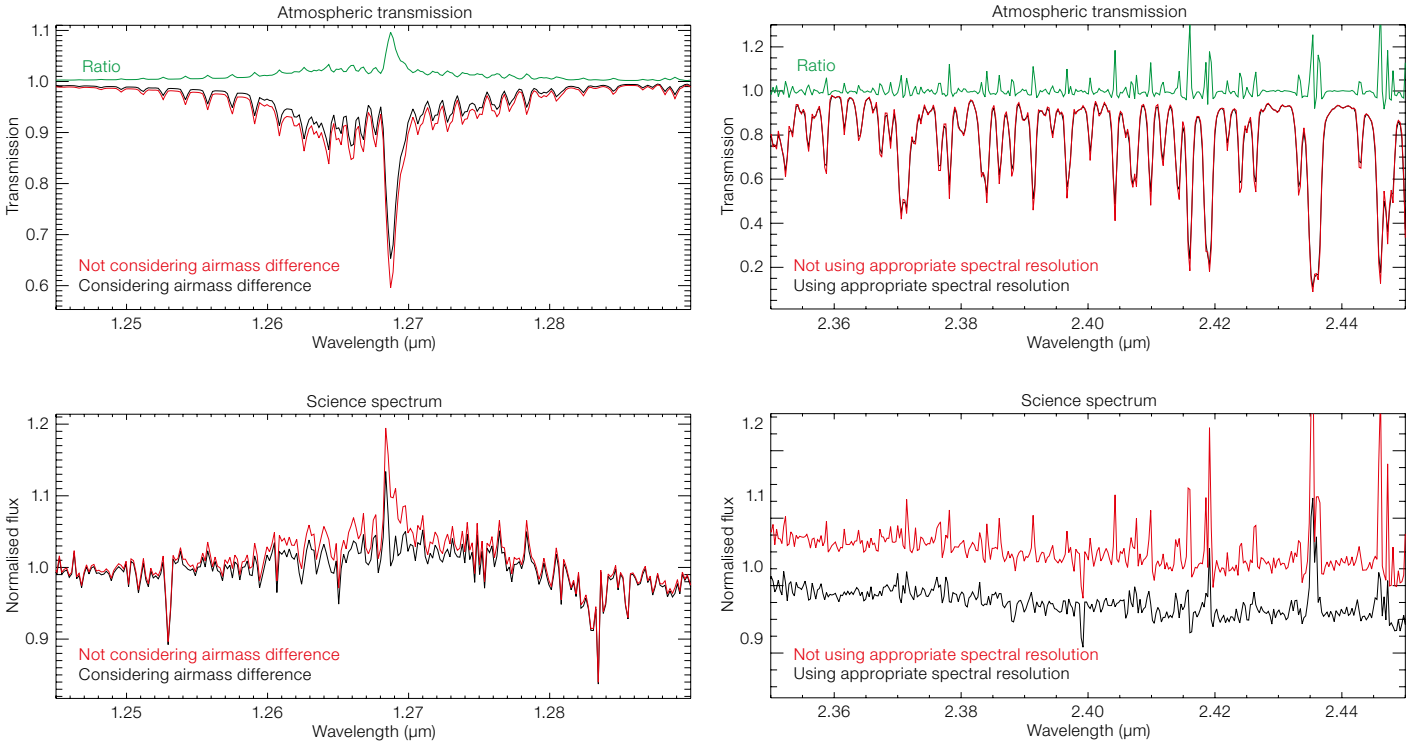

Figure 2. Comparison between the outcome of different molecfit models that account for (black) and ignore (red) the airmass difference between the standard star and the science spectra. The top panel shows the atmospheric transmissions and their ratio (in green). The airmass difference between the two models is $\Delta z = 0.34$. The bottom panel compares the science spectra corrected with these different transmissions. The dataset used here is KMOS.2016-12-21T03:18:57.095.

Figure 3. Comparison between the outcome of different molecfit models that account for (black) and ignore (red) the differences in spectral resolution between the arm used to observe the standard star and the arm used to observe the scientific target. The top panel shows the atmospheric transmissions and their ratios (in green). The bottom panel compares the telluric-corrected science spectra (arbitrarily shifted). The file used here is KMOS.2017-02-13T05:45:03.492.

directly, because of the complicated multi-extension structure that requires special treatment. In order to provide a convenient interface, the molecfit algorithms have been integrated into the KMOS pipeline, which now offers three strategies to correct for telluric absorptions in the observations:

1. Use the telluric standard star spectrum directly to correct the science data, i.e., the empirical method.
2. Use the standard star spectrum as reference to model the atmosphere and derive its transmission to correct science data on the same night (we call this the molecfit on-standard approach).
3. Use one science spectrum as a reference to model the atmosphere and derive its transmission to correct the science spectrum itself or other science data in the same observing block (we define this as the molecfit on-science approach).

The empirical method is much faster, but generally does not return the best results. Nevertheless, it is useful for a quick look at the data or in those cases where the atmospheric fit does not converge. The molecfit methods are computationally slower but return the best results in the vast majority of cases. Both the molecfit on-standard and on-science approaches model the atmosphere by fitting a number of telluric absorption features in a reference spectrum. In the on-standard approach, the default wavelength regions of the recipe can safely be used, whereas for the on-science approach it is advisable to carefully adjust the fitting regions avoiding intrinsic features of the science spectrum. Then, the full telluric correction is obtained for the entire wavelength range and it accounts for the difference in airmass between the reference and science spectra. A set of static calibration files provide the recipes with tables giving the wavelength-dependent instrument spectral resolution and instrument response for each integral field unit (IFU), grating, and instrument rotator angle. Figure 4 illustrates the data reduction cascades due to the two different molecfit approaches. For each spectrum, the user can select a reference scientific exposure from which to obtain the atmospheric transmission. It can be the same target or another; for example, a bright target can be used to compute the correction for all other observations in the same observing block. The loop is rerun for each input exposure accounting for changes in airmass and spectral resolution.

All three correction strategies have been integrated into the data reduction workflow that can be executed within the EsoReflex data reduction environment (Freudling et al., 2013). The KMOS workflow includes automatic organisation of the data and interactive tools to visualise and control the telluric correction as well as other reduction steps (Figure 5). In particular, it includes a tool to select

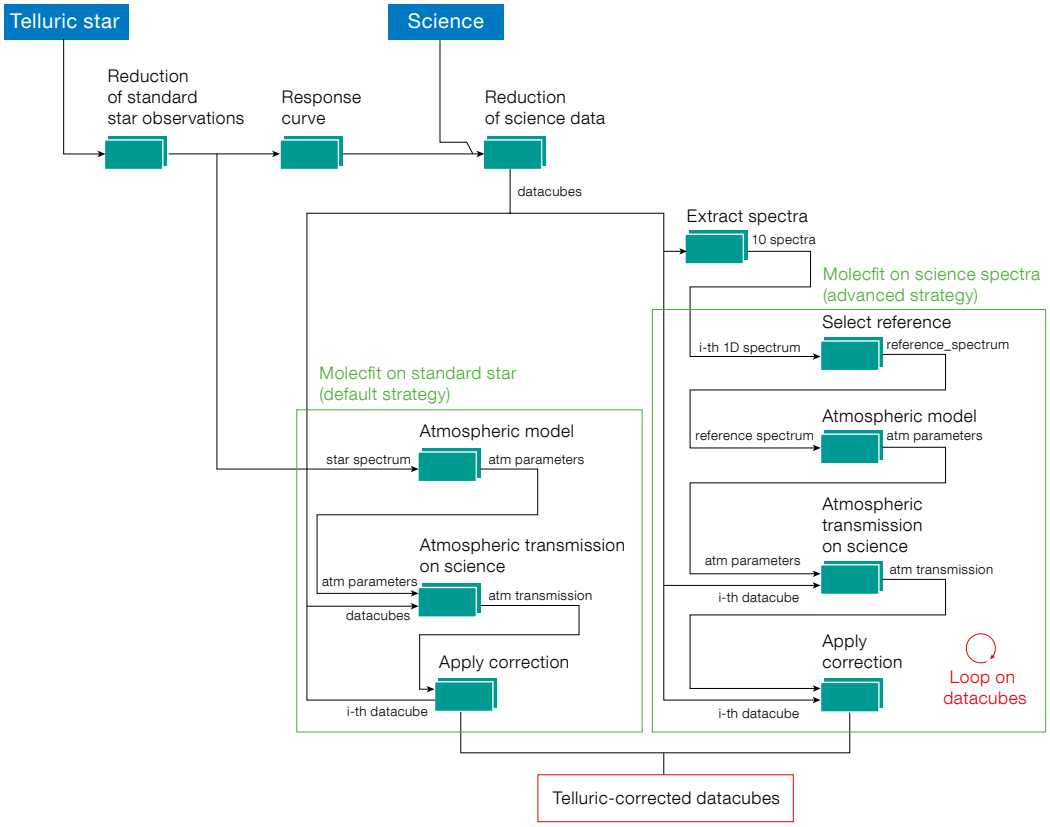

Figure 4. Schematic representation of the two molecfit strategies implemented in the KMOS EsoReflex workflow. The default molecfit on-standard approach (on the left) obtains atmospheric parameters from a telluric standard observation before computing the atmospheric transmission at the airmass and spectral resolution of the scientific exposure. In the molecfit on-science approach (on the right), the process is applied directly to the science exposures.

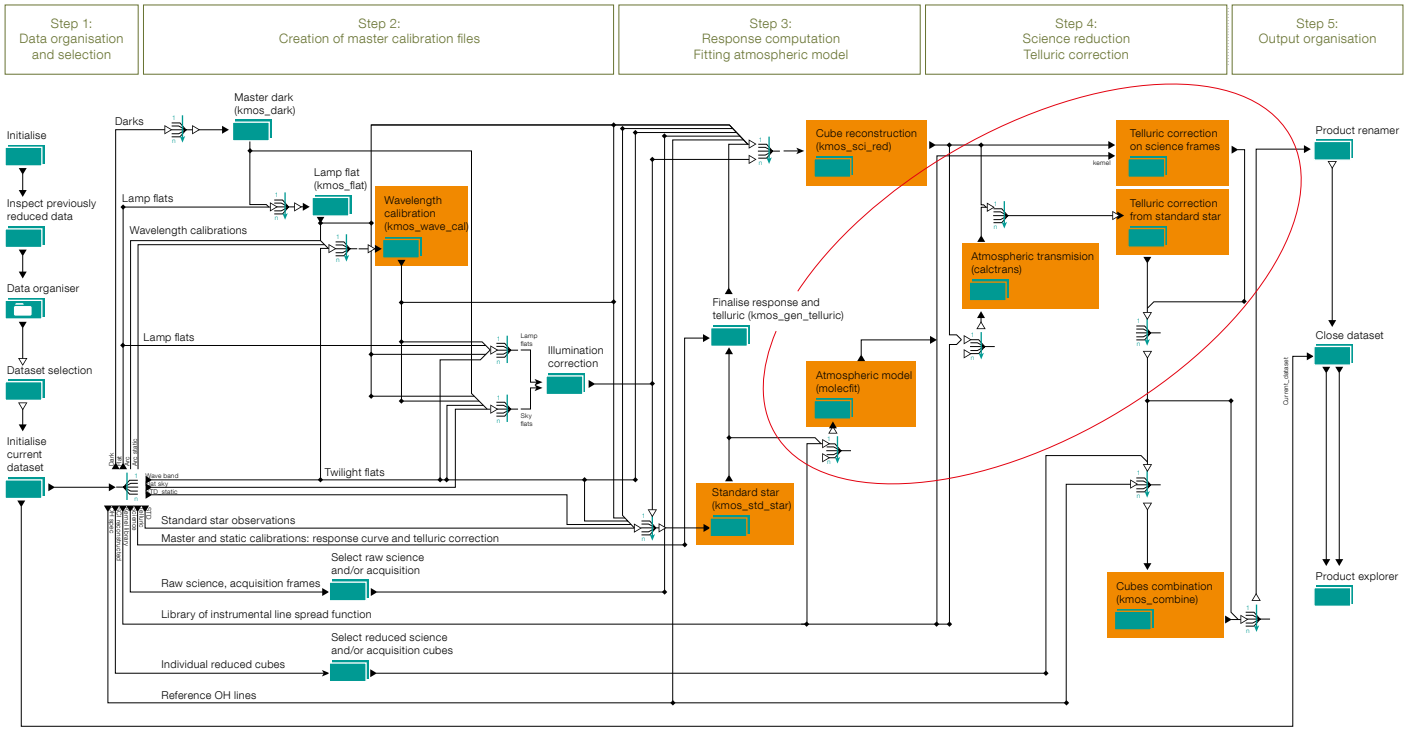

Figure 5 (below). The EsoReflex KMOS workflow. Each green box represents a step in the data reduction chain. Orange boxes identify interactive components in which the user has the opportunity to inspect the products of that specific step and re-run the corresponding recipe with different parameters. Interactive modules that are specific to telluric correction are marked by the red ellipse. User-defined scripts can be plugged into the workflow as well.

wavelength regions and the reference spectra to fit the atmosphere, which are fundamental steps in the on-science approach. An EsoReflex tutorial[5] (Coccato et al., 2019) that guides the user through the data reduction and an updated pipeline manual are available at the ESO instrument pipelines webpage[6].

The on-standard molecfit approach is used for the in-house ESO reduction of KMOS observations for the ESO archive; these reduced data products will be available to the astronomical community soon through the ESO archive science portal[7]. Improvements with respect to this method can be obtained case by case with the on-science molecfit approach. Indeed, this approach limits the differences in the molecule column densities between the scientific spectrum and the target spectrum that arise simply by looking at different locations on the sky (despite closeness in time or airmass). The on-science method, however, requires interactive selection of bright science spectra to use as references, and a careful selection of the wavelength ranges to fit. For those reasons it is not used for the archive products. In future, the molecfit tools will be integrated into all the near- and mid-infrared instrument pipelines and workflows to grant the user flexibility to perform telluric correction in the most efficient way.

References

Clough, S. A., Iacono, M. J. & Moncet, J.-L. 2005, J. Geophys. Res., 97, 1576
Coccato, L. et al. 2019, Reflex KMOS tutorial, issue 6.0
Davies, R. et al. 2013, A&A, 558, 56
Freudling, W. et al. 2013, A&A, 559, 96
Kausch, W. et al. 2015, A&A, 576, 78
Sharples, R. et al. 2013, The Messenger, 151, 21
Smette, A. et al. 2015, A&A, 576, 77

Links

[1] Atmospheric & Environmental Research (AER) Radiative Transfer Working Group Website: http://rtweb.aer.com/
[2] HITRAN database: https://hitran.org/home/
[3] National Centers for Environmental Information Global Data Assimilation System (GDAS): https://www.ncdc.noaa.gov/data-access/model-data/model-datasets/global-data-assimilation-system-gdas
[4] ESA Michelson Interferometer for Passive Atmospheric Sounding: https://earth.esa.int/web/guest/missions/esa-operational-eo-missions/envisat/instruments/mipas
[5] The Reflex KMOS tutorial (Coccato et al. 2019) can be downloaded from the following link: http://www.eso.org/sci/software/pipelines/
[6] VLT instrument pipelines: http://www.eso.org/sci/software/pipelines/
[7] ESO Science Archive Portal: http://archive.eso.org/scienceportal/

M. Cabral/ESO

The VLT/I at sunset.

DOI: 10.18727/0722-6691/5149

Bringing the New Adaptive Optics Module for Interferometry (NAOMI) into Operation

Frédéric Gonté[1]
Jose Antonio Abad[1]
Roberto Abuter[1]
Emmanuel Aller Carpentier[1]
Jaime Alonso[1]
Luigi Andofalto[1]
Pablo Barriga[1]
Jean-Philippe Berger[2]
Jean-Luc Beuzit[2]
Israel Blanchard[1]
Henri Bonnet[1]
Guillaume Bourdarot[2]
Pierre Bourget[1]
Roland Brast[1]
Paul Bristow[1]
Luis Caniguante[1]
Susana Cerda[1]
Claudia Cid[1]
Alex Correa[1]
Eric Cottalorda[2]
Benjamin Courtney-Barrer[1]
Pascaline Darré[1]
Bernard Delabre[1]
Alain Delboulbé[2]
Roderick Dembet[1]
Ronald Donaldson[1]
Reinhold Dorn[1]
Jorge Dupeyron[1]
Christophe Dupuy[1]
Sebastian Egner[1]
Frank Eisenhauer[5]
Lorena Faundez[1]
Enrico Fedrigo[1]
Gerhard Fischer[1]
Christoph Frank[1]
Eloy Fuenteseca[1]
Philippe Gitton[1]
Thibaut Guerlet[1]
Sylvain Guieu[2]
Pablo Gutierrez[1]
Pierre Haguenauer[1]
Andreas Haimerl[1]
Xavier Haubois[1]
Cédric Heritier[1]
Stefan Huber[1]
Norbert Hubin[1]
Paul Jolley[1]
Laurent Jocou[2]
Jean-Paul Kirchbauer[1]
Johann Kolb[1]
Johan Kosmalski[1]
Peter Krempl[3]
Carlos La Fuente[1]
Jean-Baptiste Le Bouquin[2]
Miska Le Louarn[1]
Paul Lilley[1]
Bruno Lopez[6]
Marcelo Lopez[1]
Yves Magnard[2]
Enrico Marchetti[1]
Stewart Mclay[1]
Anthony Meilland[6]
Alexander Meister[1]
Antoine Mérand[1]
Thibaut Moulin[2]
Luca Pasquini[1]
Jérôme Paufique[1]
Isabelle Percheron[1]
Lorenzo Pettazzi[1]
Oliver Pfuhl[5]
Duc Phan[1]
Andres Pino[1]
Werther Pirani[1]
Jutta Quentin[1]
Andrew Rakich[1]
Andrés Ramirez[1]
Robert Ridings[1]
Mario Riedel[1]
Javier Reyes[1]
Sylvain Rochat[2]
Juan Sanchez[1]
Gonsalo Santos Tomás[1]
Christian Schmid[1]
Pavel Shchekaturov[4]
Nicolas Schuhler[1]
Matthias Seidel[1]
Christian Soenke[1]
Eric Stadler[2]
Christian Stephan[1]
Marcos Suárez[1]
Mirko Todorović[1]
Guillermo Valdes[1]
Cristophe Verinaud[1]
Julien Woillez[1]
Gérard Zins[1]
Sebastian Zúñiga-Fernández[1,7,8]

[1] ESO
[2] Institut de Planétologie et d'Astrophysique de Grenoble (IPAG), Université Grenoble Alpes, CNRS, France
[3] KRP Mechatec GmbH, Garching, Germany
[4] Pactum LTD, London, UK
[5] Max Planck Institute for Extraterrestrial Physics, Garching, Germany
[6] Laboratoire Lagrange, Université Côte d'Azur, Observatoire de la Côte d'Azur, CNRS, France
[7] Universidad de Valparaíso, Instituto de Física y Astronomía (IFA), Chile
[8] Núcleo Milenio de Formación Planetaria (NPF), Valparaíso, Chile

NAOMI was developed by a consortium composed of IPAG and ESO. Its Provisional Acceptance Chile review was held in April 2019. The NAOMI systems that have been installed on the Auxiliary Telescopes make the Very Large Telescope Interferometer (VLTI) and its instruments much less dependent on the atmospheric and dome seeing conditions. NAOMI increases the interferometer's operability and improves the performance of its instruments and, very early on, was identified as being critical to the VLTI. In this article, we review the project, describe its principles and architecture, and offer a preview of the improvements it brings to VLTI instruments.

Context

Adaptive optics were considered for interferometric instruments even before non-interferometric instruments, as the measurement of high-quality interferometric observables depends strongly on the wavefront quality. Therefore, the implementation of the adaptive optics (AO) systems on the Auxiliary and Unit Telescopes (ATs and UTs) of the VLTI has been recommended ever since the launch of the VLTI project (Beckers, 1990). Consequently, between 2003 and 2005 the UTs were equipped with the visible Multi-Application Curvature Adaptive Optics systems (MACAO; Arsenault, 2003); later, in 2016, the UT AO coverage was extended into the infrared with the Coudé Infrared Adaptive Optics system (CIAO; Scheithauer, 2016).

The Auxiliary Telescopes

Although the design concept for the ATs developed by the Institut de Radioastronomie Millimétrique (IRAM; Von Der Lühe, 1997) included an AO system, this was omitted when construction started owing to a lack of resources, both in terms of personnel and funds. Instead, a tip/tilt corrector based on the System for Tip-tilt Removal with Avalanche Photodiodes (STRAP; Bonaccini, 1997) and a fast steering mirror was studied and implemented (Koehler, 2002, 2004). The ATs, depicted in Figure 1, each have a primary mirror of 1.8-metre diameter. They are

used by the VLTI for around 75% of the available nights.

NAOMI

NAOMI has completely replaced STRAP and is now the only wavefront correction system available on the ATs. It has three main components that are fully embedded in the telescopes: a wavefront sensor; a deformable mirror; and a real-time computer. The wavefront sensor was developed at ESO headquarters; it is a Shack–Hartmann Sensor sensitive to visible wavelengths with a 4 × 4 lenslet array, of which 12 sub-apertures are used. The low number of sub-pupils was driven by the requirement to maintain a high sensitivity for the VLTI-AT array. The detector is an off the shelf EM-CCD camera iXon ultra 897 developed by ANDOR (UK). The wavefront sensor is also integrated on a field-tracking stage to pick up the correct field. A neutral density filter wheel has been integrated just above the wavefront sensor to adjust the illumination in case of high flux, and a notch filter has been integrated into the wavefront sensor optics to reject any contamination from the lasers of the Adaptive Optics Facility (AOF; Arsenault, 2017) implemented on UT4. The full wavefront sensor and its filter wheel are installed in the lower part of the Relay Optics Structure. It receives the visible part of the light after the M9 dichroic mirror which redirects the infrared component to the VLTI instruments.

The corrective optics (Le Bouquin, 2018), developed by IPAG, consist of a deformable mirror (DM241), which has 17 actuators across its clear aperture, produced by ALPAO France, and which is integrated in a motorised gimbal mount. It is installed at the M6 pupil location in the coudé train. In addition to compensating for atmospheric turbulence, it provides the chopping capability required by MATISSE. The DM241 has a clear aperture of 37.5 mm, but NAOMI uses only the central part over a 28-mm (11-actuator) diameter pupil as seen in Figure 2 (right).

The deformable mirrors were characterised at room temperature at IPAG and then in a thermal chamber between 5 and 20 degrees C at ESO headquarters. The outcome convinced the project team that a temperature-controlled calibration bench was necessary at Paranal. IPAG finalised this bench, which is now used as a maintenance tool on Paranal. We discovered on Paranal that the deformable mirror had a more complex thermal dependence than previously understood and that the mirror displayed unpredictable behaviour. It is therefore necessary to calibrate the deformable mirror on sky at each target acquisition. The result of the characterisation of the mirrors was presented at the Adaptive Optics for Extremely Large Telescopes (AO4ELT) conference in June 2019[1] (see Haguenauer, 2019).

The real-time computing unit is based on the ESO-standard SPARTA Light platform (Suárez Valles, 2012) and has been customised by PACTUM Ltd for the NAOMI project. It uses the same platform as for the CIAO of the UTs, which facilitated its development in Garching and simplifies the operation on Paranal. The hardware is implemented in the electronics rack of the signal cabinet (see Figure 1). This unit makes the acquisition on the Shack–Hartmann Sensor, analyses the wavefront aberration and the pupil derotation to be corrected, calculates the correction to be applied to the deformable mirror and then sends the command to the mirror. Since the deformable mirror and the

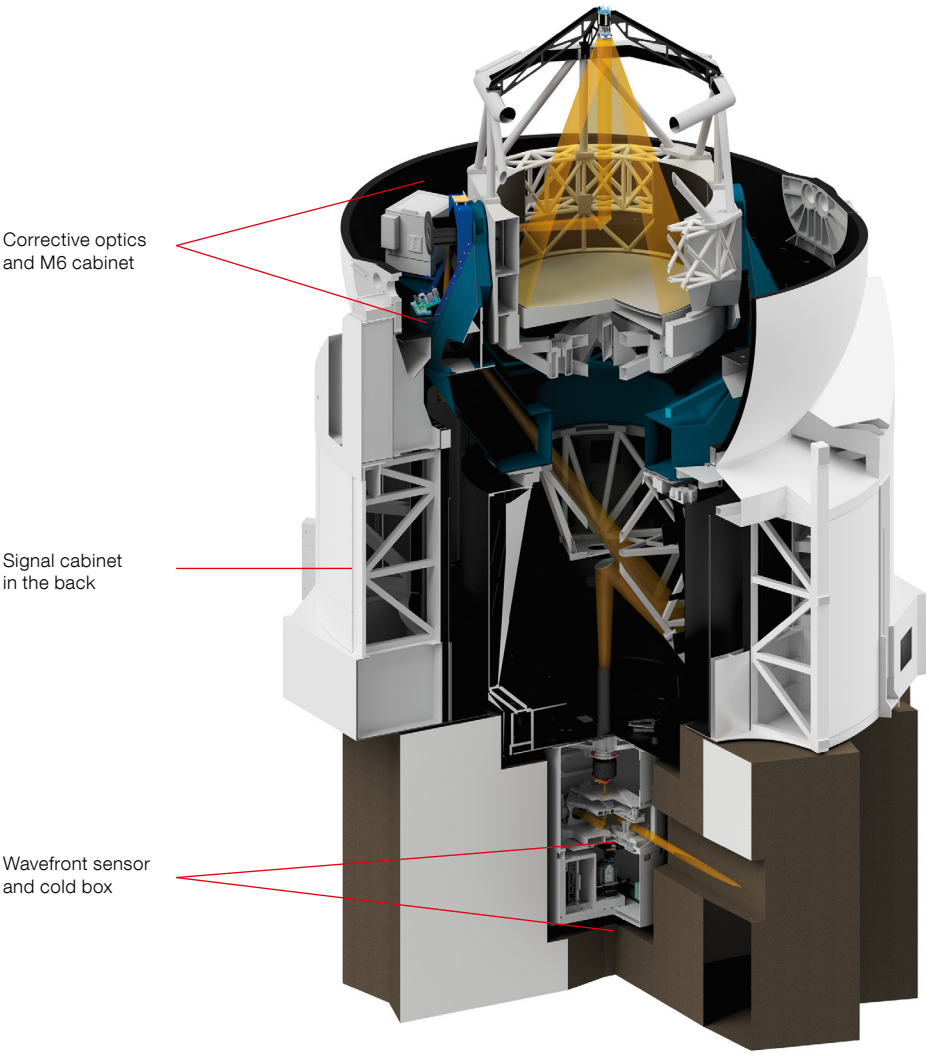

Peter Krempl

Figure 1. 3D cross-sectional view of an AT showing the locations of the NAOMI components. The corrective optics and its electronics are implemented at the level of the azimuth; the wavefront sensor and its electronics are implemented in the lower part of the Relay Optics Structure. The real-time computer and the remaining control electronics are implemented in the signal cabinet.

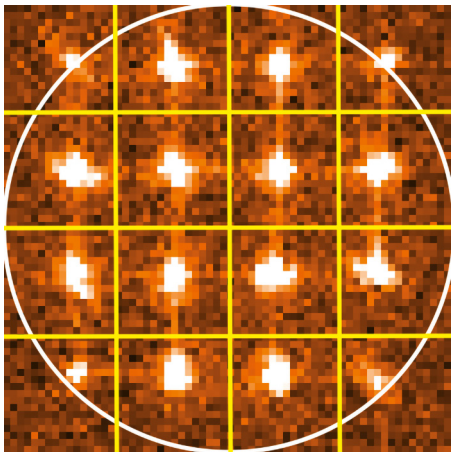

Figure 2. Real-time displays from the real-time computer. The left picture shows the Shack–Hartmann image. The four unused spots at the corners are vignetted at more than 50% by the pupil (represented by a white circle). The sub-apertures are represented in yellow. The picture on the right shows the voltage applied to the actuators of the deformable mirror, the white circle indicating the pupil footprint.

ANDOR camera are commercial products, interfaces between SPARTA light and these components had to be developed. The real-time computer measures 24 gradients on the wavefront sensor at a frequency up to 500 Hz and corrects up to 14 modes on the deformable mirror depending of the brightness of the star.

Manufacturing, Assembly, Integration and Testing (MAIT)

The MAIT phase began in January 2017 with several activities in parallel. IPAG worked on the deformable mirror characterisation, the corrective optics integration and its dedicated electronics while ESO worked on the wavefront sensor, the electronics, the real-time computer, the software and the test bench. The integration and alignment of the NAOMI test bench were carried out by members of the ESO Mechanical Engineering and Optical Engineering Departments. The goal was to replicate as accurately as possible the behaviour of an on-sky target in the laboratory as it would be observed by an AT at Paranal.

The bench consisted of an optical table and a replica of the Relay Optics Structure used by the AT. The optical table facilitated simulation of sky and AT behaviour. An artificial on-sky target was created via a monomode fibre connected to a halogen lamp. A pupil mask was used to define the spider of the AT (the spider is the strut that supports the mirror) while the deformable mirror itself simulated the atmospheric turbulence thanks to its high density of actuators. IPAG provided phase maps for different levels of turbulence which were run in parallel to the applied correction by the AO loop. This approach was much more flexible and more useful than using a turbulence generator with phase plates. Finally, a derotator integrated into the Relay Optics Structure was used to create the pupil rotation on the wavefront sensor to be fully representative of the Paranal conditions. An infrared camera was integrated into the bench to record the resulting star-like image. This same camera was later re-used during the Assembly, Integration and Verification (AIV) phase for the stand-alone characterisation of NAOMI on sky.

The NAOMI software is fully embedded in the AT software. It was developed in the control model implemented at ESO headquarters before being tested on the NAOMI test bench. The ESO software department obtained two years of external support from CNRS in order to ensure the project team had the required skills. The real-time computer software followed the same approach with model-based testing before its integration onto the test bench and was delivered by PACTUM Ltd.

A prototype of the wavefront sensor was first developed to validate the opto-mechanical concept as well as the integration and alignment procedure. The required mechanical improvement to the design was then made by KRP Mechatec GmbH who also provided the tooling required for the MAIT and the AIV. The electronics development and integration were supported by the electronics groups at ESO in order to account for the evolution of the ATs and to conduct a thorough analysis of the cabling and interface.

The system test began in November 2017, led by the system engineer and the AO engineer while other team members produced and tested the final versions of the electronics, wavefront sensors and corrective optics. In addition to the NAOMI test bench, the project team developed dedicated test benches for the electronics, the wavefront sensor and the corrective optics. This allowed the

Figure 3. NAOMI test bench in integration. The corrective optics are seen at the top right.

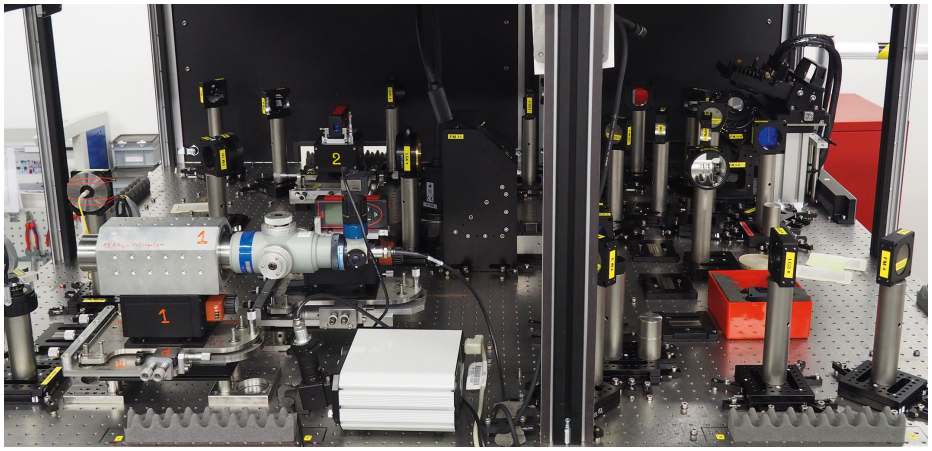

Emmanuel Aller Carpentier

Thibaut Moulin

Figure 4. Some of the members of the NAOMI project team during AIV; first row, from left to right: Thibaut Guerlet, Christian Soenke, Sylvain Rochat, Luis Caniguante; second row, left to right: Pascaline Darré, Pabio Gutierrez, Emmanuel Aller Carpentier, Frederic Gonté, Roderick Dembet, Stefan Huber, Alain Delboulbé, Peter Krempl, Laurent Jocou, Pierre Bourget, Sylvain Guieu, Thibaut Moulin.

verification of all of the components to be delivered to Paranal independently of the main NAOMI test bench, which was fully dedicated to the NAOMI functional and system test.

In parallel with the systems test, the AIV team and several engineers from Paranal were trained on the test bench every time a corrective optics or a wavefront sensor needed to be exchanged to ensure a high level of confidence in the procedures. Provisional Acceptance Europe, held in July 2018, concluded these system tests.

Assembly, Integration and Verification

AIV was prepared well before the arrival of the NAOMI equipment on Paranal. Several missions to Chile were necessary to verify the ATs, check the interfaces, and ensure the feasibility of the AIV plan via discussions with Paranal staff. The plan accounted for various factors, including the availability of tools such as the crane, the staff, the locations where various activities had to be performed, and the logistics of accommodating the 14-member project team at the Residencia.

It became apparent that science operations of the VLTI with ATs would have to be suspended during AIV of NAOMI; which necessitated minimising the time required for AIV. The NAOMI AIV was the first time that a system was implemented simultaneously on four telescopes at Paranal. To mitigate the risks, the main procedures were fully rehearsed before the start of AIV. The plan also included adequate contingency in the schedule, and redundancies in the staff competences.

AIV began on 6 September 2018, following a few days of preparation during which the four Relay Optics Structures were removed and transported to the New Integration Hall and the first AT was moved to the service station to allow the removal of the fast steering mirror and the implementation of the corrective optics.

Many activities were then carried out in parallel, with three teams focusing on different aspects of the implementation. The first team took care of the cooling and cabling upgrade of the Relay Optics Structure and the implementation of the NAOMI components. The second worked on the replacement and upgrade of the electronics cabinets while the third focussed on the internal re-alignment of the ATs with the corrective optics (Figure 5). With so many activities in parallel, regular reorganisation and reassignment of tasks was necessary, requiring the staff to be flexible.

The assembly and integration part of the AIV proceeded faster than planned, and on 18 September the first AT was ready for the first stand-alone verification on sky, during which the functionalities and AO performance could be evaluated (see Figure 6). Soon after, two telescopes were available for verification working together with the VLTI. It was impressive to see the NAOMI team simultaneously in the New Integration Hall, in the AT Service station, in the VLTI building, and in the Control Room working hard toward getting the first closed-loop with NAOMI. The AIV included 32 missions from Europe, with an average of nine project members working at Paranal over a two-month period.

Julien Woillez

Figure 5. Intervention at the beginning of the night on the corrective optics of AT4 conducted by Pascaline Darré and Sylvain Guieu.

Pierre Haguenauer

Figure 6. Acquisition of a star with the infrared Strehl camera (*H*-band) in open loop (left) and in closed loop (right) for quasi-instantaneous Strehl measurement (50 ms integration time) during the stand-alone verification of AT1.

Commissioning

The NAOMI project had two commissioning periods led by IPAG and supported by ESO; these involved 14 missions. During this time NAOMI was also commissioned on the current instrument suite at VLTI: GRAVITY (GRAVITY Collaboration et al., 2017), the Multi AperTure mid-Infrared SpectroScopic Experiment (MATISSE; Lopez, 2014) and the Precision Integrated Optics Near Infrared ExpeRiment (PIONIER; Zins, 2011). Commissioning began with the first light of NAOMI using the four ATs and GRAVITY on 20 October. It was dedicated to verifying functionality with the VLTI and ensuring stable operation. In order to measure how NAOMI improved the performance of the PIONIER and GRAVITY instruments, several indicators were monitored, including throughput, flux drop-out estimators and fringe tracking residuals. All measurements were compared against tip/tilt-only correction. The chopping capability was functionally tested with MATISSE. The reliability of the NAOMI system was analysed and found slightly non-compliant owing to a few issues that had a minor impact on operation. At the end of the first commissioning on 17 November the ATs were transferred back into science operation.

The ESO team with the support of IPAG continued to follow the performance of NAOMI closely during these operations. The team made extensive use of the Garching Remote Access Facility before the second commissioning, in order to solve issues discovered by the Paranal operation team.

The second commissioning period, which began on 25 February 2019, focused on the VLTI instrument performance gains resulting from NAOMI, in particular the improvement for faint stars, with lower than average seeing and the AT dome seeing effect. NAOMI greatly improves the injection flux in the spatial filters and/or the fibres of the interferometric instruments. It improves the signal to noise of each instrument and significantly reduces the loss of fringes on the Gravity Fringe Tracker. NAOMI is much more robust to atmospheric conditions than STRAP. It corrects the dome seeing observed with low wind conditions and corrects the atmospheric seeing well above 1.4 arcseconds. The performances of VLTI instruments with NAOMI are detailed in Woillez et al. (2019).

Operations

NAOMI is now fully integrated in the operation of the VLTI. A typical observing night always follows the same procedure: two hours before sunset, the VLTI start-up procedure is launched, the functionalities of each subsystem are automatically verified, and the optical path is validated up to the InfraRed Imaging Sensor (IRIS; Gitton, 2004) in the VLTI Laboratory — allowing the verification of the alignment of the pupil and of the field. After twilight, the first preset on the selected target can be launched by the instrument. The sky coordinates are sent to the VLTI which propagates them to each AT.

NAOMI has a specific acquisition procedure called discoball to detect any object within 22.4 arcseconds. This permits precise centring of the AT in the 6-arcsecond acquisition field of view of NAOMI and subsequent closing of the loop. The field of view in the closed loop is 2.25 arcseconds. The full process between the launch of the preset and the closed loop is automatic, requiring approximately 140 seconds. A manual procedure can be used for very specific targets, such as a close binary. At the end of the night, the NAOMI system is automatically re-checked while the ATs are being closed and set in standby mode for the day. The day team then checks the calibration data and applies any corrections that may be needed before the next VLTI start up.

All the telescopes used by the VLTI are now in operation with adaptive optics systems as recommended by Pierre Léna (Léna, 1987) and Jacques Maurice Beckers (Beckers, 1990); we remain indebted to them for their vision.

References

Arsenault, R. et al. 2003, The Messenger, 112, 7
Arsenault, R. et al. 2017, The Messenger, 168, 8
Beckers, J. M. et al. 1990, The Messenger, 60, 1
Bonaccini, D. et al. 1997, Proc. SPIE, 3126, 77
Gitton, P. et al. 2004, Proc. SPIE, 5491, 944
Gravity Collaboration 2017, The Messenger, 170, 10
Haguenauer, P. & Guieu, S. 2019, Proc. AO4ELT conference, in press
Koehler, B. et al. 2004, The Messenger, 115, 15
Koehler, B. et al. 2002, The Messenger, 110, 21
Le Bouquin, J. B. et al. 2018, Proc. SPIE, 1070371
Léna, P. 1987, The Messenger, 50, 53
Lopez, B. et al. 2014, The Messenger, 157, 5
Scheithauer, S. et al. 2016, Proc. SPIE, 9909, 99092L
Suárez Valles, M. 2012, Proc. SPIE, 8447, 84472Q
Woillez, J. et al. 2015, The Messenger, 162, 18
Woillez, J. et al. 2019, A&A, 629, A41
Zins, G. et al. 2011, The Messenger, 146, 12

Links

[1] Adaptive Optics for Extremely Large Telescopes Conference (A04ELT) held in Québec City, Canada in June 2019: http://ao4elt6.copl.ulaval.ca/

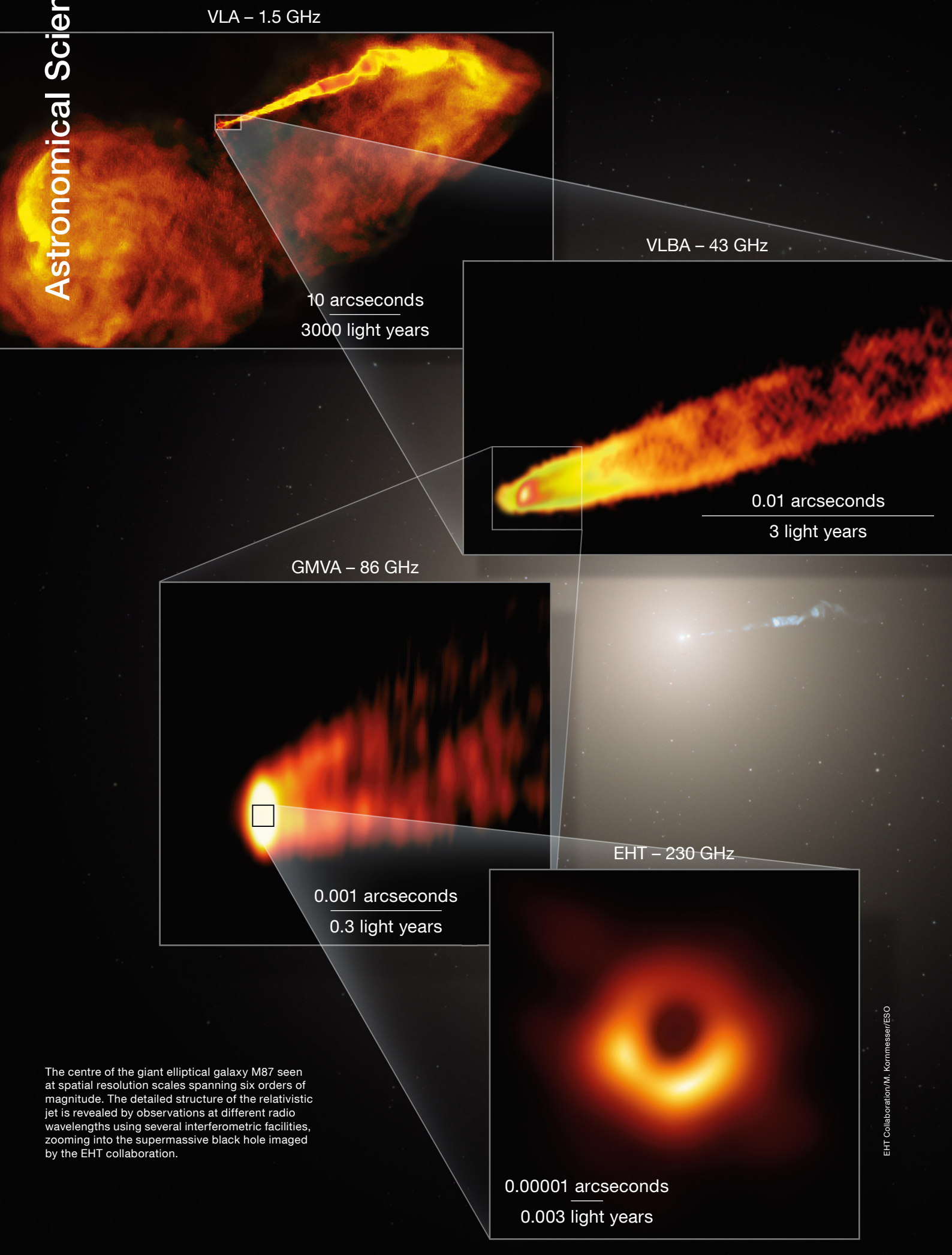

The centre of the giant elliptical galaxy M87 seen at spatial resolution scales spanning six orders of magnitude. The detailed structure of the relativistic jet is revealed by observations at different radio wavelengths using several interferometric facilities, zooming into the supermassive black hole imaged by the EHT collaboration.

EHT Collaboration/M. Kornmesser/ESO

DOI: 10.18727/0722-6691/5150

First M87 Event Horizon Telescope Results and the Role of ALMA

Ciriaco Goddi[1,2]
Geoff Crew[3]
Violette Impellizzeri[4]
Iván Martí-Vidal[5,6]
Lynn D. Matthews[3]
Hugo Messias[4]
Helge Rottmann[7]
Walter Alef[7]
Lindy Blackburn[8]
Thomas Bronzwaer[1]
Chi-Kwan Chan[9]
Jordy Davelaar[1]
Roger Deane[10]
Jason Dexter[11]
Shep Doeleman[8]
Heino Falcke[1]
Vincent L. Fish[3]
Raquel Fraga-Encinas[1]
Christian M. Fromm[12]
Ruben Herrero-Illana[18]
Sara Issaoun[1]
David James[8]
Michael Janssen[1]
Michael Kramer[7]
Thomas P. Krichbaum[7]
Mariafelicia De Laurentis[19,20]
Elisabetta Liuzzo[21]
Yosuke Mizuno[12]
Monika Moscibrodzka[1]
Iniyan Natarajan[10]
Oliver Porth[14]
Luciano Rezzolla[12]
Kazi Rygl[21]
Freek Roelofs[1]
Eduardo Ros[7]
Alan L. Roy[7]
Lijing Shao[17,7]
Huib Jan van Langevelde[13,2]
Ilse van Bemmel[13]
Remo Tilanus[1,2]
Pablo Torne[15,7]
Maciek Wielgus[8]
Ziri Younsi[16,12]
J. Anton Zensus[7]
on behalf of the Event Horizon Telescope collaboration

[1] Department of Astrophysics, Institute for Mathematics, Astrophysics and Particle Physics (IMAPP), Radboud University, Nijmegen, the Netherlands
[2] Leiden Observatory—Allegro, Leiden University, Leiden, the Netherlands
[3] Massachusetts Institute of Technology Haystack Observatory, Westford, USA
[4] Joint ALMA Observatory, Vitacura, Santiago de Chile, Chile
[5] Onsala Space Observatory, Chalmers University of Technology, Sweden
[6] Department of Astronomy and Astrophysics/Astronomical Observatory, University of Valencia, Spain
[7] Max-Planck-Institut für Radioastronomie (MPIfR), Bonn, Germany
[8] Center for Astrophysics | Harvard & Smithsonian, Cambridge, USA
[9] Steward Observatory and Department of Astronomy, University of Arizona Tucson, USA
[10] Centre for Radio Astronomy Techniques and Technologies, Department of Physics and Electronics, Rhodes University, Grahamstown, South Africa
[11] Max-Planck-Institut für Extraterrestrische Physik, Garching, Germany
[12] Institut für Theoretische Physik, Goethe Universität, Frankfurt am Main, Germany
[13] Joint Institute for VLBI ERIC (JIVE), Dwingeloo, the Netherlands
[14] Anton Pannekoek Institute for Astronomy, University of Amsterdam, the Netherlands
[15] Instituto de Radioastronomía Milimétrica, IRAM, Granada, Spain
[16] Mullard Space Science Laboratory, University College London, Dorking, UK
[17] Kavli Institute for Astronomy and Astrophysics, Peking University, Beijing, China
[18] ESO
[19] Dipartimento di Fisica “E. Pancini,” Universitá di Napoli “Federico II”, Naples, Italy
[20] INFN Sez. di Napoli, Compl. Univ. di Monte S. Angelo, Naples, Italy
[21] INAF–Istituto di Radioastronomia, Bologna, Italy

In April 2019, the Event Horizon Telescope (EHT) collaboration revealed the first image of the candidate supermassive black hole (SMBH) at the centre of the giant elliptical galaxy Messier 87 (M87). This event-horizon-scale image shows a ring of glowing plasma with a dark patch at the centre, which is interpreted as the shadow of the black hole. This breakthrough result, which represents a powerful confirmation of Einstein’s theory of gravity, or general relativity, was made possible by assembling a global network of radio telescopes operating at millimetre wavelengths that for the first time included the Atacama Large Millimeter/submillimeter Array (ALMA). The addition of ALMA as an anchor station has enabled a giant leap forward by increasing the sensitivity limits of the EHT by an order of magnitude, effectively turning it into an imaging array. The published image demonstrates that it is now possible to directly study the event horizon shadows of SMBHs via electromagnetic radiation, thereby transforming this elusive frontier from a mathematical concept into an astrophysical reality. The expansion of the array over the next few years will include new stations on different continents — and eventually satellites in space. This will provide progressively sharper and higher-fidelity images of SMBH candidates, and potentially even movies of the hot plasma orbiting around SMBHs. These improvements will shed light on the processes of black hole accretion and jet formation on event-horizon scales, thereby enabling more precise tests of general relativity in the truly strong field regime.

Supermassive black holes and their shadows: a fundamental prediction of general relativity

Black holes are perhaps the most fundamental and striking prediction of Einstein’s General Theory of Relativity (GR), and are at the heart of fundamental questions attempting to unify GR and quantum mechanics. Despite their importance, they remain one of the least tested concepts in GR. Since the 1970s, astronomers have been accumulating indirect evidence for the existence of black holes by studying the effects of their gravitational interaction with their surrounding environment. The first such evidence came from the prototypical high-mass X-ray binary Cygnus X-1, where a star orbits an unseen compact object of ~ 15 solar masses, apparently feeding on material from its stellar companion at only 0.2 au. More evidence has come from studies of the Galactic Centre, where ~ 30 stars have been tracked in tight, fast orbits (up to 10 000 km s^{-1}) around a radio point source named Sagittarius A* or Sgr A* (Gillessen et al., 2009), practically ruling out all mechanisms

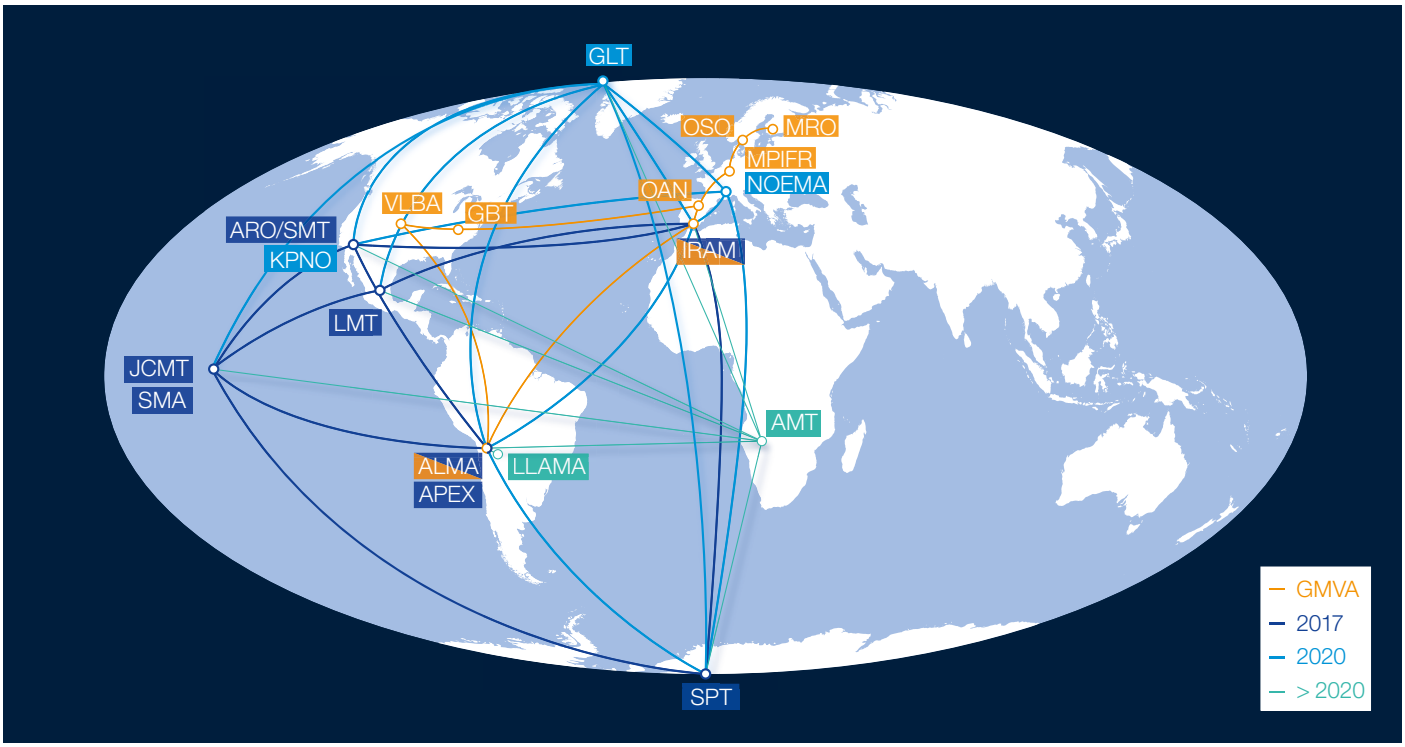

Figure 1. Locations of the participating telescopes of the Event Horizon Telescope (EHT; shown in blue) and the Global mm-VLBI Array (GMVA; shown in yellow) during the 2017 global VLBI campaign. Additional telescopes that will observe in 2020 are shown in light blue; the GLT also joined in the campaign conducted in 2018. Planned telescopes that may join the EHT in the future are shown in green.

responsible for their motions, except for a black hole with a mass of about four million solar masses.

Perhaps the most compelling evidence came in 2015, with the detection by the advanced Laser Interferometer Gravitational-Wave Observatory (LIGO) of gravitational waves: ripples in space-time produced by the merger of two stellar-mass black holes (Abbot et al., 2016). Despite this breakthrough discovery, there was until very recently no direct evidence for the existence of an event horizon, the defining feature of a black hole and a one-way causal boundary in spacetime from which nothing (including photons) can escape. On 10 April 2019, the EHT provided the very first resolved images of a black hole, demonstrating that they are now observable astrophysical objects and opening a new and previously near-unimaginable window onto black hole studies.

In order to conduct tests of GR using astrophysical black holes, it is crucial to observationally resolve the gravitational sphere of influence of the black hole, down to scales comparable to its event horizon. For a non-rotating black hole, the radius of the event horizon is equal to its Schwarzschild radius:
$R_{Sch} = 2\ GM_{BH}/c^2 = 2\ r_g$,
where r_g is the gravitational radius, M_{BH} is the black hole mass, G is the gravitational constant, and c is the speed of light. The angular size, subtended by a non-rotating BH with diameter 2 R_{Sch} is:
$\theta_{Sch} = 2\ R_{Sch}/D \approx 40\ (M_{BH}/10^6\ M_\odot)$(kpc/$D$)
in microarcseconds (μas), where the black-hole mass is expressed in units of one million solar masses and the black hole's distance (D) is in kiloparsecs. For stellar-mass black holes (with masses of a few to tens of solar masses), θ_{Sch} lies well below the resolving power of any current telescope. SMBHs, which are thought to reside at the centre of most galaxies, are millions to billions of times the mass of the Sun, but as they are located at much greater distances, their apparent angular sizes are also generally too small to be resolved using conventional observing techniques. Fortunately, there are two notable exceptions: Sgr A* and the nucleus of M87.

Sgr A* and the nucleus of M87: the "largest" black hole shadows in our sky

Sgr A*, at the centre of our own Galaxy, hosts the closest and best constrained candidate SMBH in the Universe. With a mass of 4.15 million solar masses and at a distance of 26 400 light years or 8.1 kpc (Gravity collaboration et al., 2019), this SMBH is a factor of a million times larger than any stellar mass black hole in the Galaxy and at least a thousand times closer than any other SMBH in other galaxies. The second-best candidate is found in the nucleus of the giant elliptical galaxy M87, the largest and most massive galaxy within the local supercluster of galaxies in the constellation of Virgo. Located 55 million light years from the Earth (or 16.8 Mpc), it hosts a black hole of 6.5 billion solar masses. Therefore, even though M87 is ~ 2000 times as distant, it is ~ 1500 times as massive as Sgr A*, yielding a (slightly) smaller but comparable angular size of the black hole shadow on the sky. Owing to the combination of their masses and proximity, both Sgr A* and the nucleus of M87 subtend the largest angular size on the sky

among all known SMBHs ($\theta_{Sch} \approx 20$ and 15 μas, respectively). This makes Sgr A* and M87 the two most suitable sources for studying the accretion process and jet formation in SMBHs, even enabling tests of GR at horizon-scale resolution.

The "shadow" of a black hole

Although by definition black holes cannot be seen, we can detect light which passes very close to the event horizon before escaping, allowing us to see what is around the black hole.

So what would a black hole actually look like if we could observe it? David Hilbert began calculating the bending of light around a Schwarzschild (non-rotating) black hole in 1917. Bardeen (1973) subsequently calculated the geometrical properties of a rotating black hole's silhouette against a bright background (an orbiting star). Although the likelihood of a black hole passing in front of a star is very small, black holes never appear "naked" in astrophysical environments since their extreme gravitational fields will pull and compress matter from their surroundings, eventually forming a disc of luminous plasma. Luminet (1979) performed simulations of a black hole surrounded by a geometrically thin, optically thick, accretion disc. Falcke, Melia and Agol (2000) demonstrated that an accreting black hole embedded in a plasma that is optically thin at millimetre wavelengths (like the plasma expected to surround Sgr A*) would produce a bright ring of emission with a dim "shadow" cast by the black hole event horizon in its interior. They suggested that such a shadow might be detectable towards the Galactic Centre using the technique of very long baseline interferometry (VLBI) at millimetre wavelengths[a].

The shadow and ring are caused by a combination of light bending and photon capture at the event horizon. The size scale of the emission ring is set by the photon capture radius R_c. For a non-rotating Schwarzschild black hole, $R_c = \sqrt{27}\, r_g \sim 2.5\, R_{Sch}$. The factor of ~ 2.5 comes from gravitational lensing, which increases the radius of the photon ring with respect to the Schwarzschild radius as seen from the observer, resulting in an angular diameter on the sky of ~ 50 and ~ 40 μas (as viewed from the Earth) for Sgr A* and M87, respectively. Although very small, this angular size can now be resolved by the VLBI technique at millimetre wavelengths using the EHT.

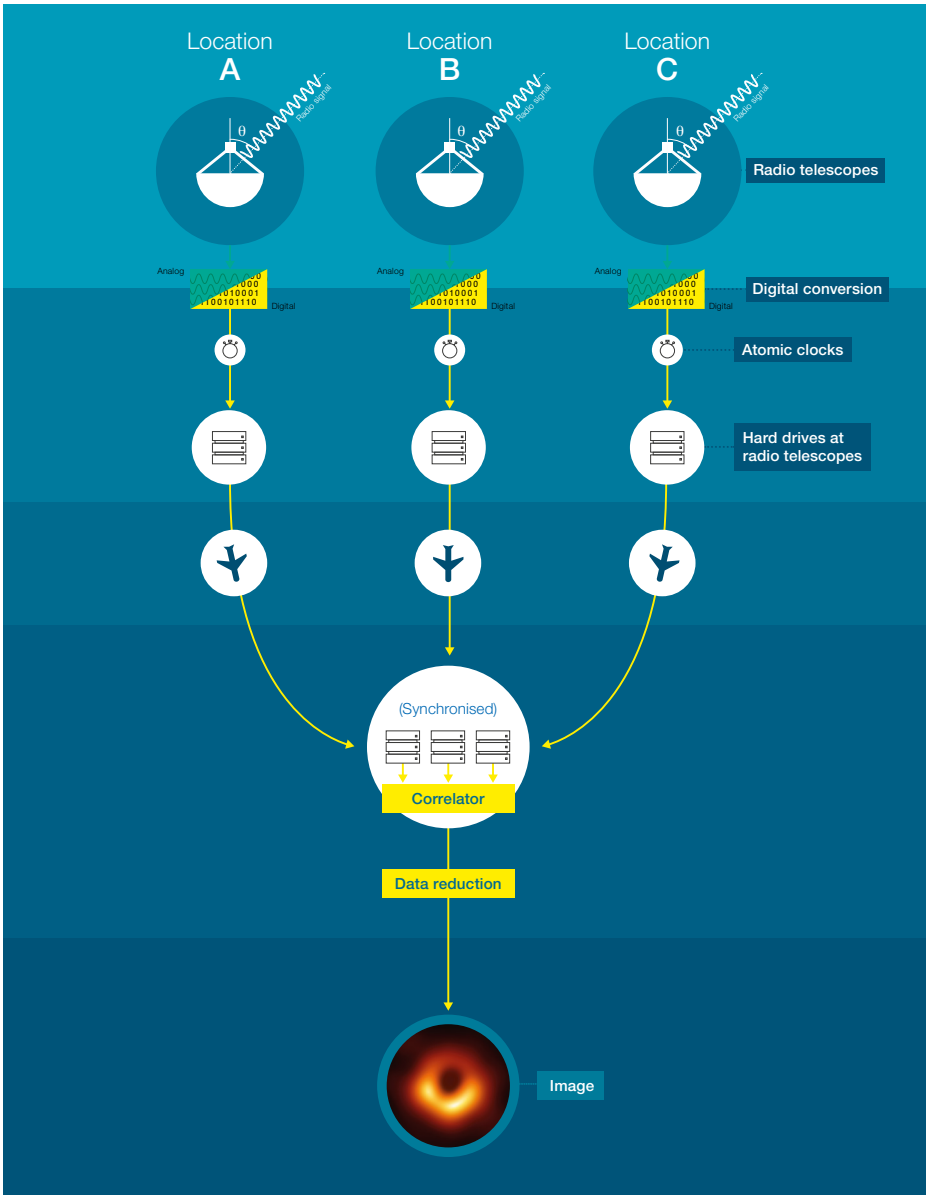

ALMA (ESO/NAOJ/NRAO), J. Pinto & N. Lira

Figure 2. A schematic diagram of the VLBI technique. Radio wave signals collected by individual antennas are converted from analogue to digital and recorded onto hard disks together with the time-stamps provided by extremely precise atomic clocks at each station. In the 2017 campaign, a total of about 4000 TB of recorded data was obtained. The data were shipped from each station to a central location where a supercomputer (the correlator) combined the signals between all pairs of antennas (synchronised using the timing information at each station). The output of the correlator is hundreds of gigabytes, which is further reduced during data calibration down to tens to hundreds of megabytes. The end product of the VLBI data processing is an astronomical image.

Imaging black holes with the Event Horizon Telescope (EHT)

The VLBI technique at millimetre wavelengths

For VLBI to work, a network of radio telescopes spread across different continents (see, for example, Figure 1) must observe the same source at exactly the same time

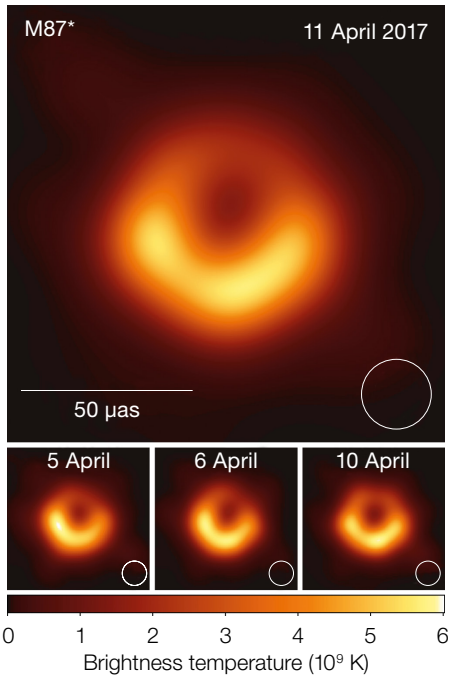

Figure 3. Image of the supermassive black hole M87* as obtained with the EHT (on four different days) in April 2017. Top panel: EHT image of M87* from observations on 11 April as a representative example of the images collected during the 2017 campaign. The angular resolution of the observation (20 μas) is shown in the lower right corner. The image is shown in units of brightness temperature. North is up and east is to the left. Bottom panels: similar images taken on different days showing the stability of the ring structure across the observing week.

and in the same frequency band. Individual antennas record their signals (plus time stamps from very precise atomic clocks) onto computer hard disks which are then shipped to a central location, where a supercomputer (called a correlator) combines (cross-correlates) the signals between all pairs of antennas, synchronising them using the recorded timing information from each station. Figure 2 is a diagram illustrating the data acquisition and processing path in a VLBI experiment.

The achievable angular resolution for an interferometer is given by $\theta \sim \lambda/B$ (in radians), where λ is the observed wavelength and B is the maximum distance between the telescopes (or baseline). Hence, higher frequencies (shorter wavelengths) and longer baselines provide the highest resolving power. At 1.3 mm (corresponding to a radio frequency of 230 GHz), Earth-diameter VLBI baselines achieve an angular resolution as fine as 20 μas, which is sufficient to resolve the shadow of both Sgr A* and M87. Therefore, the VLBI technique effectively mimics a virtual telescope with the size of the Earth.

While VLBI is well-established at centimetre wavelengths, its extension to wavelengths as short as 1.3 mm only began in the 1990s (for example, Padin et al., 1990; Krichbaum et al., 1997; Doeleman & Krichbaum, 1999). Challenges at shorter wavelengths include the reduced aperture efficiency and small diameter of radiotelescopes, increased noise in radio receiver electronics, higher atmospheric opacity, and above all, stronger distortion effects on the wavefronts from water vapour in the troposphere, which limits the phase coherence to only a few seconds. By 2003, several active galactic nuclei (AGN) had been detected on intercontinental baselines between Pico Veleta (Spain) and the Heinrich Hertz Telescope (HHT – Arizona, USA) at wavelengths of both 1 and 2 mm (Krichbaum et al., 2004; Doeleman et al., 2005).

Formation of the EHT project

Early pathfinder experiments (Krichbaum et al., 1998) detected Sgr A* with the baseline between Pico Veleta and the Plateau de Bure Interferometer, but the resolution was insufficient to probe horizon scales. In the mid-2000s, a focused effort to boost sensitivity through increased bandwidth led to the development of fully digital VLBI backends, with the goal of intercontinental 1.3-mm VLBI of Sgr A*. These systems were deployed at sites in Arizona, California, and Hawai'i, and event-horizon-scale structures were detected in both Sgr A* and M87 (Doeleman et al., 2008, 2012). These precursory scientific results motivated a strategy aimed at building a global 1.3-mm VLBI array capable of imaging the shadows of the SMBHs in both Sgr A* and M87, and spurred on the formation of the EHT project, which was proposed during the US 2010 Decadal Survey (Doeleman et al., 2009a)[b].

Since then, the EHT collaboration (or EHTC)[1] has grown to include over 250 members representing ~ 60 institutes, operating in over 20 countries/regions. The key elements of the roadmap towards an imaging array were the addition of new sites to better sample the Fourier plane, and the improvement in sensitivity needed to detect weak signals on short timescales (Doeleman et al., 2010). Two technological developments were crucial for the latter: (1) improvement in the observing bandwidth by increasing recording rates — over the last 10 years, EHT data rates increased from 4 to 64 Gb per second (Gbps); and (2) development of phased-array systems to combine the collecting area of existing connected-element (sub)millimetre interferometers, which has led to the inclusion in the EHT of ALMA and the Submillimeter Array (SMA) and the future incorporation of the NOrthern Extended Millimeter Array (NOEMA).

Phasing ALMA: turning ALMA into a giant single-dish VLBI station

ALMA is the most sensitive (sub)millimetre-wavelength telescope ever built. It consists of 54 12-metre and 12 7-metre antennas located on the Chajnantor plateau in the Atacama desert in Chile, the highest, driest (accessible) desert on the Earth, and it ordinarily operates as a connected-element interferometer. Although the implementation of a VLBI mode was not part of the baseline project, the desirability of phasing the entire array for VLBI had been recognised (Wright et al., 2001; Shaver, 2003) and some of the architecture needed to sum signals from all ALMA antennas was built into the ALMA correlator (Escoffier et al., 2007).

Motivated by the prospect of using ALMA for horizon-scale observations of supermassive black holes (Doeleman et al., 2009a, 2010), the case for phasing ALMA was renewed. An international team, led by Doeleman at MIT Haystack Observatory, proposed an ALMA Phasing Project (APP) to the US National Science Foundation. The APP was accepted by the ALMA Board in 2011 and was completed in 2018 thanks to an international effort with contributors from the USA, Europe, and Asia.

The heart of the APP is a beamformer system, which electronically combines

the collecting area of ALMA by aligning the signals from individual ALMA antennas in phase to form a coherent sum signal. Currently, up to 43 12-metre antennas are used for the phased array, but the number may be smaller depending on the array configuration and the weather conditions. This effectively turns ALMA into a giant virtual single dish (hereinafter called "phased ALMA"), and is equivalent to adding a ~ 70-metre dish to existing mm-VLBI arrays. In order to phase ALMA successfully and incorporate it as a VLBI station, the APP had to add several new hardware and software components. These included an optical fibre link system to transport the phased-sum signal from the ALMA Array Operations Site (at an altitude of 5100 m) to the ALMA Operations Support Facility (at 2900 m), where a set of Mark 6 VLBI recorders was installed. ALMA's original rubidium clock was replaced with a more precise hydrogen maser (required to properly tune and synchronise the signals in the VLBI array). Numerous software enhancements were also required, including the implementation of an ALMA VLBI Observing Mode (VOM) and a phase solver to adjust the phase of each of the ALMA antennas during observations to allow coherent summation of their signals. The initial scope of the APP effort and implementation can be found in Doeleman et al. (2010); the final working implementation is described in Matthews et al. (2018) and Goddi et al. (2019).

A broad science case for the use of the ALMA Phasing System was assembled by the international community in white papers[c] (Fish et al., 2013; Tilanus et al., 2014). Starting in 2016, VLBI as an observing mode was made available to the astronomy community through the normal ALMA proposal system, with an

Figure 4. The supermassive black hole at the centre of M87. Left: The black hole feeds on a swirling disc of glowing plasma (shown in red), driving a powerful relativistic jet across several thousands of light years (shown in grey; simulation by Davelaar et al. 2018). Bottom right: Approaching the black hole, gravity is so strong that light is severely bent, creating a bright (almost circular) ring. The north–south asymmetry in the emission ring is produced by relativistic beaming and Doppler boosting (matter in the bottom part of the image is moving toward the observer) and is mediated by the black hole spin (which is pointing away from Earth and rotating clockwise). Gravitational lensing magnifies the apparent size of the black hole's event horizon into a larger dark shadow. The emission between the photon ring and the event horizon is due to emitting plasma either in the accretion flow and/or at the footprint of the jet (this emission is generally too dim to be detected by the EHT; see Younsi et al., in preparation for detail). Top right: While the EHT can zoom in very close to the event horizon, down to scales of only 0.01 light years (or 3.7 light days), i.e., a region comparable to the size of our Solar System, the relativistic jet (extended across several thousand light years) can be probed using ALMA intra-baselines, recorded during the EHT observations (greyscale image; Goddi et al. 2019 and in prep.).

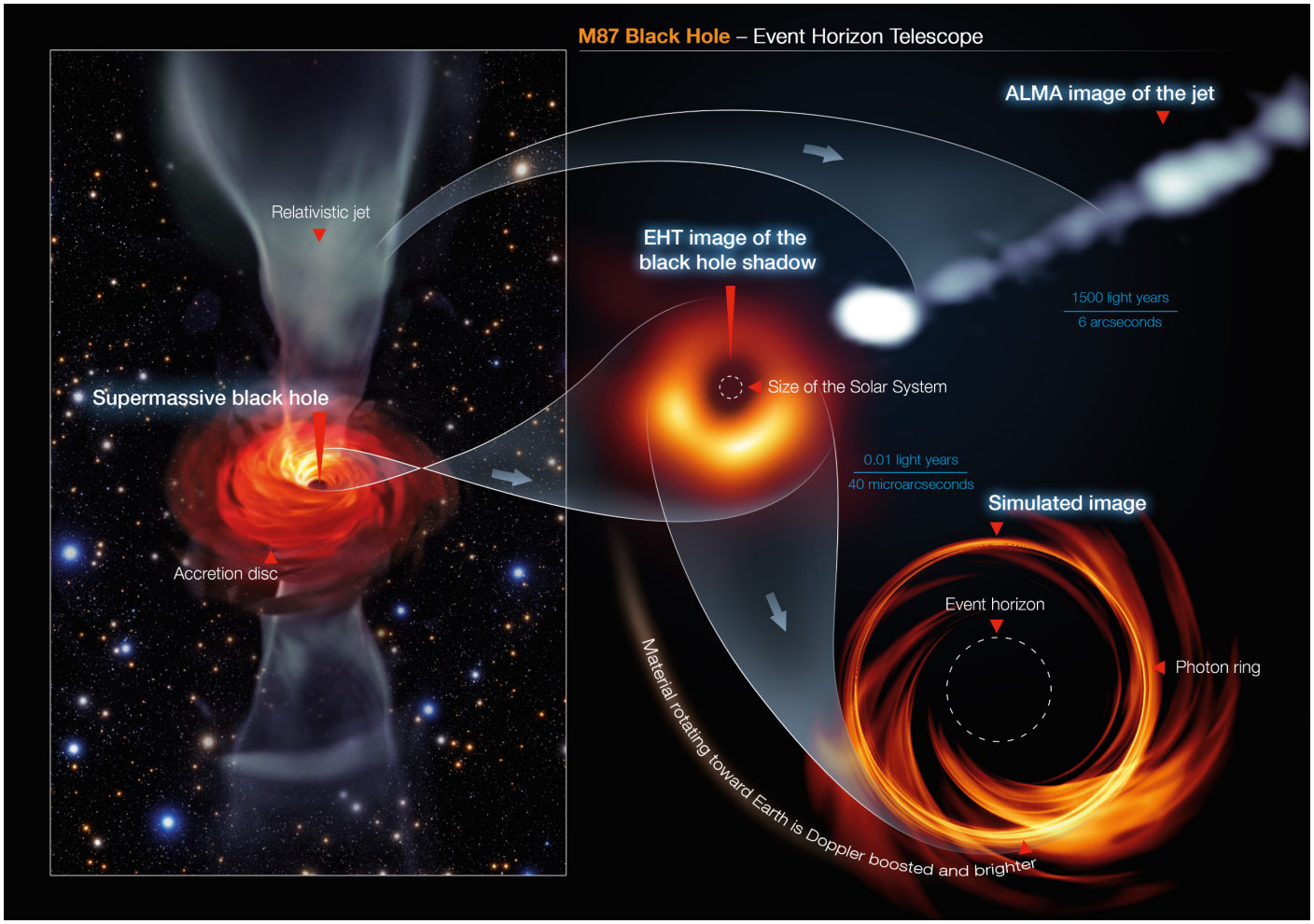

C. Goddi, Z. Younsi, J. Davelaar/M.Kornmesser/ESO

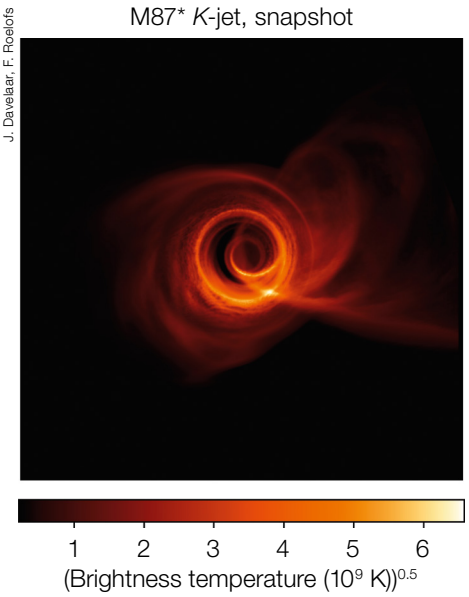

Figure 5. Black hole model for M87* used for the image reconstructions shown in Figure 6. This specific model has a relatively bright jet footprint appearing in front of the photon ring and a more extended jet emission extending towards west. Note the bright knot to the south-west at the point where the jet sheath crosses the photon ring in projection (see Davelaar et al., 2019).

expected maximum time allocation of ~ 5 % of the total ALMA observing time.

Impact of ALMA in the EHT array

Owing to the combination of a large effective aperture, its central location in the VLBI array, excellent typical atmospheric conditions and ultra-low noise receivers, the addition of ALMA drastically changed the overall capabilities of the global EHT array, boosting the achievable signal-to-noise ratio (SNR) of VLBI baselines by more than an order of magnitude with respect to the first horizon-scale detections (Doeleman at al., 2008, 2012). More specifically, the inclusion of ALMA in the EHT provides three key advantages: a boost in sensitivity; improved baseline coverage; and an accurate measurement of the absolute flux-density scale and polarisation fractions of EHT targets (using standard ALMA interferometric data). We expand on these characteristics below.

I. The median thermal noise of non-ALMA baselines is 7 mJy, and 0.7 mJy in ALMA baselines; for M87 this corresponds to SNR > 10 on non-ALMA baselines and > 100 on ALMA baselines. Therefore, the addition of ALMA into the EHT array greatly facilitates detections, especially for weak signals (for example, long baseline length or bad weather). Using ALMA as a highly sensitive reference station has enabled critical corrections for ionospheric and tropospheric distortions at the other EHT sites (see EHTC et al., 2019c for details).
II. ALMA has a central location in the EHT array (see Figure 1), and is therefore essential for the baseline coverage and image fidelity. Even though ALMA and the Atacama Pathfinder Experiment (APEX) are extremely close geographically, ALMA's superior sensitivity allows the EHT to detect signals with the required 10-second integration times between all baselines, i.e., to find VLBI fringe solutions, which has a dramatic impact on the imaging capability of the EHT (see Figure 6).
III. VLBI observations with ALMA also provide connected-element interferometric data, which are archived, as with any standard ALMA project, and are available to the user in the ALMA archive (after the appropriate proprietary period). As outlined in Goddi et al. (2019), the calibration of such interferometric data allows one to determine the absolute amplitude calibration of the co-located sites ALMA–APEX in physical flux-density (i.e, Jy). This, in turn, allows us to bootstrap source fluxes and calibrate longer baselines across the entire array (i.e., network calibration). In addition, since VLBI observations are always performed in full-polarisation mode (in order to supply input to the polarisation conversion process at the VLBI correlators — see Martí-Vidal et al., 2016; Goddi et al., 2019), the ALMA full-polarisation interferometric datasets can be used to derive mm-wavelength emission and polarisation properties of each target observed by the EHT on arcsecond scales (Goddi et al., in preparation).

The first global VLBI campaigns with ALMA

Phased ALMA joined the EHT array for the first time in April 2017, performing VLBI observations with an array capable of imaging its key science targets. The global array included eight telescopes in six different geographical sites: the South Pole Telescope (SPT), the Arizona Radio Observatory's Submillimeter Telescope (SMT), the Large Millimeter Telescope Alfonso Serrano (LMT) in Mexico, the IRAM 30-metre telescope in Spain, the SMA and the James Clerk Maxwell Telescope (JCMT) in Hawai'i, and APEX and ALMA in Chile. These telescopes provided baseline lengths up to 10 700 km towards M87, resulting in an array with a resolution of ~ 20 μas (details are provided in EHTC et al., 2019b).

Besides the EHT, which operates at a wavelength of 1.3 mm (i.e., a frequency of 230 GHz, ALMA Band 6), complementary VLBI observations with ALMA were also conducted at 3.5 mm or 86 GHz (ALMA Band 3) in concert with the Global mm-VLBI Array (GMVA)[3], which consists of up to 18 telescopes located in Europe, North America, and Asia. Figure 1 displays the geographical locations of all the participating telescopes in the EHT and the GMVA in 2017 (plus additional telescopes that joined after or plan to join in the near future).

The EHT 2017 science observing campaign was scheduled for April when Sgr A* and M87 are night-time sources and tropospheric conditions tend to be the best, averaged over all sites in the array. At that time, ALMA was in a more compact configuration as required for phased array operations. About 40 EHT astronomers travelled to four continents

Figure 6. Image reconstructions from synthetic data generated using the M87* model displayed in Figure 5 as input. Each panel shows a reconstruction from simulated observations with a different array: 2017 EHT array (left column); planned 2020 array (middle column); and a future EHT array including AMT in Namibia, and LLAMA in Argentina (right column). A comparison between the top row (with ALMA) and the middle row (without ALMA) highlights the importance of ALMA, demonstrating that the shadow feature can only be recovered if ALMA is part of the array. A comparison between the middle row and the bottom row (where APEX is also excluded) clearly demonstrates that, even with a single-dish telescope in the same geographical location of ALMA, it is not possible to recover an image with sufficiently high fidelity to discern the shadow. Although with future arrays the quality of the reconstructed image will improve and it will be possible to recover new features (for example, the jet), the addition of new stations cannot fully compensate for the loss of ALMA (middle and right columns).

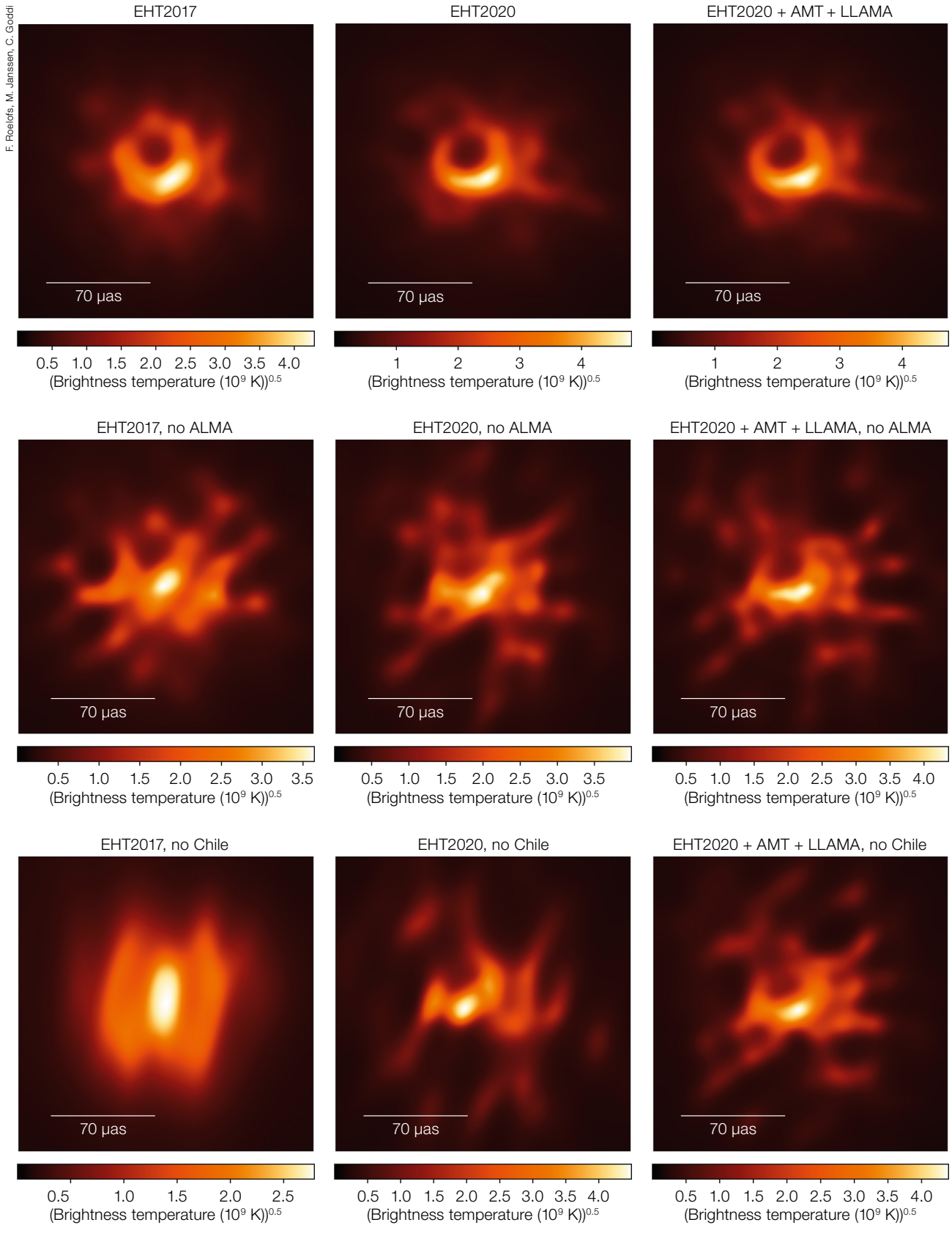
F. Roelofs, M. Janssen, C. Goddi
EHT2017
EHT2020
EHT2020 + AMT + LLAMA
70 μas
70 μas
70 μas
0.5 1.0 1.5 2.0 2.5 3.0 3.5 4.0
1 2 3 4
1 2 3 4
(Brightness temperature (10^9 K))^0.5
EHT2017, no ALMA
EHT2020, no ALMA
EHT2020 + AMT + LLAMA, no ALMA
70 μas
70 μas
70 μas
0.5 1.0 1.5 2.0 2.5 3.0 3.5
0.5 1.0 1.5 2.0 2.5 3.0 3.5
0.5 1.0 1.5 2.0 2.5 3.0 3.5 4.0
(Brightness temperature (10^9 K))^0.5
EHT2017, no Chile
EHT2020, no Chile
EHT2020 + AMT + LLAMA, no Chile
70 μas
70 μas
70 μas
0.5 1.0 1.5 2.0 2.5
0.5 1.0 1.5 2.0 2.5 3.0 3.5 4.0
0.5 1.0 1.5 2.0 2.5 3.0 3.5 4.0
(Brightness temperature (10^9 K))^0.5

and drove to mountaintops to carry out the observations, which included six science targets: the primary EHT targets, Sgr A* and M87, and the AGN targets, 3C 279, OJ 287, Centaurus A, and NGC 1052[d]. Weather is a crucial factor for VLBI observations at mm wavelengths, which is why the EHT uses flexible observing schedules with windows that are about twice as long as the approved number of observing nights. An array-wide go/no-go decision was made a few hours before the start of each observing night, based on the weather conditions and predictions at each site, as well as technical readiness at each of the participating telescopes. Observations were triggered over a 10-night window 5–14 April 2017 — on 5, 6, 7, 10, and 11 April. During the whole campaign, the weather was good to excellent at most stations. In addition to favourable weather conditions, the VLBI-specific technical setup and operations at all sites were successful, which resulted in fringe detections across the entire array.

By the end of the campaign, 96 disk modules were used, each containing eight helium-filled hard disks (of either six or eight terabyte [TB] capacity), corresponding to more than 5 petabytes (PB) of (removable) storage; about 4 PB of data were eventually recorded in total. Given this huge volume of data, the observing campaign VLBI data could not be transferred over the internet, but were shipped from each remote station to the two EHT correlator centres for processing (the shipping took at least several days, and many months in the case of the South Pole telescope).

Path to the image

The EHT data were correlated at the MIT Haystack Observatory in Westford, USA and at the MPIfR in Bonn, Germany. Three independent data calibration pipelines and three imaging pipelines, each using a different software package and associated methodology, were used for the data processing in order to produce images independently. This approach encourages the data analysis and science teams to minimise their biases in terms of both methodology and human decision making; further details of this are provided in EHTC et al. (2019c,d). Multiple independent analyses were also performed in order to verify the results (EHTC et al., 2019e,f). After about two years of dedicated work by many dozens of EHT scientists in multiple working groups (from instrument through data processing to theory), the collaboration was finally ready to communicate our breakthrough to the world.

The breakthrough: first image of a black hole shadow

The first image of a black hole was published by the EHT Collaboration on 10 April 2019 in a series of six scientific publications (EHTC et al., 2019a,b,c,d,e,f). The announcement and the historic image were released worldwide in six simultaneous press conferences — in Washington, Brussels, Santiago, Shanghai, Taipei and Tokyo — with additional satellite events in Rome, Madrid, Munich, Leiden and Nijmegen, amongst others. The core of M87, as imaged with the EHT, was renamed M87*, in line with the name of the black hole candidate at the centre of the Galaxy, Sgr A*.

The most striking feature of the image (displayed in Figure 3) is a bright circular ring with an asymmetric brightness distribution and a dark region at its centre, which identifies the black hole shadow. The ring reveals the curvature of spacetime due to the extreme gravitational field around a SMBH, which bends light around it, creating an almost circular shadow at its centre. In fact, GR predicts the shadow to be circular to within a few percent, whereas alternative theories of gravity predict distorted, non-circular shapes (Younsi et al., 2016; also see Figure 7 of Goddi et al., 2017).

The ring has a measured diameter of 42 ± 3 μas and the central brightness depression has a contrast ratio > 10:1. The measured angular size, assuming a distance of 16.8 Mpc (EHTC et al., 2019f), implies a black hole mass of $M = (6.5 \pm 0.7) \times 10^9\ M_\odot$, or 6.5 billion times the mass of the Sun (consistent with one earlier mass measurement — Gebhardt et al., 2011). To convert the measured diameter of the ring into the mass of the black hole, the radiating plasma around the black hole was modelled with general relativistic calculations spanning a wide range of possible accretion states (see next subsection). By tracing the peak of the emission in the ring we can determine the shape of the image, which is close to circular with an axial ratio 4:3 (corresponding to a 10% deviation from circularity). The emission in the ring is asymmetric and is brighter in the south, which can be explained as relativistic beaming of plasma rotating (close to the speed of light) in the clockwise direction around the black hole as seen by the observer (i.e., the bottom part of the emission ring is Doppler-boosted towards the Earth). Based on our modelling and information on the inclination angle of the relativistic jet (observed on larger scales), we derive the sense of rotation of the black hole to be in the clockwise direction, i.e., the spin axis of the black hole points away from us.

A number of elements reinforce the robustness of the result. The data analysis used four independent data sets taken on four different days (spanning a one-week observing window) in two separate frequency bands (centered at 227 and 229 GHz). The top part of Figure 3 shows an image of M87* on 11 April, while the bottom panels show similar images from three different days. The diameter and width of the ring remain stable and the image features are broadly consistent across all four observing days, except the position angle of the bright part in the asymmetric azimuthal profile, which varies in the range 150–200 degrees measured from north towards the east between the first two days and the last two days.

Overall, the size, circularity, asymmetry, and brightness contrast of the observed image are consistent with the shadow of a "Kerr" black hole as predicted by GR and provide the strongest evidence to date of the existence of SMBHs in the nuclei of external galaxies.

Modelling and physical interpretation of the black hole image

The appearance of M87* has been modelled using 3D general-relativistic magnetohydrodynamic (GRMHD) simulations, which provide the physical conditions of

the plasma and magnetic field surrounding the black hole. GR ray-tracing radiative-transfer (GRRT) codes then take this GRMHD simulation data as input and calculate the black hole's appearance from the emitted radiation field. Approximately 60 000 simulated images were produced in the process (see EHTC et al., 2019e). Figure 4 showcases the main components of the M87 SMBH and their characteristic scales by comparing observed and simulated images (for one specific set of models). In particular, in the simulation to the left (which combines emission at wavelengths of 7, 3, and 1 mm; see Davelaar et al., 2018 for details), one can see that the SMBH is embedded in an accretion flow and powers a bipolar relativistic jet.

Zooming in closer to the centre (the simulation to the right in Figure 4 shows emission at 1 mm; Younsi et al., in preparation), hot magnetised plasma orbiting and accreting onto the black hole creates the familiar emission ring structure around the event horizon. As stated earlier, the size of the ring is set by the photon capture radius: photons approaching the black hole with an impact parameter $b < R_c$ are captured and disappear into the black hole; photons with $b > R_c$ escape to infinity; photons with $b = R_c$ are captured on an unstable circular orbit and produce the so-called lensed photon ring.

While the EHT can resolve down to scales of 0.01 light years (or 3.7 light-days), i.e., a region comparable to the size of our Solar System, the jet extends to much larger scales across several thousand light years and can be probed using shorter baselines and/or lower frequencies. In Figure 4 (top right), we show an image of the M87 jet, which extends across about 20 arcseconds, corresponding to 5000 light years, obtained at 1.3 mm using ALMA interferometric data (with maximum baseline lengths of only a few hundred metres) acquired simultaneously with the EHT observations (Goddi et al., 2019 and in preparation). The science section image (p. 24) showcases a montage of images of the M87 relativistic jet observed at several radio wavelengths with multiple interferometers at progressively higher angular resolution overlaid on the HST optical image: the VLA at 21 cm, VLBA at 7 mm, GMVA at 3 mm, and EHT at 1.3 mm.

Implications of the black hole shadow on tests of GR and complementarity with LIGO

Simulated images can be used to test basic properties of black holes as predicted in GR (for example, Psaltis et al., 2015), or in alternative theories of gravity (Younsi et al., 2016; Mizuno et al., 2018). They can also be used to test alternatives to black holes (Olivares et al., 2019). We estimate a deviation from circularity of < 10 %, so we can set an initial limit on relative deviations from GR. Although it is difficult to rule out alternatives to black holes in GR — a shadow can be produced by any compact object with unstable circular photon orbits (Mizuno et al., 2018) — we can readily exclude exotic alternatives to black holes, such as naked singularities or wormholes, which predict much smaller shadows than we have measured, whereas others like boson stars and gravastars need to be analysed with more care (Olivares et al., 2019); also see EHTC et al. (2019e) for further details.

It is worth pointing out that the EHT result provides a new way to study black hole spacetimes and is complementary to the detection experiments of gravitational waves from merging stellar-mass black holes with LIGO/Virgo (Abbott et al., 2016). There are at least two main complementary aspects between gravitational-wave and electromagnetic observations of black holes:

1. Since EHT targets SMBHs and LIGO mainly targets stellar-mass black holes, combining measurements from both methods we can test whether one of the most fundamental properties of black holes in GR, that their size scales linearly with mass, actually holds over eight orders of magnitude.
2. Gravitational wave experiments cannot rely on the possibility of multiple and repeated measurements of the same source, whereas the EHT can be used to measure the shadow shape of M87 with ever increasing precision, leading to progressively better constraints on black hole parameters and their spacetime.

Importance of ALMA in imaging M87

The most straightforward way to visualise how the loss of specific stations changes the baseline coverage and sensitivity, thereby affecting the resulting images, is by performing simulated observations. Instrument simulators were specifically built for the EHT to tie theoretical models to instrument measurements. In particular, they can generate realistic synthetic data, taking as input GRMHD model images, and performing synthetic observations using a specific EHT array and observing schedule (see EHTC et al., 2019d,e). As a demonstration, in Figure 5 we show a GRMHD simulation of the jet-launching region of M87 from Davelaar et al. (2019). This specific model has a relatively bright jet footprint appearing in front of the photon ring and a more extended jet emission extending towards west. We can then test how well the input image (the ground truth) can be recovered with the current EHT array and analyse the effect of adding new stations and/or excluding existing stations.

Figure 6 shows some examples of reconstructed images of M87, using the model shown in Figure 5 as the input model, produced with one specific EHT synthetic data generation pipeline (details are reported in Roelofs, Janssen and EHTC, submitted). For instance, using the EHT array and schedule that observed on 11 April 2017, the resulting simulated image (shown in the left panel, top row of Figure 6) is similar to the one actually observed by the EHT. The middle and bottom rows show simulated images without ALMA, which best showcase its importance by clearly demonstrating that the familiar ring structure cannot be reconstructed when ALMA is not part of the array. Although APEX shares the same geographical location as ALMA and therefore should provide similar baseline coverage, the quality of the reconstructed image is not sufficient to discern the ring when APEX is in the array and ALMA is excluded. These simulations clearly substantiate the need for ALMA's sensitivity, which allows for numerous and strong detections of weak signal[e].

By adding new stations, the quality of the reconstructed image improves and new features (for example, the jet) can be recovered (see middle and right columns in the top row of Figure 6), but these new stations cannot fully compensate for the loss of ALMA (see middle and right columns in the middle and bottom rows).

Future directions

The first EHT image of M87 has provided very strong evidence for the existence of an event horizon and supports the notion of SMBHs being located at the centre of galaxies. SMBHs present a new tool to explore gravity at its most extreme limit and on a mass scale that was hitherto inaccessible. Ongoing analysis of existing data and future EHT observations will further help us understand the nature of black holes and will provide even more stringent tests of GR.

Future observations and detailed analysis of M87 data will explore the shape and time variability of the shadow more accurately. The EHT is in the process of studying the magnetised plasma around M87 in polarised light, which will allow us to investigate the mechanism by which black holes launch and power their relativistic jets.

As for Sgr A*, the mass-to-distance ratio is accurately measured from stellar orbits in the near-infrared (Gravity Collaboration et al., 2019), so measuring the shadow shape and diameter provides a null hypothesis test of GR (Psaltis et al., 2015). Since its mass is three orders of magnitude smaller than that of M87*, the dynamical timescales are minutes instead of days; therefore observing the shadow of Sgr A* will require accounting for this variability as well as the mitigation of scattering effects caused by the interstellar medium (Johnson, 2016). Time-dependent non-imaging analysis can potentially be used to track orbits of hot spots near the black hole (Broderick & Loeb, 2006; Doeleman et al., 2009b; Roelofs et al., 2017), as reported recently on the basis of interferometric observations in the near-infrared (Gravity Collaboration et al., 2018). Real-time movies may also become possible via interferometric dynamical imaging (Johnson et al., 2017). Time-domain studies and movies of black holes can then be used to study black hole accretion and to map the black hole spacetime, leading directly to measurements of black hole spin and tests of the “no hair” theorem (Broderick et al., 2014).

Although the focus of this article is the first EHT result from the 2017 campaign, it is noteworthy that enhancement of the EHT’s capabilities over the coming years will bring more exciting scientific results. In 2018, the Greenland Telescope (GLT) joined the EHT (and GMVA) and VLBI observations were conducted as part of ALMA Cycle 5 (the analysis of these observations is still ongoing). In 2019, EHT observations were abandoned because of operational difficulties at a small number of key EHT sites. For 2020, observations are planned during ALMA Cycle 7 and will include new telescopes: Kitt Peak National Observatory (KPNO) in Arizona, and the NOEMA interferometer in France. These new stations will provide intermediate baselines ($\lesssim$ 1000 km) in Europe (NOEMA–IRAM-30m) and important short baselines in the USA (KPNO–SMT) ($\lesssim$ 100 km), thus further extending the baseline coverage for both M87 and Sgr A*. The possible future addition of the Africa Millimeter Telescope (AMT) in Namibia (Backes et al., 2016) and the Large Latin American Millimeter Array (LLAMA) in Argentina will add further baseline coverage, including the long baselines oriented east-west (AMT–ALMA) and the intermediate baseline LLAMA–ALMA (180 km). In particular, the addition of short/intermediate baselines of the order of a few hundred km, which are sensitive to extended emission from the jet on scales > 100 μas, may enable us to trace the jet down to the SMBH and directly image the jet launching. See the middle and right columns of Figure 6 to evaluate the impact of these new stations in recovering the jet structure; the location of the new stations is also displayed in Figure 1.

Higher-resolution images can be achieved by going to a shorter wavelength (0.87 mm or 345 GHz, i.e., ALMA Band 7). A future array that combines observations at both 1.3 and 0.87 mm will improve the imaging dynamic range, while multi-frequency VLBI would also open up spectral index and rotation measure studies.

In the more distant future, extending VLBI into space would provide the increased angular resolution necessary to image finer structures and dynamics near the black hole shadow (Fish et al., 2019; Palumbo et al., 2019; Roelofs et al., 2019). An order of magnitude increase in angular resolution would allow us to perform precision tests of GR and to measure parameters like black hole spin. While current terrestrial VLBI at 1.3 mm can resolve the black hole shadow only in Sgr A* and M87, adding satellites in space would significantly expand the range of sources that can be resolved on horizon scales. Combining ground-based VLBI at 0.87 mm with space-based VLBI at longer wavelengths would provide better matching beam sizes, which are important for spectral index and rotation measure studies. Studying nearby low-luminosity AGN could fill the gaps in black hole mass, accretion/jet power, and host galaxy type between Sgr A* and M87. Therefore all these developments will open up very exciting and new scientific possibilities in the coming decades.

Finally, if we were to discover a radio pulsar on a tight orbit (period < 1 year) around Sgr A*, this would allow us to measure the black hole properties (mass, distance and spin) more accurately than currently possible with orbiting stars targeted by the AO-assisted, two-object, multiple beam-combiner interferometric VLTI instrument, GRAVITY, leading to a clean test of the no-hair theorem (Psaltis, Wex & Kramer, 2016). The detection of a magnetar at a projected distance of 0.1 pc from Sgr A* (Eatough et al., 2013) suggests that finding a pulsar in a close orbit around Sgr A* should be possible, and the recent detection of the Vela pulsar with phased ALMA (Liu et al., 2019) opens up the possibility of pulsar searches with ALMA at high frequencies (where the effect of interstellar scattering is lower). The combination of the far-field measurements (100s–1000s r_g) based on pulsars and stars, with the near-field tests from imaging of black hole shadows (10s rg), has the power to reveal deviations from the Kerr metric and provide a fundamental test of GR (Goddi et al., 2017), potentially leading to a breakthrough in our understanding of physics in the strong gravity regime.

Acknowledgements

The authors would like to acknowledge all the scientists, institutes, observatories and funding agencies who are part of and collectively support the EHT project. The APP was supported by a Major Research Instrumentation award from the National Science Foundation (NSF; award 1126433), an ALMA

North American Development Augmentation award, ALMA North America (NA) Cycle 3 and Cycle 4 Study awards, and an ALMA NA Cycle 5 Development award. The EHT project has been supported by multiple grants from many independent funding agencies, including the ERC Synergy Grant "Black-HoleCam: Imaging the Event Horizon of Black Holes" (Grant 610058) and several USA NSF grants (including AST-1310896, AST-1440254, and OISE-1743747). For the complete list of funding grants and acknowledgements please see EHT Collaboration et al. (2019a); they have not been reproduced here for reasons of space and readability. We gratefully acknowledge the support provided by the staff of the ALMA observatory.

This paper makes use of the following ALMA data: ADS/JAO.ALMA#2016.1.01154.V.

ALMA is a partnership of ESO (representing its member states), NSF (USA) and NINS (Japan), together with NRC (Canada), MOST and ASIAA (Taiwan), and KASI (Republic of Korea), in cooperation with the Republic of Chile. The Joint ALMA Observatory is operated by ESO, AUI/NRAO and NAOJ.

References

Abbot, B. P. et al. 2016, Phys. Rev. Lett., 116, 061102
Backes, M. et al. 2016, Proc. of High Energy Astro physics in Southern Africa (HEASA 2016), South African Astronomical Observatory (SAAO), (Cape Town, South Africa), 029
Bardeen, J. M. 1973, in Black Holes, ed. DeWitt, C. & DeWitt, B. S., 215
Broderick, A. E. & Loeb, A. 2006, MNRAS, 367, 905
Broderick, A. E. et al. 2014, ApJ, 784, 7
Davelaar, J. et al. 2018, Computational Astrophysics and Cosmology, 5, 1
Davelaar, J. et al. 2019, arXiv:1906.10065
Doeleman, S. & Krichbaum, T. 1999, 2nd millimeter-VLBI science workshop, ed. Greve, A. & Krichbaum, T. P., (St. Martin d'Heres, France), 73
Doeleman, S. et al. 2005, ASPC, 340, 605
Doeleman, S. et al. 2008, Nature, 455, 78
Doeleman, S. et al. 2009a, astro2010, 68
Doeleman, S. et al. 2009b, ApJ, 695, 59
Doeleman, S. 2010, EVN Symposium Proceedings, 53
Doeleman, S. et al. 2012, Science, 338, 355
Eatough, R. et al. 2013, Nature, 501, 391
EHT Collaboration et al. 2019a, ApJ, 875, L1
EHT Collaboration et al. 2019b, ApJ, 875, L2
EHT Collaboration et al. 2019c, ApJ, 875, L3
EHT Collaboration et al. 2019d, ApJ, 875, L4
EHT Collaboration et al. 2019e, ApJ, 875, L5
EHT Collaboration et al. 2019f, ApJ, 875, L6
Escoffier, R. P. et al. 2007, A&A, 462, 801
Falcke, H., Melia, F. & Agol, E. 2000, ApJ, 528, 13
Falcke, H. et al. 2012, The Messenger, 149, 50
Falcke, H. 2017, J. Phys., Conference Series 942, 012001
Fish, V. et al. 2013, arXiv:1309.3519
Fish, V. et al. 2019, arXiv:1903.09539
Gebhardt, K. et al. 2011, ApJ, 729, 119
Gillessen, S. et al. 2009, ApJ, 692, 1075
Goddi, C. et al. 2017, IJMP, 26, 1730001
Goddi, C. et al. 2019, PASP, 131, 075003
Gravity collaboration et al. 2018, A&A, 618, 15
Gravity collaboration et al. 2019, A&A, 625, 10
Janssen, M. et al. 2019, A&A, 626, 75
Johnson, M. 2016, ApJ, 833, 74
Johnson, M. et al. 2017, ApJ, 850, 172
Krichbaum, T. et al. 1997, A&A, 323, 17
Krichbaum, T. et al. 1998, A&A, 335, 106
Krichbaum, T. et al. 2004, EVN Symposium Proceedings, 15
Liu, K. et al. 2019, submitted to ApJ
Luminet, J.-P. 1979, A&A, 75, 228
Luminet, J.-P. 2019, arXiv:1902.11196
Martí-Vidal, I. et al. 2016, A&A, 587, A143
Matthews, L. D. et al. 2018, PASP, 130, 015002
Moscibrodzka, M. et al. 2014, A&A, 570, 7
Mizuno, Y. et al. 2018, Nature Astronomy, 2, 585
Olivares, H. et al., arxiv:1809.08682
Padin, S. et al. 1990, ApJ, 360, 11
Palumbo, D. et al. 2019, ApJ, 881, 62
Psaltis, D. et al. 2015, ApJ, 814, 115
Psaltis, D., Wex, N. & Kramer, M. 2016, ApJ, 818, 121
Roelofs, F. et al. 2017, ApJ, 847, 55
Roelofs, F. et al. 2019, A&A, 625, 124
Roelofs, F., Janssen, M. and EHTC, submitted to A&A
Shaver, P. A. 2003, Proc. of the workshop "The Mass of Galaxies at Low and High Redshift", ESO Astrophysics Symposia, ed. Bender, R. & Renzini, A., 357
Tilanus, R. et al. 2014, arXiv:1406.4650
Wright, M. et al. 2001, ALMA Memo, 382
Younsi, Z. et al. 2016, Phys. Rev. D, 94, 084025

Links

[1] The Event Horizon Telescope webpage: http://eventhorizontelescope.org/
[2] The Global mm-VLBI Array webpage: http://www3.mpifr-bonn.mpg.de/div/vlbi/globalmm/
[3] Astronet 2007: https://www.eso.org/public/archives/oldpdfs/Astronet_ScienceVision_lowres.pdf

Notes

[a] We refer to Luminet (2019) for a comprehensive review of the history of early numerical simulations of black-hole imaging during the period 1972–2002 and Falcke (2017) for a review of past, current and future efforts to image black holes.
[b] The strategic importance of millimetre-VLBI for event-horizon-scale imaging of the Galactic Centre was also recognised in the European Science Vision for astronomy, Astronet 2007[3].
[c] In building the science case for phased ALMA, astronomers from all ALMA regions were asked for input at a variety of meetings in the USA and Europe, including an ESO workshop (see Falcke et al., 2012).
[d] In addition to being scientific targets, AGN observations are very important to facilitate the intensity and polarisation calibration of the entire VLBI array.
[e] APEX participation is nevertheless extremely important as it provides the ALMA–APEX short baseline (2.6 km), which allows the robust absolute calibration of visibility amplitudes (i.e., telescope sensitivities).

Y. Beletsky/ESO

The groundbreaking ALMA array is composed of 66 giant antennas situated on the Chajnantor Plateau in the Chilean Andes.

DOI: 10.18727/0722-6691/5151

The Physics at High Angular resolution in Nearby GalaxieS (PHANGS) Surveys

Eva Schinnerer[1,2]
Adam Leroy[3]
Guillermo Blanc[4,5]
Eric Emsellem[6,7]
Annie Hughes[8]
Erik Rosolowsky[9]
Andreas Schruba[10]
Frank Bigiel[11]
Andres Escala[5]
Brent Groves[12]
Kathryn Kreckel[1]
Diederik Kruijssen[13]
Janice Lee[14]
Sharon Meidt[15]
Jerome Pety[16]
Patricia Sanchez-Blazquez[17]
Karin Sandstrom[18]
Antonio Usero[19]
Ashley Barnes[11]
Francesco Belfiore[6]
Ivana Bešlić[11]
Rupali Chandar[20]
Dimitris Chatzigiannakis[11]
Melanie Chevance[13]
Enrico Congiu[4]
Daniel Dale[21]
Christopher Faesi[1]
Molly Gallagher[3]
Axel Garcia-Rodriguez[19]
Simon Glover[22]
Kathryn Grasha[12]
Jonathan Henshaw[1]
Cinthya Herrera[16]
I-Ting Ho[1]
Alexander Hygate[1]
Maria Jimenez-Donaire[23]
Sarah Kessler[3]
Jenny Kim[13]
Ralf Klessen[22]
Eric Koch[9]
Philipp Lang[1]
Kirsten Larson[14]
Alexandra Le Reste[8]
Daizhong Liu[1]
Rebecca McElroy[1]
Joseph Nofech[9]
Eve Ostriker[24]
Ismael Pessa Gutierrez[1]
Johannes Puschnig[11]
Miguel Querejeta[5,19]
Alessandro Razza[5,6]
Toshiki Saito[1]
Francesco Santoro[1]
Sophia Stuber[1]
Jiayi Sun[3]
David Thilker[25]
Jordan Turner[21]
Leonardo Ubeda[26]
Jose Utreras[5]
Dyas Utomo[3]
Schuyler van Dyk[14]
Jacob Ward[13]
Brad Whitmore[26]

[1] Max Planck Institute for Astronomy, Heidelberg, Germany
[2] Associate Scientist, National Radio Astronomy Observatory, Charlottesville, USA
[3] The Ohio State University, Columbus, USA
[4] The Observatories of the Carnegie Institution for Science, Pasadena, USA
[5] Universidad de Chile, Santiago, Chile
[6] ESO
[7] Univ. Lyon, Univ. Lyon I, ENS Lyon, CNRS, CRAL, Saint-Genis-Laval, France
[8] CNRS/IRAP & UPS-OMP, Toulouse, France
[9] University of Alberta, Edmonton, Canada
[10] Max Planck Institute for Extraterrestrial Physics, Garching, Germany
[11] AIfA University Bonn, Bonn, Germany
[12] Australian National University, Canberra, Australia
[13] ARI/ZAH University Heidelberg, Germany
[14] CalTech/IPAC, Pasadena, USA
[15] Ghent University, Belgium
[16] Institut de Radio Astronomie Millimétrique, Saint Martin d'Hères, France
[17] Universidad Autónoma de Madrid, Spain
[18] University of California San Diego, La Jolla, USA
[19] Observatorio Astronómico National (IGN), Madrid, Spain
[20] University of Toledo, Toledo, USA
[21] University of Wyoming, Laramie, USA
[22] ITA/ZAH University Heidelberg, Germany
[23] CfA/Harvard & Smithsonian, Cambridge, USA
[24] Princeton University, USA
[25] Johns Hopkins University, Baltimore, USA
[26] Space Telescope Science Institute, Baltimore, USA

A major advance in understanding the process of star formation will come from charting the connections between cold (molecular) gas and young stars on the scale of individual molecular clouds, HII regions, and star clusters. For the first time, the ESO facilities ALMA and MUSE, in combination with HST, offer the opportunity to survey the properties of these regions and clusters across a large sample of galaxies, capturing the range of diverse galactic environments found in the local universe. Guided by theoretical models and simulations, the PHANGS collaboration has begun an endeavour which aims to reveal the physical processes controlling the process of star formation in galaxies.

Understanding the physics of star formation from detailed studies of nearby galaxies

For more than 10 Gyr, most stars have been formed in galactic disc-like systems in a secular mode. Star formation in galactic discs, including in our own Milky Way, is thus intimately linked to the formation of structure. As far as we know, the overwhelming bulk of star formation in these galaxy discs occurs in cold, well-shielded giant molecular clouds (GMCs). Therefore, the birth of stars in GMCs is connected to the structural and chemical evolution of galaxies, and the build-up of their stellar mass. Understanding this process — its triggers, efficiency, key timescales and dependence on environment — is a crucial goal of modern astrophysics.

Despite decades of intense observational and theoretical studies (for example, see the review by Kennicutt & Evans, 2012), major questions remain. How do the properties of these GMCs depend on their parent galaxy and on their location within the galaxy? How do the efficiency, duration and output of star formation depend on the hosting GMC, the dynamical environment in the galaxy, and the properties of the host galaxy? Do different clouds and different environments produce different cluster or stellar populations? How do clouds evolve? Does star formation accelerate over time or proceed at a steady pace? Which feedback mechanisms dominate the destruction of clouds in which environments? How does stellar feedback shape the larger structures of gas, metals, and eventually stars inside a galaxy?

These remain open questions because addressing them requires surveys that combine high resolution and high sensitivity. GMCs are the fundamental units of the cold interstellar medium (ISM). They sit at the interface between the large-scale physics of galactic discs and the small-scale physics of star formation. With sizes of ~ 100 pc, studying these clouds requires high physical resolution. Over the last decade, observations of individual galaxies, including the Milky Way, have replaced the old idea of a universal population of GMCs with a more diverse, dynamical view of clouds. But these previous-generation studies have been confined to individual galaxies, and often to small regions inside those galaxies. Before now it has simply been too expensive to survey molecular clouds across the whole galaxy population, and as a result, we still lack a rigorous statistical characterisation of GMC populations and properties across a representative sample of star-forming galaxy discs. Consequently, our understanding of the link between GMC properties and star formation is also in its infancy.

Our understanding of the time evolution of star formation regions has been similarly constrained by observations. Over time, an individual star formation region evolves from a GMC to an exposed stellar cluster, with turbulence, gravitational contraction, and stellar feedback all playing key but weakly constrained roles. Again, the key physics is accessible only from highly resolved observations. Here, a multi-wavelength approach is required. Observations of optical line emission from ionised gas are indispensable to probe the HII regions created by young stars, optical and ultraviolet observations probe the young stellar populations themselves, while longer wavelength observations measure the cold gas. To capture the violent cycling between ISM phases, all of these observations must at least isolate individual star-forming regions. Again, these requirements have been so strict that most key work on this topic has so far been restricted to case studies, mostly focused on the Milky Way or Local Group targets.

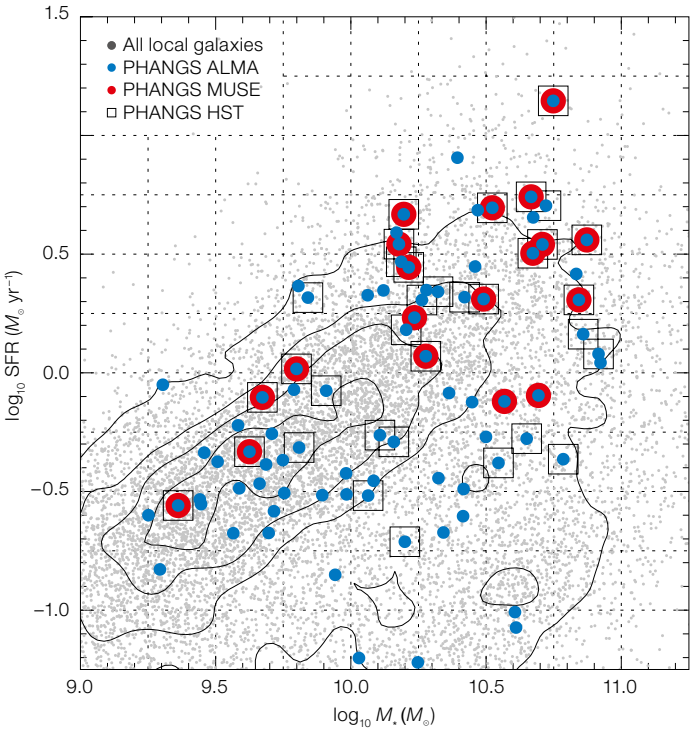

Figure 1. The PHANGS ALMA and PHANGS MUSE samples. PHANGS ALMA targets all of the closest massive, star-forming galaxies and PHANGS MUSE focuses on a key subset of these targets. Both samples achieve good coverage in the M-SFR* plane, covering the kinds of systems where most stars form. The galaxies targeted by ALMA (blue filled circles), MUSE (red circles), and HST (black squares) are shown with respect to the distribution of local galaxies.

The transformational power of ALMA and MUSE

The advent of two ESO flagship facilities dramatically changed the observational landscape in this field. The Atacama Large Millimeter/submillimeter Array (ALMA) can map cloud-scale CO (2–1) emission — a key tracer of molecular gas mass and kinematics — over the entire disc of a nearby (d ~ 15 Mpc) galaxy in about two hours of main array time. This is an improvement of roughly two orders of magnitude in survey speed compared to previous instruments, opening the transformational opportunity to survey GMCs across the whole nearby galaxy population.

Meanwhile the Multi Unit Spectroscopic Explorer (MUSE) at the VLT can capture the full optical spectrum with the same resolution and field of view as ALMA. MUSE spectral maps reveal the location, kinematics, and physical properties of HII regions, supernova remnants (SNe), and planetary nebulae (PNe). At the same time, MUSE captures the underlying stellar structures (spirals, bars, clusters) and populations that represent the dynamical drivers and outputs of the star formation process. With its large field of view, fantastic sensitivity, wavelength coverage, and sampling of the other stages of the star formation process, MUSE represents the perfect complement to ALMA.

PHANGS ALMA and PHANGS MUSE observations

Recognising this opportunity, the PHANGS collaboration proposed ambitious observational campaigns that aimed to use ALMA and MUSE to address the open questions in this field. The PHANGS ALMA and PHANGS MUSE surveys sample the full time sequence of the star formation process at resolutions matched to individual clouds across a representative sample of local galaxies. By combining resolution and physical detail using a survey type approach, these programmes aim to link the detailed physics of star formation to our understanding of galaxy evolution.

A representative sample of local star-forming galaxies

Detailed studies of clouds, HII regions, and cloud evolution have so far

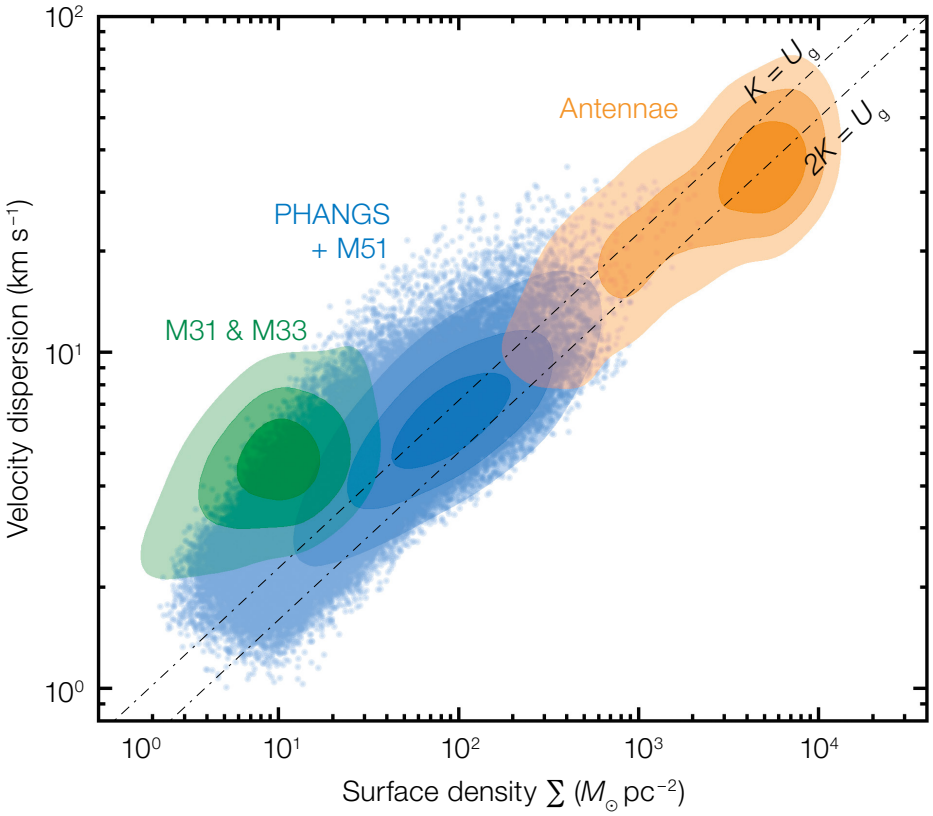

Figure 2. Molecular clouds in PHANGS ALMA. Line width at a fixed size scale (120 pc) as a function of gas surface density for the first ~ 10 PHANGS ALMA targets (blue) and several literature targets including the Antennae galaxies (NGC 4038/39). The figure, adapted from Sun et al. (2018), shows the properties of ~ 30 000 individual cloud-scale measurements (i.e., the equivalent of ~ 30 000 GMCs). The clouds span a wide range of surface density, line width, and internal (turbulent) pressure, but a relatively modest range of dynamical state (ratio of kinetic (K) to potential (U) energy). The visible variations in cloud properties can be mapped back to the locations of clouds inside the galaxy and the properties of the host galaxy.

been mostly restricted to individual case studies. Gas content, galaxy growth, and star formation are now understood to vary in important ways as a function of stellar mass (M_*) and specific star formation rate (sSFR). A key goal of PHANGS is to link the detailed physics of star formation to our understanding of galaxy evolution. To achieve this, both surveys aim to sample the so-called main sequence of star-forming galaxies, i.e., the M_*–SFR correlation that persists across redshift. To this end, PHANGS targets all massive ($9.5 < \log(M_*/M_\odot) < 11.0$), actively star-forming ($\log(\mathrm{sSFR/yr^{-1}}) > -11$) galaxies within D ~ 17 Mpc that are not too edge-on ($I < 75$ degrees) and which are easily observable with ALMA and MUSE (–75 < declination < 20 degrees). These criteria yield ~ 80 galaxies (see Figure 1) that sample the local M_*–SFR relation very well.

Cloud-scale surveys

The key physics described above plays out at the cloud scale, which is 50–150 pc. This is about the scale height of the cold gas disc, about the scale at which supernovae are expected to stir turbulence, and about the radius of a massive GMC. Current models of star formation and feedback predict a deep link between GMC properties, star formation, and feedback, setting the conditions for star formation to occur, its efficiency and duration. Violent cycling between stages of the star formation process also becomes visible at roughly this resolution.

ALMA and MUSE are efficient survey instruments thanks to their ~ one arcsecond resolution. We designed the sample to be close enough that this resolution corresponds to this key cloud scale. At this resolution, both instruments can still cover an area that includes most of the massive star formation in each target. Reaching these GMC scales in nearby galaxies allows us to connect detailed Galactic studies of Milky Way clouds to global galaxy properties, to make measurements that test theories and numerical prescriptions for star formation and feedback, and to resolve the time evolution of the ISM.

Resolving the star-forming units in nearby galaxies

Molecular clouds across galaxy discs with PHANGS ALMA

PHANGS ALMA resolves the molecular gas reservoir into individual GMCs across the full disc in ~ 80 targets. The survey focuses on mapping CO(2–1) line emission, which arises from the cold, molecular gas that forms stars. When complete, PHANGS ALMA will characterise more than 100 000 massive GMCs, roughly 100 times the number of clouds known in the Milky Way. Key science goals of PHANGS ALMA include:

A. *Uncover the dependence of molecular cloud populations on host galaxy and local galactic environment.*
Case studies of cloud properties in individual galaxies have already indicated that the distribution of cloud mass and the corresponding gravitational state are changing as a function of environment. The statistics provided by PHANGS ALMA will not only allow for a systematic assessment of these changes, but also identify the parameters that set or control the structure of the cold ISM. Figure 3 shows results from a pilot study using our first ~ 10 targets (Sun et al., 2018). These already reveal strong, systematic variations in the physical state of molecular gas across the galaxy population.

B. *Measure the efficiency of star formation by comparing the rate at which molecular gas forms stars to the gravitational freefall time.*
This efficiency per freefall time is a central parameter in many star formation theories. It captures the degree

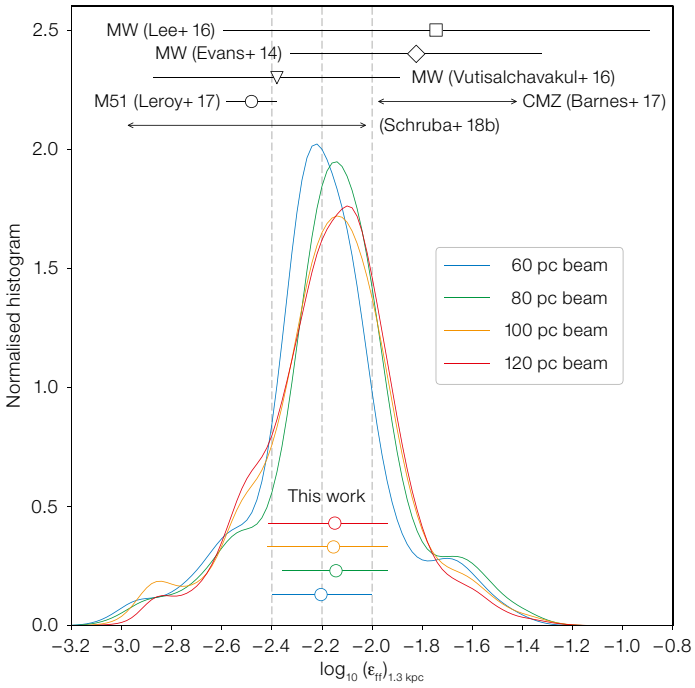

Figure 3. The distribution of star formation efficiency per freefall time ε_{ff}. The fraction of gas mass converted to stars per gravitational freefall time in the first ~ 10 PHANGS ALMA targets (from Utomo et al., 2018). This efficiency per freefall time ε_{ff} is a key benchmark for theory, capturing the inefficiency of star formation relative to gravitational collapse. It is uniquely accessible to PHANGS ALMA because the high-resolution ALMA imaging allows us to estimate the mean density of the molecular gas.

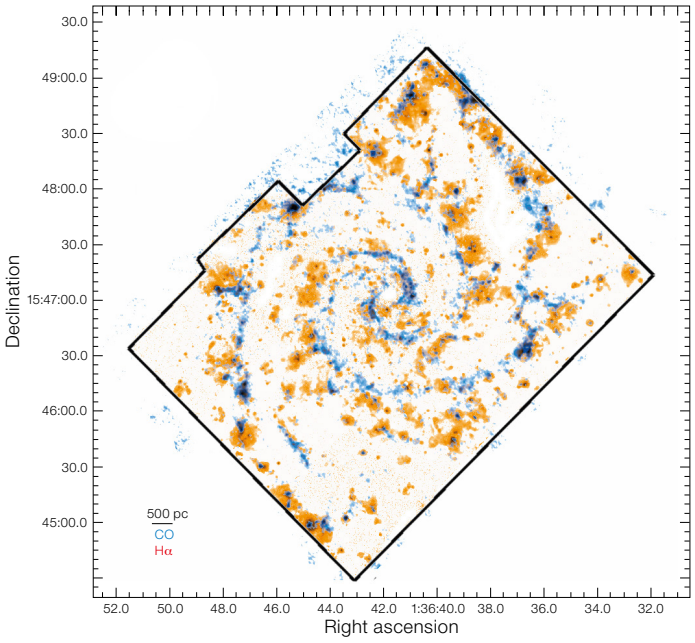

Figure 4. PHANGS ALMA and MUSE observations show the evolution of star-forming regions. ALMA observations of the cold gas reservoir (blue; CO [2–1]) overlaid with the PHANGS MUSE view of ongoing star formation activity (orange; Hα) in the the nearby spiral galaxy NGC628 (Kreckel et al., 2018). The molecular clouds seen in blue often appear visibly offset from the HII regions created by massive young stars. As gas flows through the spiral arms, cold, dense clouds visibly evolve into young star-forming regions. A key goal of PHANGS is to use statistical and dynamical modeling of these data to constrain the life cycle of molecular clouds.

to which star formation is slowed or curtailed by feedback, turbulence, and other means and represents a specific prediction of many models. Because this measurement requires knowing the gas density, it also requires high-resolution imaging. Already, using our first ~ 10 galaxies, PHANGS ALMA has provided the most definitive measurement of this quantity to date in normal local disc galaxies (Utomo et al., 2018).

C. *Quantify the life-cycle of molecular clouds.*
At high resolution, star-forming regions appear in discrete evolutionary states using ALMA and MUSE – that is as clouds, HII regions, and young star clusters (beautifully demonstrated in Figure 4, adapted from Kreckel et al., 2018). Via statistical and dynamical modelling, such observations constrain the evolution from diffuse gas to dense clouds to HII regions to clusters. The dominant feedback mechanism and timescale for cloud dispersal in different environments are still unknown and will be constrained via modelling.

At the time of writing, the observations for the Large Programme that forms the core of PHANGS ALMA are almost complete. All calibrated data products, cloud catalogues, and a host of other high-level data products are expected to be released to the community in 2020. Science papers addressing our key goals have already begun to appear.

Star-forming regions and stellar structures with PHANGS MUSE

Star formation and feedback are violent, rapid processes, with key roles played by ionising radiation, radiation pressure, stellar winds, and supernovae — all phenomena traced through the ionised gas phase. These sources of feedback impact, destroy, and reshape the cold gas that will form the next generation of stars. Meanwhile, the young stars deposit new metals into the ISM, while new material for future star formation must flow in through the galaxy disc. Star formation itself may be shaped by the underlying stellar potential, with important roles played by spirals, bars, and central stellar structures revealed by their stellar population distributions and kinematics. Resolving star-forming regions and stellar discs with PHANGS MUSE (which started as a Large Programme in ESO Period 100) will provide us with a dynamic view of star formation, stellar feedback and chemical enrichment of disc galaxies, allowing us to address the following:

A. *Estimate the timescales of the star formation process.* This is closely related to modelling the life cycle of molecular clouds. MUSE and ALMA working together (illustrated in Figure 4, adapted from Kreckel et al., 2018) offer the chance to address open questions: How long does star formation take to set in once a molecular cloud has formed? How long does stellar feedback take to disperse

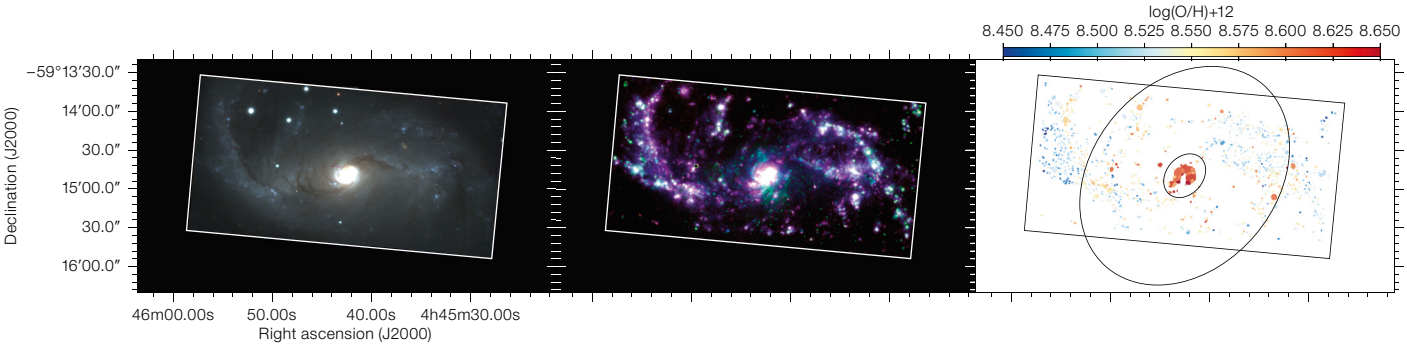

Figure 5. The PHANGS MUSE view of starlight, ionised gas and metals. PHANGS MUSE observations of NGC1672. Left: Simulated *gri* three-colour image derived from MUSE, showing starlight and prominent dust lanes. Middle: Emission line maps (red: Hα, green: [OIII], blue: [SII]) revealing active star formation and diverse physical conditions. Right: For each HII region in the galaxy, we use the MUSE spectra to estimate the metallicity. Even before removing the radial gradient, spatial correlations in metallicity, including azimuthal variations, are apparent. These trace the diffusion of metals and the flows of enriched and pristine gas across the galaxy.

a cloud? Is star formation triggered within a galactic disc (i.e., in spiral arms) or is it a stochastic process?

B. *Quantify the strength of stellar feedback across environment and scale.* Stellar feedback comes in many forms, including ionising radiation, radiation pressure, stellar winds, and supernova explosions. The high physical resolution and wide wavelength coverage provided by MUSE allow us to separate and characterise HII regions, SNe remnants and PNe (for example, Kreckel et al., 2017, apply this method to our pilot data). Together with the ALMA data, the MUSE cubes can directly assess the interactions between the warm gas (10 000 K), the cold gas (< 100 K), and the young stellar population.

C. *Measure the diffusion of metals and chemical enrichment.* The details of metal production and diffusion remain major open questions in the chemical evolution of galaxies. With metallicity estimates for ~ 15 000 HII regions across 19 galaxies, PHANGS MUSE gives us a powerful handle on how metals are built and distributed. Patterns in the small-scale distribution of metals (see Figure 5) constrain the flows of pristine and enriched gas in and out of galaxies, and the redistribution of metals from their birth sites to the surrounding medium.

PHANGS MUSE targets 19 nearby star-forming galaxies that are also targets of PHANGS ALMA. We expect to identify and characterise ~ 15 000 resolved star-forming regions, measuring metallicity and other physical diagnostics for each. MUSE also captures a host of PNe and SNe remnants (for example, Kreckel et al., 2017) and yields exquisite stellar and gas kinematics, offering signatures of stellar feedback and (with ALMA) the relative motion of different phases of the ISM. Full spectral fitting of the MUSE datacubes will produce "movies" of stellar mass in several bins of ages and metallicities. The survey is currently approximately three-quarters done, with a full release of major data products expected by 2021.

PHANGS beyond ALMA and MUSE

Young stars and stellar clusters with PHANGS HST

Direct observations of young stellar clusters offer a powerful complement to the observations of clouds by ALMA and those of HII regions and integrated starlight by MUSE. These clusters have typical sizes of a few parsecs, and so observing them requires the resolving power of the Hubble Space Telescope (HST). As of 2019, PHANGS HST (Principal Investigator: Janice Lee, Infrared Processing and Analysis Center [IPAC] at Caltech, USA), has been observing an overlapping sample with the goal of connecting young star clusters to the cold and warm gas traced by ALMA and MUSE.

The PHANGS HST Large Programme builds on the successful Legacy Extra-Galactic Ultraviolet Survey (LEGUS) Treasury programme, using a similar five-filter observing strategy with the Wide Field Camera 3 (WFC3) camera. PHANGS HST expands from LEGUS towards more massive (more Milky Way-like) galaxies and focuses on regions covered by ALMA and MUSE (see Figure 6). When completed, it will cover 38 disc galaxies. We expect the high-resolution ultraviolet and optical imaging from PHANGS HST to yield catalogues of 100 000 star clusters and associations.

Combining HST with ALMA and MUSE will dramatically improve our answers to the questions listed above (for example, from much improved knowledge of the young stellar population) and also constrain: (a) the timescale for the removal of gas from young stellar clusters (YSC); (b) the relation between the YSC and GMC mass functions; (c) the link between cloud properties and the fraction of stars formed in clusters; and (d) the connection between the multi-scale structure visible in young starlight and cold gas structure. The release of joint HST-ALMA data products revealing the detailed properties of stellar clusters and gas clouds will be a key part of the PHANGS legacy and will help lay the scientific groundwork for future facilities like the James Webb Space Telescope (JWST).

Other major efforts

Building around the core ALMA, MUSE, and HST samples, the PHANGS team is committed to building a complete characterisation of the stellar, gas, and kinematic structure of our sample. Key efforts include: (1) making high quality maps of

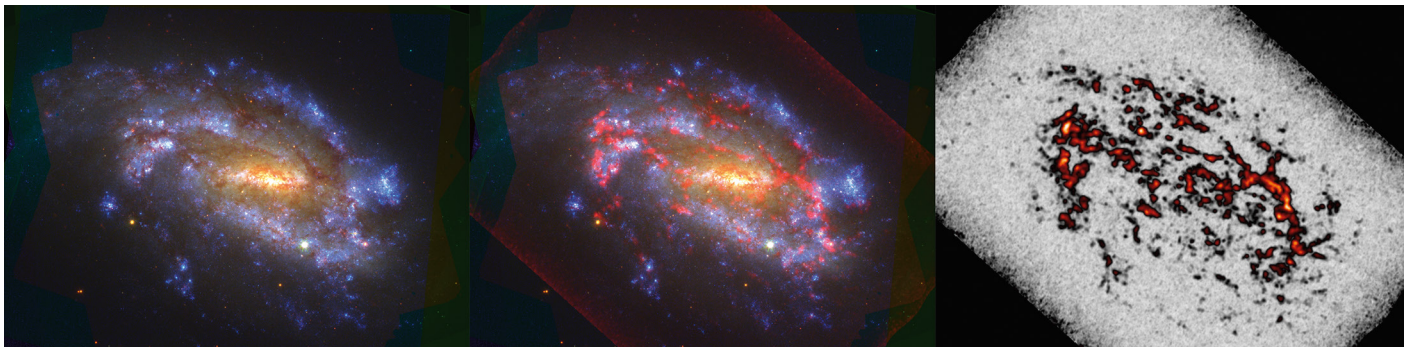

Figure 6. HST and ALMA probing the life-cycle of star formation regions. PHANGS HST and PHANGS ALMA observations of the nearby spiral galaxy NGC1559. The high angular resolution afforded by HST allows for the identification of individual young star clusters that have just emerged from their birth cloud as seen by ALMA. Optical light (HST red: white light, green: *H*-band, blue: near ultraviolet; left), with the molecular gas distribution added in red (middle). The distribution of molecular gas (ALMA; right) is remarkably similar to that of the dust lanes seen in optical light.

the stellar mass distribution for each target using Spitzer and Wide-field Infrared Survey Explorer (WISE data); (2) assembling new and archival narrow-band imaging of the Hα emission line for the whole PHANGS ALMA sample; (3) using the Indian Space Research Organization (ISRO) AstroSat satellite to obtain high-angular-resolution imaging of far-ultraviolet emission for a subset of targets; (4) new and archival Very Large Array observations of the 21-cm line to trace the atomic gas reservoir; (5) construction of detailed environmental masks; (6) reprocessing, fitting, and analysis of archival infrared (Spitzer, Herschel, WISE) and ultraviolet (Galaxy Evolution Explorer, GALEX) observations; and (7) observations of high critical density tracers of "dense gas" using ALMA, the Institut de radioastronomie millimétrique (IRAM) facilities, and the Green Bank Telescope. These efforts leverage a diverse, distributed team and promise to pair the unprecedented ALMA and MUSE data with the most complete view of stellar and gas structure for any sample to date.

Synergy of observations and theory

The combination of ALMA, MUSE, HST and the deep supporting observations represents a complex, high-dimensional data set. The full exploitation of such a unique resource requires a close synergy between careful observational analysis, modelling and statistical analysis techniques, numerical simulations, and analytic theory. With this in mind, PHANGS has pursued development of new tools and close comparison with numerical modelling and theory as a core activity. The development of new statistical tools focuses on robust statistical characterisation of the full multi-dimensional, multi-scale data set, with a focus on moving resolved studies of nearby galaxies into the "big data" regime. The team is also running dedicated state-of-the-art simulations. Our observations capture the underlying physical processes filtered through a complex combination of projection, chemistry, and radiative transfer. Implementing a realistic forward modelling perspective into the PHANGS theoretical efforts is therefore key to both uncovering the underlying physics that drives star formation and constructing new innovative tracers.

A modern scientific collaboration

The PHANGS collaboration brings together experts on ISM physics, dynamics, stellar populations, and galaxy evolution. It includes expertise distributed across different wavelengths and combines both observational and theoretical points of view. PHANGS started in 2015 with a small group of enthusiasts dedicated to seizing the opportunities described above. Today, PHANGS is a medium-sized collaboration distributed around the globe (with substantial representation in Australia, Europe, Chile, and North America).

The team is committed to diversity. We aim to fill scientific leadership roles with a mixture of junior and senior scientists and to enhance the visibility of female scientists. Currently about half of all leadership positions are occupied by female scientists. Following good practice of other large collaborations, "builder status" has been granted to junior scientists who have spent significant time generating data products for use by the astronomical community. Junior scientists have also taken on high profile roles such as leading follow-up proposals and planning the next generation of PHANGS projects.

Acknowledgements

We would like to thank all the staff at ESO, JAO, and NRAO who have been supporting the preparation, conduction and delivery of these unique datasets, and more generally, devoting efforts to make such a challenging observational campaign a reality.

References

Kennicutt, R. C. & Evans, N. J. 2012, ARA&A, 50, 531
Kreckel, K. et al. 2017, ApJ, 834, 174K
Kreckel, K. et al. 2018, ApJ, 863L, 21K
Sun, J. et al. 2018, ApJ, 860, 172S
Utomo, D. et al. 2018, ApJ, 861L, 18U

Links

[1] PHANGS survey webpage: http://www.phangs.org/

Construction has started on the foundations of ESO's Extremely Large Telescope (ELT) at Cerro Armazones. Once complete, the telescope will be the largest ground-based telescope in operation, weighing 3400 tonnes.

On 28 August 2019, ESO, MetricArts and Microsoft Chile received the 2019 award for "Digital Transformation and Industry 4.0" from the Chilean Association of Information Technology Companies (ACTI). This was in recognition of their efforts to integrate artificial intelligence into operations at Paranal Observatory.

Monica Solis

DOI: 10.18727/0722-6691/5152

Total Solar Eclipse Over La Silla

Laura Ventura[1]
Claudio Melo[1]
Lars Lindberg Christensen[1]
Mariya Lyubenova[1]
Fernando Comerón[1]

[1] ESO

On Tuesday 2 July 2019, in the late afternoon, a total solar eclipse took place over ESO's La Silla Observatory; totality lasted 1 minute and 52 seconds. For this very special event, ESO decided to open the doors of the observatory to the public, providing over one thousand visitors with a unique vantage point from which to witness this spectacular natural phenomenon.

The solar eclipse of 2 July 2019, whose path of totality included La Silla Observatory, provided a stunning culmination to the celebrations of the 50th anniversary of La Silla, ESO's first observatory, which was inaugurated on 25 March 1969. The thousands of visitors who came to La Silla for the eclipse were only a small fraction of the hundreds of thousands of people who travelled from all over the world to the narrow strip of land that would find itself under the shadow of the Moon for almost two minutes.

By 2011, ESO's education and Public Outreach Department had already received the first requests from the public to come to La Silla to witness the 2019 eclipse and/or to take pictures, videos and make precise measurements. An outline of the eclipse project was drafted in 2013, and a project plan for a big public event was prepared and approved by the ESO Directors Team in June 2018, one year before the event.

The La Silla site provides a stunning setting, combining an astronomical observatory and a beautiful landscape; in addition, given the high likelihood of good observing conditions during the event, it became a desirable location to enjoy the eclipse. For that reason, ESO decided to open the observatory to as many visitors as the infrastructure and logistics would allow.

Figure 1. La Silla during the total solar eclipse, which resulted in almost two minutes of totality at 20:39 UT.

ESO/R. Lucchesi

ESO/M. Zamani

Figure 2. The President of the Republic of Chile, Sebastián Piñera, pictured with Chilean high school students while visiting La Silla.

In addition to the general public, La Silla was honoured to welcome the President of the Republic of Chile, Sebastián Piñera and his wife, Cecilia Morel. They were accompanied by the Ministers of Science, Technology, Knowledge and Innovation, Andrés Couve, and of Education, Marcela Cubillos, as well as by the Undersecretaries of Foreign Affairs, Carolina Valdivia, and of Tourism, Mónica Zalaquett, along with other authorities from the Ministries of Science and Foreign Affairs and members of the National Congress. Although the President and the First Lady could not stay at La Silla for the eclipse, they had the opportunity of visiting the 3.6-metre telescope, where they were received by the Director General of ESO, the President of the ESO Council, and other members of the ESO management. After this visit, both the President of Chile and the ESO Director General gave speeches at a tent set up to host over 60 media representatives — both national and international — who had registered to provide live coverage of the event. They then moved to the VIP area, by the New Technology Telescope (NTT), where they met with diplomatic representatives of ESO Member States and Partners, and other distinguished guests.

As a symbol of the deep appreciation of ESO toward the local community which has hosted its first observatory for these past 50 years, ESO had the pleasure of inviting a large group of students and senior citizens from the municipalities of La Higuera, La Serena, and Coquimbo to witness the eclipse from La Silla. The group, who had a special meeting with President Piñera and the First Lady, engaged in a lively conversation with them. In addition to the students from the Coquimbo Region, La Silla also hosted the sixteen winners of a contest organised by CONICYT, the National Council of Science and Technology of Chile, among children selected from schools across the country.

Most of the members of the ESO Science Outreach Network (ESON), ESO's network of outreach representatives in the Member States and beyond, were present at La Silla as well. For them, the eclipse was the highlight of a tour of the ESO facilities in Chile that included Paranal and the Atacama Large Millimeter/submillimeter Array (ALMA). Other members of this tour group included eight social media influencers selected from 300 participants in a #MeetESO social media competition[1] including the winner of the La Silla Total Eclipse Public Competition[2].

A total solar eclipse offers a rare possibility to carry out scientific experiments targeting the physical properties of the lower solar corona, observation of which is difficult even from space-based probes. La Silla hosted an array of scientific and outreach observations carried out by teams that used dedicated equipment to perform a variety of observations, described in Christensen et al. on p. 47. Notably, even the NTT was used to obtain spectroscopy of the solar corona, an observation that critically depended on perfect synchronisation — a miscalculation could have resulted in direct exposure to the radiation of the solar surface and severe damage to the telescope optics and instrument. The experience of the telescope operators ensured that this was expertly avoided (see Dennefeld et al., p. 54). Another notable experiment included the use of the Rapid Action Telescope for Transient Objects (TAROT) to reproduce the famous Eddington experiment during the historical eclipse of 1919, when the deflection of the light from stars near the line of sight of the Sun was used to verify the predictions of Einstein's general theory of relativity.

Aside from the special guests mentioned above, over 700 people travelled to La Silla. Around a tenth of these visitors came from Chile, with the rest travelling from abroad — mostly Europe and North America. An area with a wonderful view of the eclipse was prepared for the public and was equipped with a large tent with seats, where snacks and beverages

Figure 3. Some of the 1000 visitors to La Silla are seen here observing the eclipse from an area near the Swedish–ESO Submillimetre Telescope (SEST), during the performance by Steve Rothery and friends.

S. Lowery

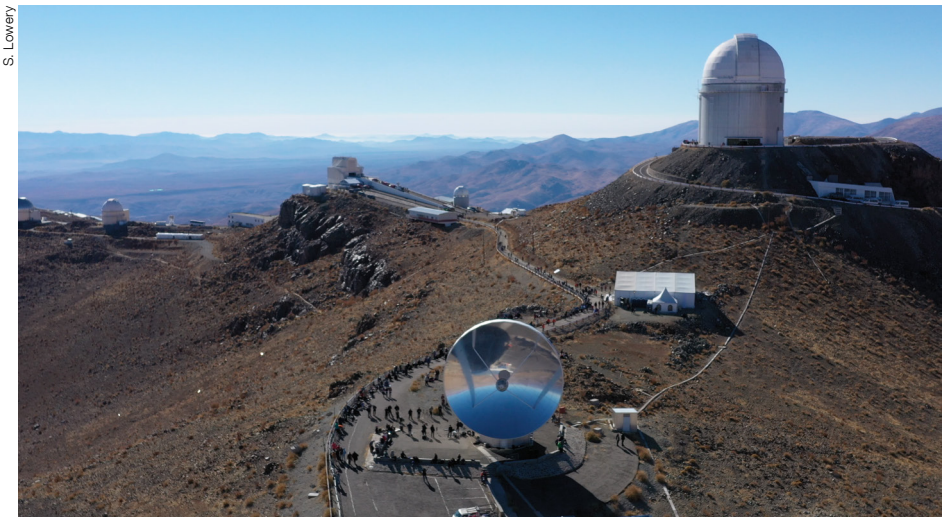

were served. Polyclinic services were installed at the former control building of the Swedish–ESO Submillimetre Telescope (SEST), and two ambulances fully equipped to provide first aid were positioned along the public viewing area. Information on the safe viewing of the eclipse had been given in advance to all those attending, and glasses with filters certified for solar viewing were distributed.

As part of the programme of activities offered for all the visitors, solar telescopes were set up for public observations before and during the partial phases of the eclipse. The visitor centre at La Silla offered a brand-new exhibition about ESO, including informative panels, the simulation of an old control room and a collection of astronomical instrumentation pieces rescued from the observatory over the course of its 50-year history, showing the evolution of detectors from photographic plates to CCDs. Two itinerant exhibitions were also installed for the occasion: the already very popular audiovisual show "ALMA sounds", created from millimetre-submillimetre signals detected by ALMA; and paintings by Chilean artist Silvana Zúñiga that, using luminescent paint, illustrate concepts like light pollution and multi-wavelength astronomy. The visitor centre also hosted public talks given by ESO experts on popular astronomy topics. Finally, public tours to the NTT and the 3.6-metre telescope were organised. The area reserved for public viewing offered ample space to set up the equipment that many visitors brought along, resulting in a truly impressive display of telescopes, cameras and a wide variety of imaging aids.

ESO made sure that the spectacle enjoyed at La Silla could be followed across the rest of the world, offering a live webcast that combined high-resolution images of the eclipsed Sun with views of the site from several vantage points, conveying the atmosphere at the observatory (see Figures 3 & 4). In addition, a team of expert photographers from ESO ensured that excellent images of high technical and artistic quality were obtained, a sample of which are shown in this article.

A special treat was a concert by British musician Steve Rothery (of Marillion fame) and his band, who performed against the impressive backdrop of the Swedish–ESO Submillimetre Telescope (SEST) antenna. The concert ended with the premiere of a new record by Steve Rothery and Riccardo Romano, a member of his band, appropriately entitled "La Silla". The performance was a collaboration with Rick Armstrong, who played bass guitar. It was an honour to host Rick Armstrong, the elder son of astronaut Neil Armstrong, particularly in the same month as the 50th anniversary of the first lunar landing.

Despite the expectation of the cold temperatures typical in July at La Silla, and the non-negligible probability of adverse meteorological conditions, the weather on the eclipse day was especially compliant, adding to the special character of the event. The sky remained clear and cloud-free for the whole day, temperatures were mild and virtually no wind blew, making the outdoors experience even more pleasant and memorable.

Figure 4. The moment worth waiting for: totality. With the Sun only 14 degrees above the horizon, day turns into twilight. The VIP platform at the NTT is seen on the right.

ESO/M. Zamani

ESO/P. Horalek

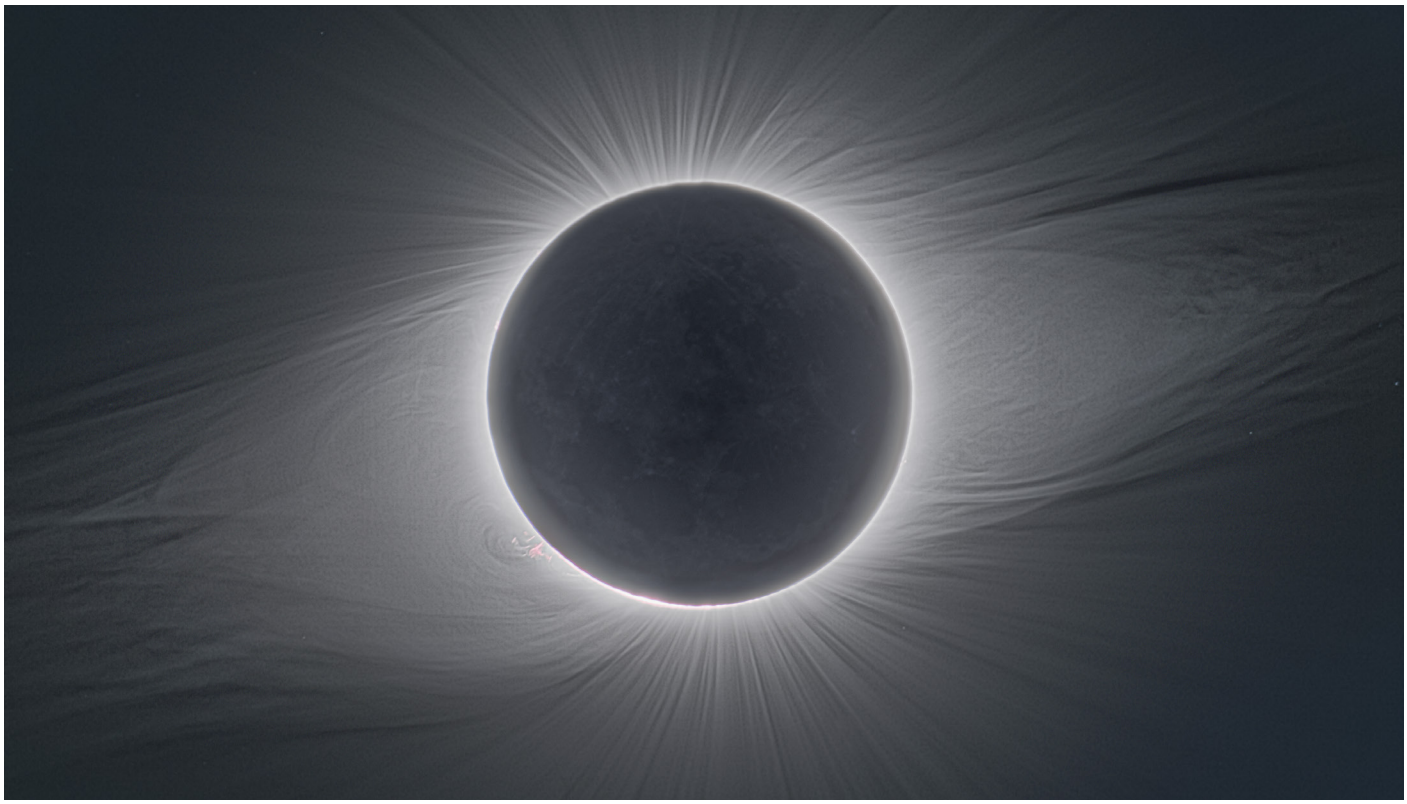

Figure 5. A composite photo with exposures of varying duration showing filamentary details in the solar corona.

As the partial eclipse phase started and progressed during the early afternoon, an atmosphere of mounting excitement built up in anticipation of the extraordinary moments to come. People witnessed the progress of the covering of the solar disc with dedicated protective glasses at the beginning, but as totality approached, the changes in illumination of the surrounding landscape became increasingly obvious, giving the scene an unreal appearance. The blue of the sky became deeper and deeper while a band of intense orange — often seen in the middle of twilight — encompassed the entire horizon. At the same time, a noticeable drop in the temperature was felt as the solar irradiation decreased.

Finally, the shadow of the Moon reached La Silla. In a matter of seconds, the sliver of the uncovered solar disc thinned until disappearing as the sky quickly darkened, stars became visible, and the solar corona shone in stark contrast with the surrounding sky and the black disc of the Moon completely covering the disc of the Sun. The corona appeared bright and compact, typical of the period near minimal solar activity, and, through the telescopes, a protuberance could be seen toward the northwest of the solar disc. Most of those witnessing the phenomenon reacted emotionally, with abundant exclamations of wonder, hugs and tears. As the first Baily's beads appeared, signalling the end of the total eclipse phase, the 1 minute and 52 seconds of totality seemed to many way too short.

The deep impressions left by totality almost turned the last partial eclipse phase — during which the solar disc progressively reappeared from behind the Moon — into an anti-climax, despite the beautiful show put on by the partially eclipsed Sun advancing toward the horizon until the end of the eclipse near sunset. Further impressions of the event can be seen online[2].

Acknowledgements

The authors feel privileged to have witnessed this once-in-a-lifetime experience at La Silla, as the next total solar eclipse visible from there will be in 2231[a]. Contemplating one of the most majestic celestial phenomena was enhanced spectacularly by excellent meteorological conditions and the wonderful landscape of ESO's first observatory. While those particular factors were beyond ESO's control, the success of the experience for visitors on that day required planning, coordination and organisation and the effort of colleagues across ESO. The authors would particularly like to thank the staff in the Department of Communication, La Silla Logistics and operations, IT support, ESO's Representation in Chile, La Silla Paranal Safety, and everybody else who worked hard in the preparation and execution of a unique event in ESO's history.

Links

[1] #MeetESO social media competition: https://www.eso.org/public/announcements/ann18088/
[2] The La Silla total eclipse public competition: https://www.eso.org/public/norway/announcements/ann18091/
[3] ESO press release for the total solar eclipse: https://www.eso.org/public/news/eso1912/

Notes

[a] This is the only total solar eclipse that will be visible from an ESO observatory for more than 212 years, when La Silla will be close to the north of the path of totality during the total solar eclipse of 28 August 2231. An annular eclipse will be visible from La Silla next century, on 9 January 2187.

DOI: 10.18727/0722-6691/5153

Science & Outreach at La Silla During the Total Solar Eclipse

Lars Lindberg Christensen[1]
Gerardo Ávila[1]
Wahab A. Baouchi[2]
Michel Boer[3]
Jean-François Le Borgne[4]
Christian Buil[5]
Manuel Castillo-Fraile[6]
Eric Denoux[7, 5]
Valérie Desnoux[5]
David Elmore[8]
Loic Eymar[3]
Robert F. Fisher[9]
Carlos Guirao[1]
Alain Klotz[4, 10]
Adrien Nicolas Klotz[10]
Julien Lecubin[11]
Kyle A. Motl[9]
Darío Pérez[12]
Miguel Pérez-Ayúcar[13]
Wouter van Reeven[13]
Xavier Regal[14]
Yoann Richaud[14]
Rico Sautile[14]
Alexandre Santerne[15]
Roy Wellington[16]
Theo Wellington[16, 17]
Padma A. Yanamandra-Fisher[9]
Joe Zender[18]

[1] ESO
[2] University of Colorado, Boulder, USA
[3] ARTEMIS-CNRS/OCA/UNS, Nice, France
[4] IRAP-Observatoire Midi Pyrénées, Toulouse, France
[5] Association AUDE, Paris, France
[6] Serco for ESA (European Space Agency), Madrid, Spain
[7] Observatoire Cor Caroli, Caussade, France
[8] Association of Universities for Research in Astronomy (AURA), Washington D.C., USA
[9] The PACA Project, Space Science Institute, Boulder, USA
[10] Université Paul Sabatier, Toulouse, France
[11] OSU PYTHEAS, Marseille, France
[12] GTlinkers, Madrid, Spain
[13] Aurora Technology for ESA (European Space Agency), Madrid, Spain
[14] Observatoire de Haute Provence/OSU PYTHEAS, Saint Michel l'Observatoire, France
[15] Aix-Marseille University/CNRS/CNES/LAM, Marseille, France
[16] Barnard-Seyfert Astronomical Society, Nashville, USA
[17] NASA Solar System Ambassador, Nashville, USA
[18] ESA (European Space Agency), Noordwijk, the Netherlands

ESA/CESAR

Figure 1. Some members of the ESA/CESAR team at their observing spot. From left to right: Manuel Castillo, Wouter van Reeven, Miguel Pérez-Ayúcar, Joe Zender and Darío Pérez de Carlos.

Total solar eclipses are rare phenomena, only occurring in a specific location once every 360 years on average. Historically, total solar eclipses have only been observed twice from large professional observatories, allowing specific science experiments to take place. On this occasion, ESO invited nearly 25 scientists, communicators and educators to observe and document the eclipse and benefit from La Silla's clear skies and its infrastructure and resources. This article presents an overview of these various activities.

Introduction

It is very rare that a total solar eclipse passes over an existing observatory with large telescopes — in fact, in the last fifty years there have only been two such opportunities: in 1961 over l'Observatoire de Haute-Provence in France, and in 1991 over Mauna Kea on the island of Hawai'i. A separate article in this issue of the Messenger (Ventura et al., p. 43) provides an overview of the total solar eclipse event at La Silla (also see ESO press release[1]).

Along with cameras and telescopes brought by 700 members of the public and more than 60 journalists, five different groups conducted outreach, education and science experiments on the day[2]. They were assigned a place on the side of the La Silla mountain just below the Visitor Centre (formerly called the Ritz building) as well as on the New Technology Telescope (NTT) platform. The two 4-metre-class telescopes at La Silla were also pointed near the Sun during the eclipse. The observations using the New Technology Telescope (NTT) are described in this issue of the Messenger (Dennefeld et al., p. 54). The eclipse was also captured with a small solar telescope called the HARPS Experiment for Light Integrated Over the Sun (HELIOS) which is installed on the catwalk of the ESO 3.6-metre telescope, and fed into the High Accuracy Radial velocity Planet Searcher (HARPS) instrument via a fibre. The high-precision spectroscopic data look promising and are currently under analysis. Two national telescopes, Exoplanets in Transits and their Atmospheres (ExTrA) and the Rapid Eye Mount telescope (REM), also attempted observations but encountered technical problems.

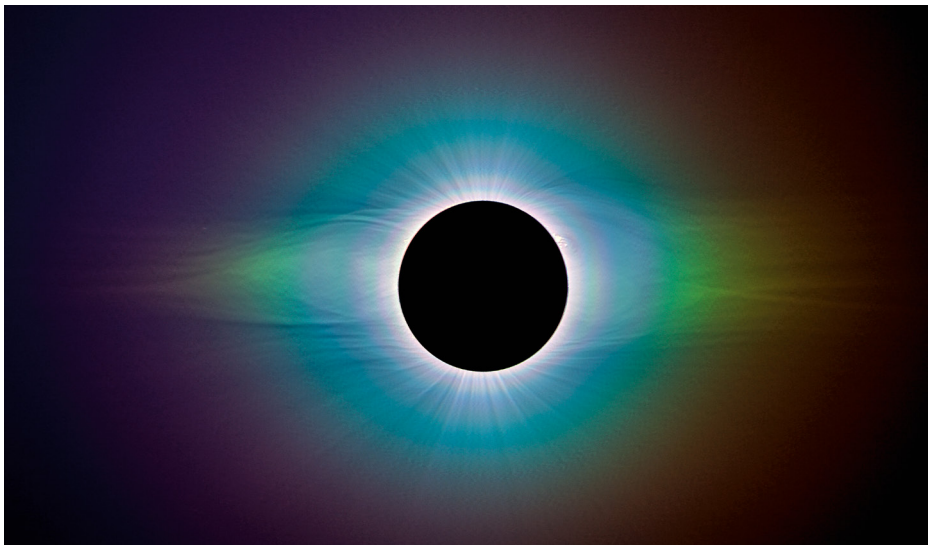

ESA/CESAR

Figure 2. This image is a combination of polarised images obtained during totality to bring out the details of coronal structures.

ESA/CESAR Activities

The primary goal of the European Space Agency (ESA) project Cooperation through Education in Science and Astronomy Research (CESAR) was to carry out scientific observations of the solar atmosphere and the Earth's ionosphere, as well as general observations for outreach and education. The results obtained to date are summarised below and online[3].

The CESAR team[a] (Figure 1) completed the following education and outreach objectives:

– Still images of the inner corona were obtained with a 1-metre focal length telescope. These were sent live (at a rate of two per minute) and posted online[4] as soon as they were processed through the servers at the European Space Astronomy Centre (ESAC) in Madrid.
– Live streaming on YouTube[5] was carried out with a 1-metre focal length telescope and a Sony Alpha 7 SII camera.
– A live Google hangout[6] included live connections to the La Silla team and talks and presentations related to solar projects and science. This was coordinated from the CESAR facilities at ESAC enabling a professional multimedia production (including mixing live video streams from different places, live images of the eclipse, presentation slides, etc.).
– In the days following the eclipse, ESA published images from the event on the main ESA webpages[7] (see Figures 2–5).

The team also completed most of its scientific objectives; at the time of writing this was the status of the (ongoing) analysis:

– Polarisation measurements were completed using the Eclipse K-corona POLarimeter (EKPOL) from the Turin—INAF Observatory using two different setups; first, the polarisation intensities of the corona were measured using observations at four different polarisation angles (0, 45, 90 and 135 degrees). From these measurements, the polarisation brightness is measured and the electron density in the corona derived. The second objective was to obtain the polarisation intensities at more polarisation angles to decrease the overall uncertainty in the computation of the polarisation brightness. EKPOL (see Zangrilli et al., 2009) is based on an optical telescope supplemented by an electronic controllable liquid-crystal variable retarder together with a specific CCD camera (funded by the ESA Faculty). EKPOL was developed as a technology demonstrator for the Metis coronagraph on Solar Orbiter (INAF) and the Association of Spacecraft for Polarimetric and Imaging Investigation of the Corona of the Sun (ASPIICS) on Proba-3 (ESA/Royal Observatory of Belgium).

Figure 3. A composite image of the solar eclipse made from ground and space observations: Proba-2 (SWAP) solar disc, CESAR corona in grey, SOHO/LASCO C2 outer corona in red, SOHO/LASCO C3 extended corona in blue.

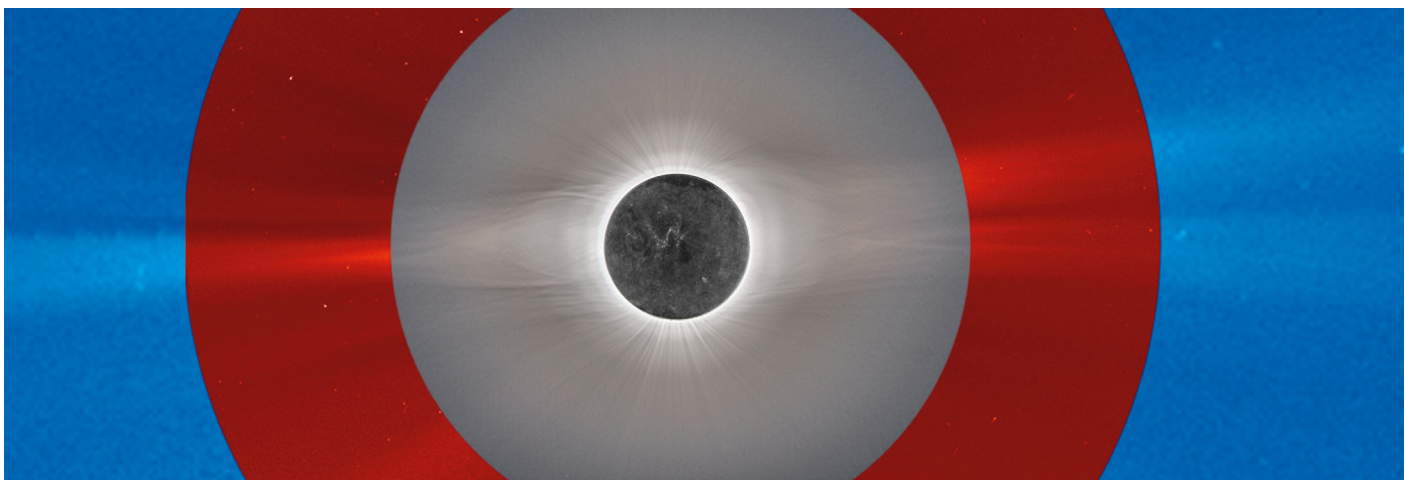

ESA/CESAR; SOHO (ESA & NASA); Proba-2: ESA/Royal Observatory of Belgium

ESA/CESAR

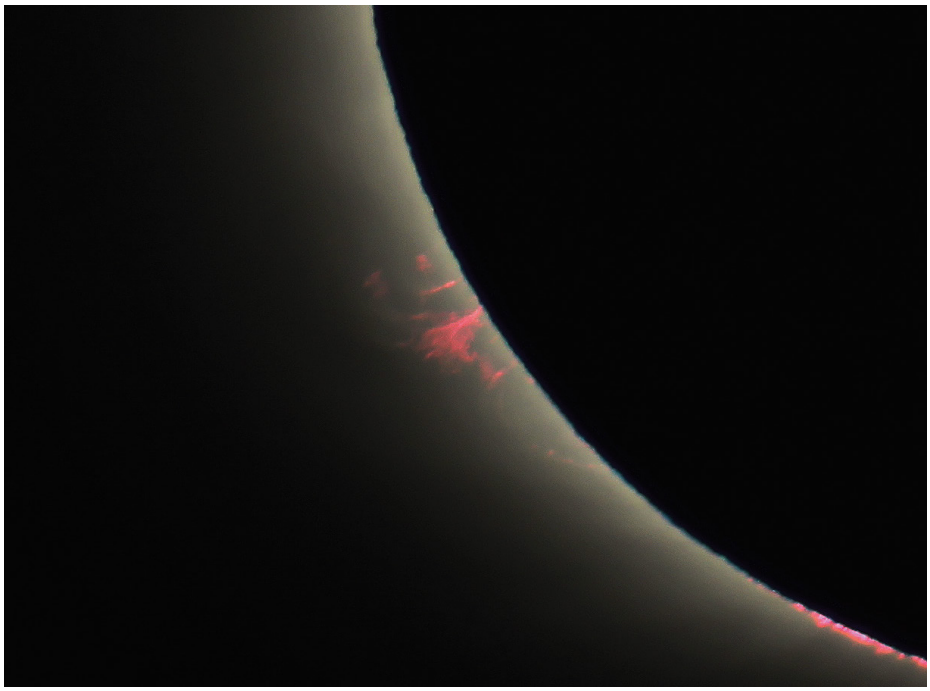

Figure 4. The Sun's chromosphere and prominence taken with a visible-light telescope (~ *f*/1000), with no filter and using a Canon 550D, during the Moon's exit (third contact).

– Independent polarisation measurements (Figure 2) were completed with simple polarisation filtering of white light (with improved equipment and procedures derived from experience gained during the total solar eclipse in the USA). A filter wheel with four polarisation angles (0, 45, 90 and 135 degrees) was used. A fifth filter position without a polariser allowed the capture of unpolarised images. The objective of this experiment was to calculate the different polarisation rates in the inner solar corona to obtain estimates of the electron content and the magnetic field. These estimates, together with physical models of the corona, can give information about the temperature and flow speed of coronal electrons.
– A flash spectrum of the chromosphere was attempted but was unsuccessful owing to the unfortunate failure of the camera two minutes before totality. It consisted of a telescope projecting an image of the Sun through a high-quality transmission diffraction grating onto a digital SLR camera without an infrared blocking filter. This configuration permits one to image the emission spectrum of the chromosphere covering wavelengths from 4000 to 10 000 Å, allowing the identification of features that are present in the photosphere but not in the chromosphere.
– The CESAR team also completed the first ever measurements of the Earth's ionosphere using a Galileo receiver to try to record changes caused by the transit of the Moon's shadow over the area of observation. The analysis is ongoing; by using multi-band and multi-constellation data from the Global Navigation Satellite System (GNSS), it is possible to analyse the total electron density perturbations with enough time resolution to reveal ionospheric irregularities during the eclipse. For this purpose, the team has a close collaboration with a GNSS research group at the Universitat Politècnica de Catalunya (UPC). The equipment provided by the Galileo Science Office at ESAC is the same as that used by the Galileo Experimentation & Scientific Tests in Antarctica project to study the effect of solar activity in the ionosphere at high latitudes.
– Surface ultraviolet irradiance measurements were also completed to observe Earth-atmospheric evidence of asymmetric ultraviolet opacity over the eclipse. This could have a bearing on how observations of the corona are interpreted. This was done in collaboration with Ralph Lorenz from Johns Hopkins University Applied Physics Lab (simple photodiode sensors equivalent to those flown on the Mars Science Laboratory Curiosity and the Beagle 2 lander). Additional low-cost ultraviolet and visible flux measurements were carried out, including measurements of a decline in all-sky brightness during totality — in a silicon solar cell, the brightness declined to < 0.02% of post-eclipse values.

The TAROT observations

One century ago, on 29 May 1919, a seminal experiment led by Arthur Eddington confirmed Albert Einstein's prediction that light can be deflected by mass. Eddington used the Sun as a mass deflector and nearby stars as the targets with which to measure the light deflection. The experiment becomes feasible during a total solar eclipse because sky brightness drops to twilight levels and stars close to the Sun can be observed.

In 1915, Einstein predicted that the apparent position of a star is shifted radially away from the centre of the Sun. He predicted an angular displacement of 1.751 arcseconds when a star grazes the Sun's limb (twice the amount expected by Newtonian mechanics). This displacement decreases as the inverse of the distance to the centre of the solar disc.

Télescope à Action Rapide pour les Objets Transitoires (TAROT; see Figure 6) is a robotic telescope that was installed at ESO's La Silla Observatory in 2006 (Klotz et al., 2013). The primary goal of the TAROT team[b] observations was to repeat the Eddington Experiment. The telescope has an aperture of 25 cm, a

Figure 5. The TAROT telescope pointing north towards the Sun during totality. The enclosure of the NTT can also be seen. This frame is taken from TAROT's webcam sequence of the full eclipse[8].

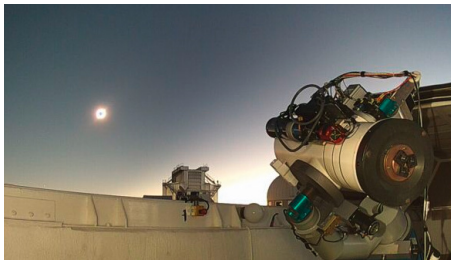

The TAROT team

CESAR/ESA

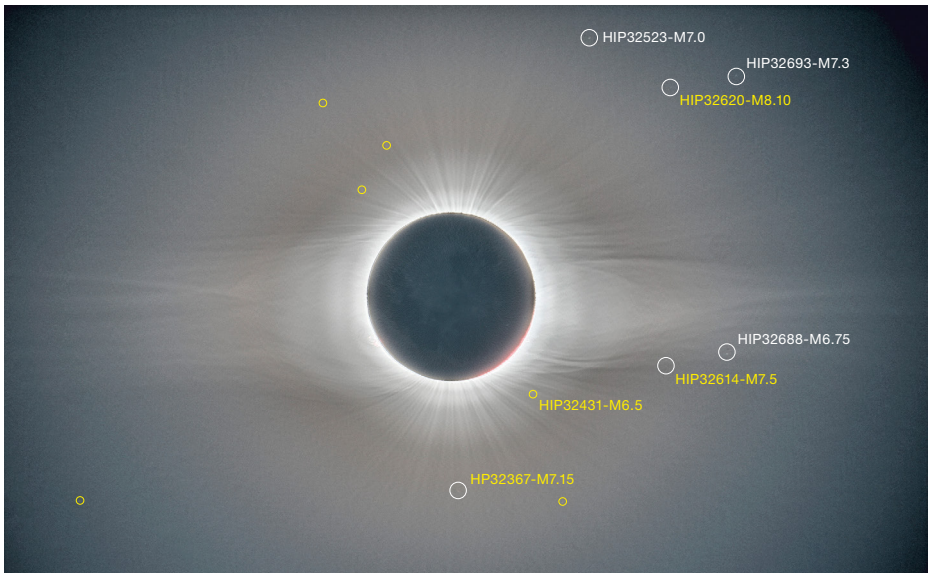

Figure 6. Stars during totality; 12 stars become visible through the extended corona, at separations less than six solar radii on sky.

focal length of 850 mm and a CCD camera that provides a field of view of 1.8 × 1.8 degrees with a spatial sampling of 3.29 arcseconds per pixel.

The stellar positions are measured experimentally on an image using Cartesian coordinates from the CCD sensor. The main difficulty is to link the Cartesian coordinates of the sensor to celestial coordinates on the sky, particularly as the light from stars recorded on the CCD is also affected by other physical effects unrelated to the Sun's gravitational field. Removing or accounting for these effects is crucial to allowing the accurate measurement of the gravitational deflection and confirming the general theory of relativity.

The most common way to calibrate these additional effects consists of recording images of field stars during a night with similar conditions to those during the eclipse: i.e., the same elevation of the stars, same optical setup, same temperature, etc. In the case of the TAROT observations, the advantage is that, as the telescope stays in the same place, the same stars that would be close to the Sun on sky during the eclipse can conveniently be observed at any period roughly six months before or after the eclipse.

The extended atmosphere of the Sun, the corona, poses another difficulty. The corona adds diffuse light which is not homogeneous because of its filamentary structure. Although very beautiful, coronal features can reduce the accuracy of the positional measurements of the stars.

Six months before the eclipse, a series of images of field stars were recorded at exactly the same elevation as during the eclipse. The analysis of these images demonstrated the ability to measure stellar positions with an accuracy on the order of ± 0.25 arcseconds, corresponding to an error of ± 15% in the value of the expected angular displacement that has been predicted by general relativity. Unfortunately, the TAROT CCD camera failed one month before the eclipse and had to be replaced two days before the eclipse. In order to have proper calibration images, the optical setup will be kept the same as during the eclipse, with the aim of recording new calibration images in January 2020.

The night before the eclipse, about 200 images were recorded in the same direction as the eclipse in order to compute the calibration coefficients between Cartesian coordinates and celestial coordinates. A second, more complex, calibration method is ongoing which involves computing the optical deformations for each image and merging all of the individual calibrations onto a master frame.

During the hour before totality, the partial eclipse was recorded with TAROT using an additional aperture solar filter. This filter was manually removed at the beginning of totality. A software script was specially written to record images during totality and to point the telescope away from the Sun when totality was over. Owing to the inherent dangers to the equipment, all of the steps were practised many times in the hours before the eclipse. In the end, image acquisition worked perfectly during the eclipse. A first analysis of the images shows that

PACA_SolPol19

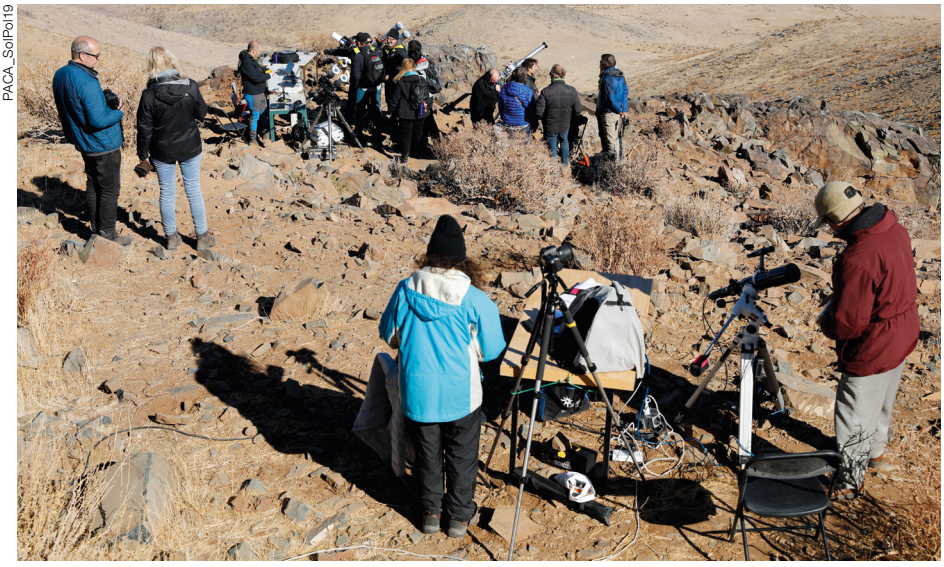

Figure 7. Part of the PACA_SolPol19 setup on one side of the La Silla mountain.

stars are detected on images with exposure times of 5 and 10 seconds. The 1-second images do not saturate the corona but stars are almost undetectable. To illustrate the principles behind this experiment an image has been synthesised using one 1-second image and with stars visible from the 5- and 10-second images (see Figure 7). The next step will be the January 2020 observations needed for calibration.

The PACA_SolPol19 Activities

The Pro-Am Collaborative Astronomy project formed a a professional-amateur collaboration PACA_SolPol19[c] is to measure the linear polarisation of the K-corona during the total eclipse. The solar corona, extending far from the Sun, is hotter than the photosphere. The outer part of the corona becomes the solar wind that moves outward through the Solar System and interstellar space, interacting with planetary atmospheres and other Solar System objects, creating space weather. The corona exhibits radial filamentary structure — bright long streamers at all latitudes during periods of high solar activity.

During low solar activity, as during this eclipse, streamers are mostly limited to lower latitudes. The corona, being thin and tenuous, is only observable during total solar eclipses or with the use of a coronagraph to block the disc of the Sun.

ESO/C. Guirao/G. Ávila

Figure 9. The CAOS group comprised Carlos Guirao and Gerardo Ávila (both from ESO), seen here on their observing post on the NTT platform.

A major unanswered question in astrophysics is how the corona is heated. Current coronagraphs block much of the inner corona, making eclipses the simplest way this region can be investigated from the ground. Since the inner corona (K-corona) is dominated by electron scattering, which is linearly polarised, observations of polarised brightness during an eclipse provide information about the distribution of polarisation and the polarisation brightness, p_B, which is related to the local electron density.

PACA_SolPol19 consisted of four mini-teams, three of them located at the La Silla Observatory (Figure 8), using one imaging telescope and two polarimetric setups (one with a programmable polarisable sensor and the other with a polarised sensor), and one imaging setup at sea level at Punta de Choros, La Higuera. All setups used the same software to acquire imaging and polarimetric data, taking advantage of similar observing conditions and initial data reduction techniques. Detailed flat-fielding, calibration, and derivation of the polarisation follow procedures used to calibrate the data from the 2017 total solar eclipse in the USA. The end goal is to measure the polarisation brightness, degree of linear polarisation and angle of linear polarisation images (Elmore et al., 2000; Lites et al., 1999; van de Hulst, 1950; Quémerais & Lamy, 2002).

The team successfully imaged the K-corona, revealing equatorial streamers (as expected for a quiet Sun), and produced a map of the polarisation brightness (see Figure 9). The colours in the polarisation brightness map represent the angle of linear polarisation, with red being the maximum. The quiet Sun exhibited polarimetric minima at the solar poles and polarimetric maxima at the solar equator, with the solar prominence exhibiting low polarisation.

In addition, the solar prominence on the north-west limb of the Sun and two stars were imaged, one towards the north east and one to the south west (tentatively

Figure 8. Left: The average total intensity of the corona. Middle: Sobel-filtered image of the solar corona. Right: The product of polarised brightness (pB) and the angle of linear polarisation, colour-coded with red indicating the maximum polarisation and green minimum polarisation.

PACA_SolPol19

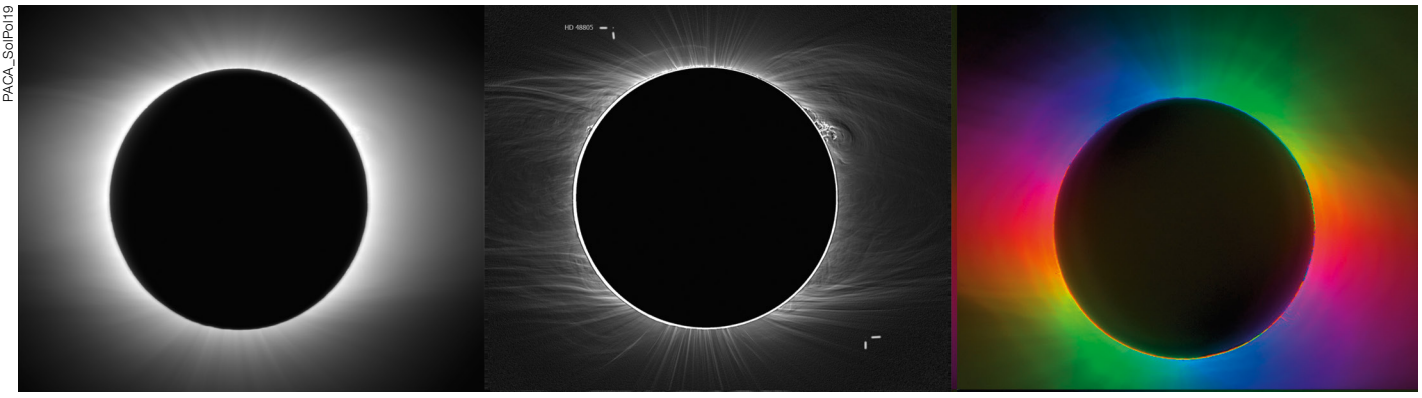

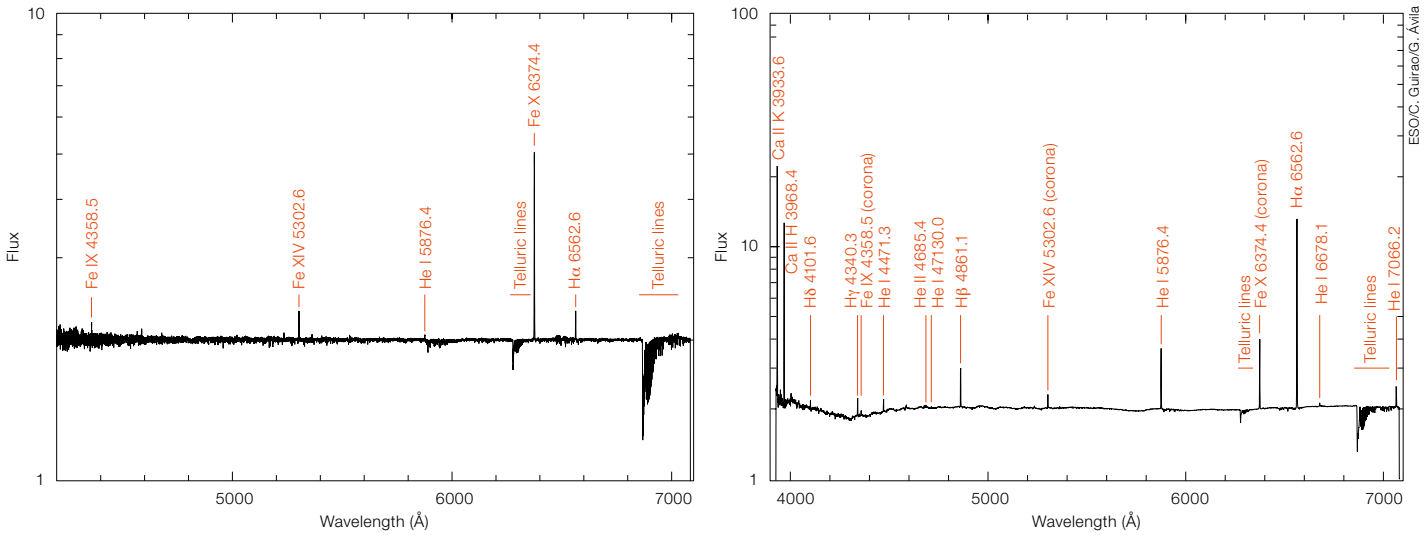

Figure 10. The two total solar eclipse spectra from the CAOS group: the spectrum of the corona (left, 10 exposures of 5 seconds) and the prominence (right, 3 exposures of 5 seconds).

identified as HD 48805 [SAO 78717] and HD 262616).

CAOS group

The group from the ESO Club of Amateurs in Optical Spectroscopy (CAOS)[d] (Figure 10) was observing from the NTT platform using a commercial 11-inch Schmidt-Cassegrain telescope and a spectrograph with a resolving power of 11 000 and spectral range of 3930–7070 Å. A commercial SBIG ST1603ME CCD camera recorded the spectra, which were calibrated with a thorium-argon hollow cathode and halogen lamps linked with a 300-µm optical fibre, for spectral calibration and order identification respectively.

Before totality, the telescope was covered with a Mylar sheet with an optical density of OD-5 to protect the instrument and our sight. In total, 13 exposures of five seconds were taken during totality. The slit of the spectrograph was placed close to the north pole of the Sun, and three of these 13 exposures showed partial illumination of the slit by a solar protuberance. The remaining 10 exposures recorded only the much weaker corona spectrum.

Both the protuberance and corona spectra (Figure 11) were reduced with the ESO–MIDAS software. The corona spectrum shows the "classical" iron (Fe XIV and Fe X) and Hα lines. The He line at 5876 Å is barely visible.

However, in the spectrum of the prominence, we found some interesting features: Ca II, five helium lines and the four hydrogen lines of the Balmer series.

ESO webcast

Starting at 19:56 CEST on 2 July 2019, a team[e] deployed by ESO provided a live webcast of the 2019 La Silla Total Solar Eclipse (see Figure 12). Organisations in the ESO Member States and beyond incorporated the webcast into public events set up for the occasion of the eclipse[9] and members of the public viewed it online in high definition on ESO's website and on ESO's YouTube channel[10]. The 4-hour live webcast was a "raw" feed without commentary regularly switching between sources, and featuring views of the Sun from three small telescopes and two cameras showing spectators at La Silla. The webcast finished

Figure 11. Part of the ESO webcast team in their working area in the shade under the Ritz (old control room building, now visitor centre). Left is engineer Lionel Gauze (APICAL), in the middle producer François Glasser (APICAL) and to the right ESO Photo Ambassador Alexandre Santerne (Aix-Marseille University/CNRS/CNES/LAM).

with a beautiful view of the Sun setting over the Pacific Ocean to conclude a day of amazing experiences at La Silla.

Considerable planning, including simulations, was carried out in the months before the eclipse. Different potential vantage points were analysed in detail using the online application The Photographer's Ephemeris[11]; this also revealed limitations in the tool's sunset times, which are most likely due to atmospheric refraction not being properly considered. The webcast was seen by tens of thousands of viewers on 2 July and has since accumulated more than 250 000 views (see Figure 13).

Acknowledgements

All authors are grateful to ESO's management for maximising the potential presented by this unique occasion.

ESA/CESAR wishes to thank the teams that made the event possible, including the ESO Department of Communication, the ESA-CESAR observing team at La Silla and at ESAC, the ESA science directorate (ESA Director of Science Günther Hasinger), ESA-Communications, the ESA-GNSS Galileo Science Office, the University of Torino and ESA faculty for the EKPOL instrument and camera and Ralph Lorenz (ultraviolet measurements), Robert Nufer and Xavier M. Jubier (cameras control SETnC and Solar Eclipse Maestro) and the BepiColombo, Solar Orbiter, Proba-2, Proba-3 and SOHO projects from ESA.

The TAROT telescopes were built and are maintained thanks to the technical and financial support of CNRS-INSU (ARTEMIS, IRAP), CNES and OSU Pytheas.

The PACA_SolPol19 Team gratefully acknowledges the support and assistance of ESO's Department of Communications, especially Fernando Comerón, and is grateful for having been selected and given the opportunity to carry out both our science and outreach experiments at La Silla.

References

Elmore, D. F. et al. 2000, SPIE, 4139, 370
van de Hulst, H. C. 1950, Bulletin of the Astronomical Institutes of the Netherlands, 11, 135
Klotz, A. et al. 2013, The Messenger, 151, 6
Lites, B. W. et al. 1999, Solar Physics, 190, 185
Quémerais, E. & Lamy, P. 2002, A&A, 393, 295
Zangrilli, L. et al. 2009, Solar Physics and Space Weather Instrumentation III, Proceedings of the SPIE, 7438, 74380W

Notes

[a] The ESA/CESAR team consists of Manuel Castillo, Wouter van Reeven, Miguel Pérez-Ayúcar, Joe Zender, Darío Pérez de Carlos, Ralph Lorenz, Michel Breitfellner, David Cabezas, Donald Merrit, and Santa Martínez.

[b] The TAROT team consists of Alain Klotz, Adrien Nicolas Klotz, Jean-François Le Borgne, Eric Denoux, Christian Buil, Valérie Desnoux, Yoann Richaud, Rico Sautile, Xavier Regal, Julien Lecubin, Loic Eymar, and Michel Boer.

[c] The PACA_SolPol19 team consists of Padma A. Yanamandra-Fisher, Robert F. Fisher, David Elmore, Wahab A. Baouchi, Kyle A. Motl, Roy Wellington, Theo Wellington and Andrei Ursache.

[d] The CAOS team consists of Carlos Guirao and Gerardo Ávila.

[e] The ESO webcasting team consists of François Glasser, Lionel Gauze, Alexandre Santerne and Lars Lindberg Christensen.

Links

1 Total Solar Eclipse: https://www.eso.org/public/news/eso1912/
2 Overview of experiments conducted at La Silla during the Total Solar Eclipse: https://www.eso.org/public/announcements/ann19031/
3 Results webpage from the CESAR team: http://cesar.esa.int/index.php?Section=Total%20Solar%20Eclipse%202019%20results
4 Archive of CESAR images: http://cesar.esa.int/sun_monitor/archive/ra/visible/2019/201907/20190702/
5 CESAR images broadcast live during eclipse: https://youtu.be/JKA2Vu_Iyik
6 CESAR live-streaming webcast from the event: https://youtu.be/OTLbIPmvn4Q
7 ESA released images from the CESAR team: https://www.esa.int/spaceinimages/content/search?SearchText=%2Beclipse+%2Bcesar+%2Bjuly+-lunar&img=1&SearchButton=Go
8 Webcast from La Silla: https://www.youtube.com/watch?v=wEiyvX9GEDI&feature=youtu.be
9 Announcement of ESO webcast: https://www.eso.org/public/announcements/ann19027/
10 The ESO webcast page: https://www.eso.org/public/events/astro-evt/solareclipse2019/webcast/
11 The Photographer's Ephemeris: app.photoephemeris.com

Figure 12. Frame from the webcast at the time of totality.

DOI: 10.18727/0722-6691/5154

Pointing the NTT at the Sun: Studying the Solar Corona During the Total Eclipse

Michel Dennefeld[1]
Serge Koutchmy[1]
François Sèvre[1]
Hassan Fathivavsari[1]
Frédéric Auchère[2]
Frédéric Baudin[2]
Shahin Abdi[2]
Peter Sinclaire[3]
Ivo Saviane[3]
Francisco Labraña[3]
Linda Schmidtobreick[3]

[1] Institut d'astrophysique de Paris (IAP), Sorbonne Université, France
[2] Institut d'astrophysique spatiale (IAS), Université Paris-Sud, France
[3] ESO

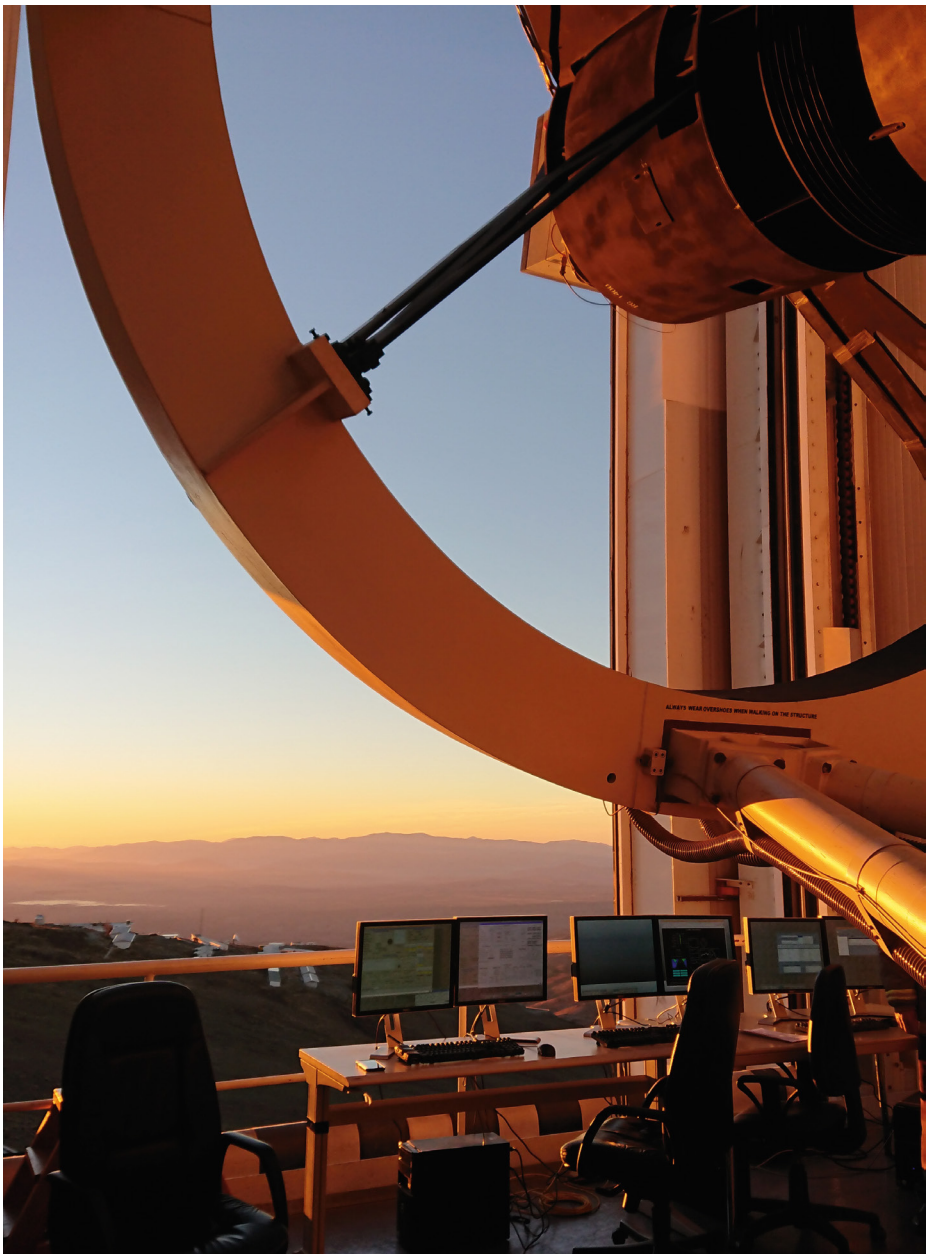

P. Sinclaire/ESO

Figure 1. The NTT pointing at the Sun, with a temporary control system set up directly in front.

As soon as we realised that the total solar eclipse of 2 July 2019 would be visible from the La Silla Observatory, we saw a rare opportunity to point a 4-metre-class telescope at the Sun to obtain spectra of its corona with unprecedented angular and spectral resolution. Despite the pessimistic reactions of many colleagues — "You are crazy, ESO will never accept..." — we pursued the idea and opened discussions with ESO in early 2018 to see how this type of observation could be carried out in practice. Our team presented a strong argument: this would not be the first time that a large telescope would be pointed at the Sun during an eclipse — it had previously been done successfully with the Observatoire de Haute-Provence (OHP) 1.93-metre telescope in 1961 (Wlérick & Fehrenbach, 1963) and the 3.6-metre Canada France Hawaii Telescope (CFHT) in 1991 (Koutchmy et al., 1994). The science case was to observe emission lines with different ionisation potentials at different positions across the corona with arcsecond angular resolution, in order to analyse the coronal heating mechanism. In the end, the team assembled included a number of people with extensive experience in both solar physics and observational techniques.

The question of which telescope to use then arose, and how we could obtain several high-resolution spectra during the short duration of totality (1m 48s). In practice, the New Technology Telescope (NTT) is the only telescope able to point as low as 13 degrees above the horizon, where totality would take place. A detailed procedure was arranged with the La Silla team to ensure the telescope could be used without risk of fire. There was, of course, no question that the telescope should be operated from a remote location (such as the Ritz control room), so computer consoles were erected right in front of the telescope (Figure 1). This allowed close monitoring, quick reaction times in case of problems, and, as a bonus, a privileged view of the eclipse — but did you ever try to read a screen with the Sun directly in front of you?! Thus, our programme using the ESO Faint Object Spectrograph and Camera v.2 (EFOSC2) at the NTT was proposed in Period 103 (Programme ID 0103.D-0139) and approved by the Observing Programmes Committee!

The main difficulty with the observation, once the above problems had been addressed, was the comparatively long

execution time needed to obtain a spectrum using the standard procedure of obtaining an image before moving to the slit — this would take more than a minute and there was no way to do the image analysis beforehand. We therefore had to rely on parameters obtained the previous night and point the telescope close to the Sun (but not at it), with the shutters closed, to first configure the mirror. It was then moved into position — defined only by coordinates and simulated coronal images — a few minutes before totality. We pointed to the west of the Sun, taking advantage of the moon protecting us from direct sunlight (Figure 2).

Exposure times had been determined weeks before through observations of the Moon; a sequence of 1-second exposures was launched with the telescope tracking normally (the Sun's motion is relatively small over the short duration of totality). The first exposures were in fact dark exposures, the Nasmyth shutter being finally opened only just before totality (C2) to obtain coronal spectra. The camera was commanded directly, without the use of Observation Blocks, allowing short total execution times of 25 s per spectrum in fast read-out mode, and the telescope was pointed away immediately at the end of totality. We obtained five good exposures of the corona, with the sixth being overexposed as Baily's beads appeared at the very end of totality (C3, Figure 2).

A high-resolution grism (Gr#20) was used with a specially manufactured offset slit (kindly provided by colleagues in Paranal) to obtain velocities and line profiles, albeit at the expense of spectral coverage. A lower-resolution, table-mounted auxiliary spectrograph was used in parallel outside the NTT to record the full coronal spectrum over a wider field of view but at a much lower spatial resolution. While the data reduction is still ongoing, preliminary results show that the coronal emission was quite weak; this is not surprising near solar activity minimum. The dominant line in the NTT spectra is the [Fe X] 6374 Å line (Figure 3). Perhaps more surprising is the Hα line, in spectra taken at the beginning and end of totality. It is of chromospheric origin, and is due to the variable illumination of the line of sight crossing low atmospheric layers

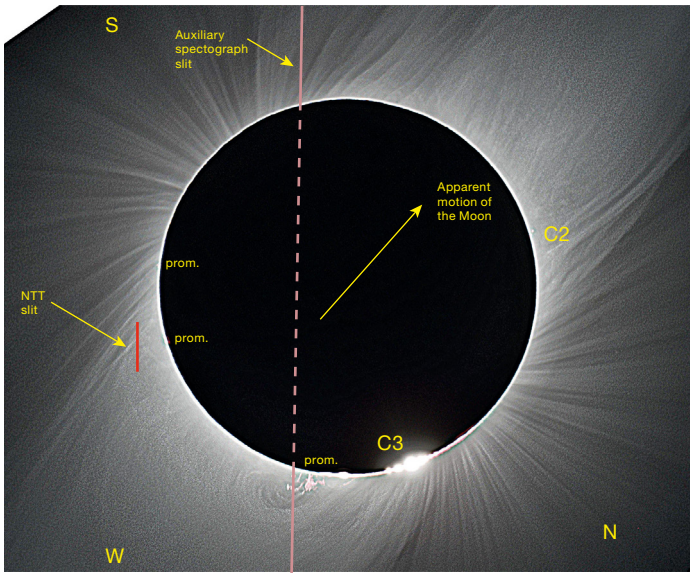

Figure 2. Slit positions plotted on a coronal image taken by Petr Horálek (ESO). Totality occurs when the lunar disc reaches the second contact point, C2 ,and lasts until it moves out at C3.

(Stellmacher & Koutchmy, 1974), as the Moon only covers the photosphere. A more careful analysis is under way to remove all artefacts, a challenging task in light of the unusual observing conditions and the fact that the telescope had to be pointed away quickly before calibrations could be obtained. Figure 3 (bottom) shows a spectrum obtained with the small auxiliary spectrograph; the lower part of the slit shows the corona, with [Fe X] dominating on the left edge. The upper part of Figure 3 shows the spectrum of a weak prominence recorded by chance (see the lower side of Figure 2), which is dominated by hydrogen and helium lines (order superposition is also present). Altogether, we obtained unique spectroscopic data during this eclipse, and we would like to warmly thank all the ESO staff who contributed to this success, both on the technical aspects and on the managerial side. A total solar eclipse is literally an extraordinary event, requiring a lot of preparatory work, but well worth the effort.

References

Wlérick, G. & Fehrenbach, C. 1963, *The Solar Corona*, Proceedings of IAU Symposium 16, ed. Evans, J. W., (New York), 199

Koutchmy, S. et al. 1994, A&A, 281, 249

Stellmacher, G. & Koutchmy, S. 1974, A&A, 35, 42

Figure 3. Top: Two EFOSC2-Gr#20 spectra of the corona taken at the same position but at two different times. The signal is dominated by the continuum of the K corona; note the presence of parasitic Hα. Bottom: Spectrum from the auxiliary spectrograph during totality.

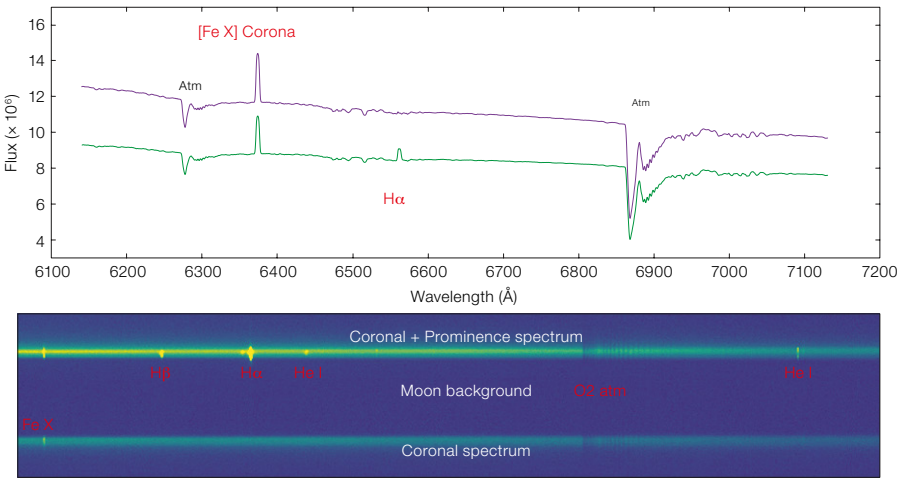

DOI: 10.18727/0722-6691/5155

Report on the ESO Workshop

KMOS@5: Star and Galaxy Formation in 3D — Challenges in KMOS 5th Year

held at ESO Headquarters, Garching, Germany, 3–6 December 2018

Eleonora Sani[1]
Michael Hilker[1]
Lodovico Coccato[1]
Suzanne Ramsay[1]
Chris Evans[2]
Myriam Rodrigues[3]
Linda Schmidtobreick[1]
Ray Sharples[4]

[1] ESO
[2] ATC, Royal Observatory Edinburgh, UK
[3] University of Oxford, UK
[4] Durham University, UK

The *K*-band Multi-Object Spectrograph (KMOS) is one of the second-generation instruments at the VLT, and has been operating for five years. To celebrate this anniversary this workshop brought together astronomers to present scientific results from KMOS and complementary instruments. The topics ranged from star formation in the Galactic centre, to stellar populations in globular clusters, to galaxy formation and evolution at various redshifts, and feedback from active galactic nuclei (AGN). Another goal of the workshop was to assess the impact of KMOS on its core science goals and to develop new strategies and programmes, also in light of future integral field unit (IFU) instruments. About 60 researchers from the astronomical community and members of the Instrument Operations Team participated in the workshop and discussed the above topics; these discussions served to identify the highest priority improvements that could increase the scientific return of KMOS in the future.

Motivations

Any advances in observational astronomy are ultimately based on the quality of observational data obtained with ever-improving, increasingly sophisticated, telescopes and instruments. KMOS enables deeper insights especially in areas related to galaxy formation and evolution, as well as a wider variety of scientific topics ranging from early stellar evolution to stellar populations and even including exoplanets.

Over the next few years, the community will have access to basic data on a large number of sources across a wide range of redshifts thanks to the upcoming or already available capabilities of survey instruments on powerful telescopes (for example, the Sloan Digital Sky Survey [SDSS], Wide Field infrared Camera for UKIRT [WFCAM], Visible and Infrared Survey Telescope for Astronomy [VISTA], VLT Survey Telescope [VST], High Acuity Wide field *K*-band Imager [HAWK-I], and Large Synoptic Survey Telescope [LSST]). The high-redshift samples will enable a new look at the early stages of the Universe when galaxies were young or still forming. Although the ensemble data already available — which have mostly been gathered by means of photometric techniques — are already providing valuable insights, a deeper understanding of the detailed physics underlying the formation and growth of galaxies requires more information about their individual properties. The coverage, in terms of star formation rates and redshifts, of the current KMOS Guaranteed Time Observation (GTO) surveys is shown in Figure 1. Such knowledge, in particular for high-redshift objects, was not sufficiently available so far. In particular, the one-dimensional spectra produced by classical spectroscopy are insufficient for a further investigation of the, often complex, galaxy morphologies and dynamics. Exactly the same limitation occurs in many other fields, for example, studies of metallicity gradients and dynamics in stellar clusters. This is indeed the framework within which KMOS is expected to play a fundamental role.

The KMOS@5 workshop aimed to bring together scientists working on all areas of star and galaxy formation and evolution using near-infrared IFU spectroscopy. The five-year milestone offered a perfect opportunity to assess the impact of KMOS on its core science cases. The workshop format allowed the exchange of strategies and ideas for analysis of the KMOS data, as well as fruitful discussion of future programmes. Finally, practical tutorials and demonstrations were offered and the users, together with the Instrument Operations Team (IOT), revised the priorities to improve and optimise the performance of KMOS over the next five years.

In the following sections we summarise some of the interesting talks and highlights from each session.

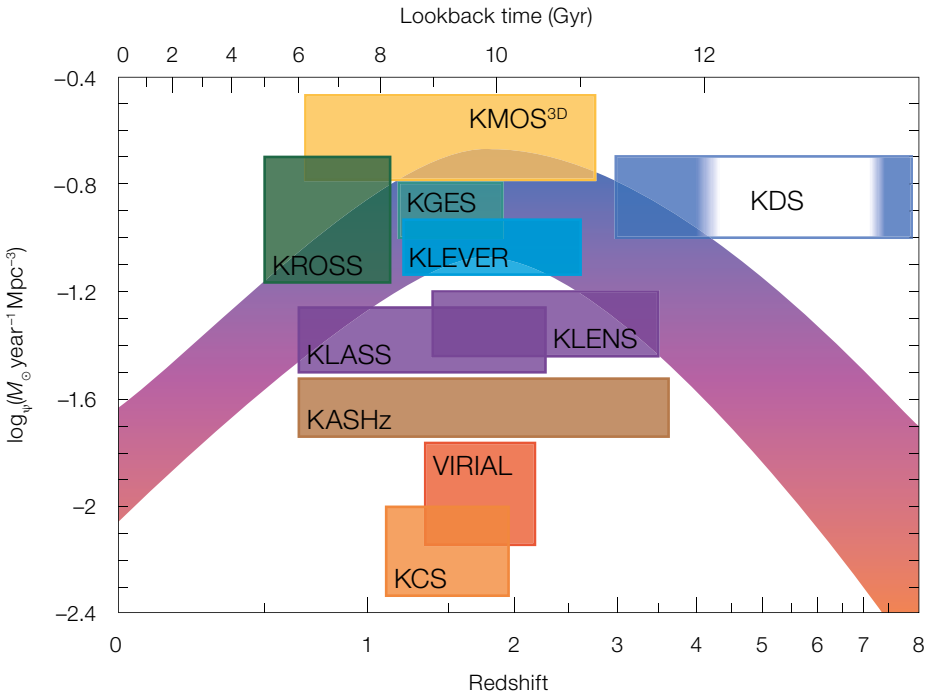

Figure 1. Cosmic star formation rate as a function of redshift and lookback time (plot from Natascha Förster-Shcreiber's talk; data from Madau & Dickinson, 2014).

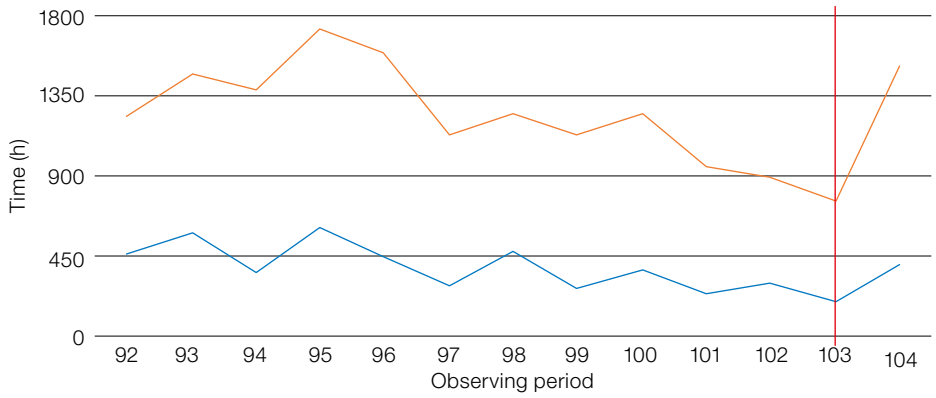

Figure 2. Requested and allocated time on KMOS. The vertical red line marks the small amount of time requested in Period 103, before the KMOS@5 workshop. The subsequent significant increase in Period 104 may be seen as the positive reaction of the community after the workshop.

Workshop opening

The meeting began with a welcome talk by Bruno Leibundgut, who presented the rising publication statistics of KMOS, which are currently dominated by GTO data, a natural consequence of the recently expired GTO time. He also showed that the demand for KMOS as measured by proposal numbers and time requested is steadily decreasing, reaching a minimum of only ~ 750 hours in Period 103 (see Figure 2). Bruno warned the participants that under-requested instruments may not be supported by ESO and have an increased risk of being decommissioned. This had the effect of shaking up the participants, and the wakeup call animated all subsequent speakers, further motivating them to illustrate the importance of KMOS for their science. It also triggered lively discussion of the future of KMOS throughout the conference.

Galactic and Local Volume science

The first scientific session concentrated on Galactic and Local Volume science with KMOS. It was convincingly shown that KMOS can be efficiently used to trace massive star formation and its feedback in both nearby star-forming galaxies as well as in the Galactic Centre and in star-forming regions of the Galactic disc.

Thanks to the multiplex capabilities of KMOS, as well as the mosaic mode with a monolithic IFU, it is possible to cover a large field of view (up to almost 1 square arcminute) and ~ 5 pc^2 of the Galactic centre have been observed. Anja Feldmeier-Krause discussed how young massive stars are centrally concentrated and that there exists a broad metallicity distribution of stars in the Nuclear Star Cluster (NSC) of the Milky Way based on ~ 700 KMOS spectra (Feldmeier-Krause et al., 2015, 2017). Anna McLeod also demonstrated that with the use of the mosaic mode of KMOS it is possible to examine the early stages of stellar feedback in star-forming molecular clouds within the Milky Way, which are only observable in the infrared because of extinction. In particular, it has become possible to trace the ionisation front and the molecular gas content at the same time. KMOS observations of massive star clusters reveal evidence for outflows and wind-blown bubbles in the environment of the clusters.

Francesco Ferraro described how the Multi-Instrument Kinematic Survey of Galactic globular clusters (MIKiS) allowed the determination of stellar kinematics across their full radial range. This survey was designed in synergy with the VLTI instruments, the Fibre Large Array Multi Element Spectrograph (FLAMES), KMOS, and the Spectrograph for INtegral Field Observations in the Near Infrared (SINFONI). Resolved kinematics of thousands of stars, combined with internal proper motions measured from Hubble Space Telescope (HST) campaigns (inner regions) and Gaia (outskirts), provide the first 3D kinematic maps of Galactic globular clusters. Surprisingly, they do not rotate as rigid bodies, but rather follow a Keplerian law with no significant evidence of intermediate mass black holes (see Ferraro et al., 2018; Lanzoni et al., 2018). The flexibility of KMOS allows studies of young massive star clusters in nearby galaxies, and Ben Davies showed how such clusters can be used as cosmic abundance probes to construct new mass-metallicity scaling relations based on red supergiants.

Galaxy assembly, dynamics and evolution

Day 2 was dedicated to galaxy assembly, and galaxy dynamics and evolution. The results of the main KMOS GTO programmes were presented, with particular focus on KLEVER (talks by the Principal Investigator Michele Cirasuolo and Mirko Curti), KROSS and KGES (Mark Swinbank and Alfred Tiley talks), and KMOS^{3D} the largest GTO programme (talks by the Principle Investigator Natascha M. Förster-Schreiber, Hannah Übler, Philipp Lang, David Wilman). Star formation rates, resolved kinematics and metallicities of more than 1000 star-forming galaxies at redshifts between 0.5 and 3 have been determined and have established the following:

i. Most galaxies (> 70%) are rotationally supported and the Hubble sequence emerged at around redshift z ~ 1.5 (Stott et al., 2016, Swinbank et al., 2017).
ii. In terms of metallicity, non-axisymmetric patterns are revealed from resolved metallicity maps, while azimuthally-averaged metallicity gradients are flat. It is also possible to characterise outflow statistics; while the incidence of star-formation-driven outflows depends on star formation properties, the fraction of AGN-driven outflows depends on the stellar mass and its concentration (Förster-Schreiber et al., 2019; Harrison et al., 2016).

A controversial topic in this session was whether the outer discs of galaxies at

redshift z ~ 1–2.5 have flat or falling rotation curves.

In his contribution, Philipp Lang discussed how a representative rotation curve for high redshift galaxies can be obtained with KMOS^{3D}; it is characterised by a significant decrease in velocity in the outer regions. Such a drop in rotation velocity can be explained by the dominance of baryons within the shallow inner dark matter potential. These results support the limited role of dark matter on disc scales (Lang et al., 2017; Übler et al., 2018). On the other hand, Alfred Tiley showed that stellar-scale rotation curves obtained from the KMOS Redshift One Spectroscopic Survey (KROSS) sample remain flat or continue to rise independently of redshift. This implies moderate to large dark matter fractions (≧ 66%) in star forming galaxies over the last 10 Gyr (Tiley et al., 2019).

On Day 3, the focus switched to lensed and very distant systems as well as AGN feedback and stellar kinematics. Results were presented from GTO surveys, such as KMOS^{3D}, the KMOS LENsing Survey (KLENS), and the KMOS Lens-Amplified Spectroscopic Survey (KLASS), related to the cosmic dawn. These surveys help in understanding the properties of distant systems. Charlotte Mason showed the first robust constraint on the intergalactic neutral hydrogen fraction at z ~ 8, inferred from deep spectroscopic limits on Lyα emission, and Marianne Girard discussed how the evolution of velocity dispersion depends on stellar mass.

AGN feedback and its effect on different stages of galaxy evolution were discussed during the afternoon, with results from the KMOS AGN Survey at High redshift (KASHz) and VIRIAL GTO programmes. Chris Harrison, Jan Scholz and Rebecca Davies argued that: (1) the most extreme gas kinematics are associated with AGN and outflows driven by low-power jets are important at low redshift; (2) there is no evidence of AGN-driven outflows quenching star formation in moderate luminosity AGN; and (3) the vast majority of the outflowing material does not have sufficient velocity to escape from the galaxy halos — rather it will be re-accreted, contributing to the build-up of stellar mass and angular momentum of the galaxies.

Trevor Mendel’s contribution dealt with the galaxy evolution mechanisms leading to massive and passive galaxies. He showed how they formed in a two-phase process: an early phase driven by rapid star formation on the main sequence, followed by the assembly of already existing stellar mass (Mendel et al., 2015). Also, such evolution can explain the typical decrease in dark matter fraction within the half-light radius.

The fourth and last workshop day was dedicated to the environment and late-stage evolution of galaxies. Alessandra Beifiori, Asmus Bohem and Sam Vaughan discussed KMOS Galaxy Cluster surveys like the KMOS Cluster Survey (KCS) and the KMOS Cluster Lensing And Supernova survey with Hubble (K-CLASH), showing that: (1) massive galaxies in big and old clusters are older than their analogues in the field; (2) gradual mass-growth mechanisms like minor mergers are favoured (Beifiori et al., 2017); (3) ram pressure stripping might compress gas in the inner discs, thus triggering star formation; and (4) non-circular motions are dominant in low-mass cluster members, thus indicating kinematic downsizing and/or interaction processes.

KMOS current and future perspectives

In addition to the scientific sessions, discussions on the present and future status of KMOS were held. We asked the audience to complete a questionnaire, and the answers were used to drive further discussions. In Figure 3 the results of the online survey are reported. Concerning the needs of the community, it is clear that archival search and pipeline improvements are two key areas of interest:

i. Querying the archive for KMOS data is tricky because so far only the central

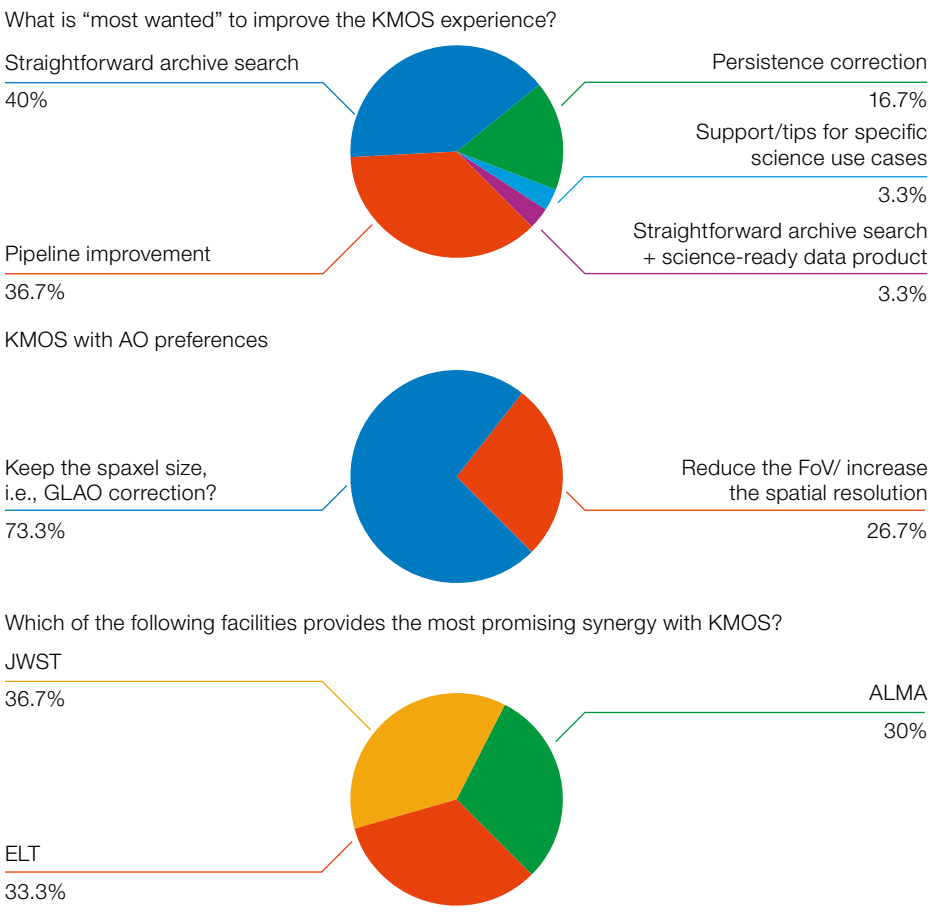

Figure 3. Online questionnaire about the most desired KMOS capabilities and synergies.

pointing coordinates of the KMOS field are searchable, rather than those of the individual targets. Such issues will be fixed shortly thanks to the new ESO Archive Science Portal and the data product release. ESO will indeed release reduced data cubes for single targets, which will be retrievable from the ESO Archive Science Portal[2].

ii. Pipeline capabilities should be improved. Since several recipes have been recently updated and released, the IOT asked the community to test the new releases and provide detailed feedback on specific tasks.

Moreover, the audience raised a concern regarding the ability of the Exposure Time Calculator (ETC) to provide the correct signal-to-noise ratio for the faintest objects. The ETC has been extensively tested on standard targets (such as stars and line-emitting regions, both Galactic and extragalactic) and it is able to provide a S/N fully consistent with the data. However, for those objects with a signal of the same order of magnitude as detector effects (i.e., variable bias, cross talk, remanence), the ETC underestimates the S/N by ~ 30% (Mason et al., 2019). The effect of imperfect sky subtraction cannot be simulated by simply scaling the S/N by a factor $\sqrt{2}$, and this, together with the above-mentioned factors, leads to the conclusion that the S/N for such extremely faint sources cannot be easily simulated within the ETC. Nonetheless, the IOT could provide the ETC with a fudge factor once the signal reaches a given threshold. A large amount of data (for example, from GTO and Large Programmes) is needed to determine this threshold, and the KMOS GTO teams together with PIs of Large Programmes are prepared to provide feedback to the IOT on this task.

We discussed possible upgrades of the instrument. The community was largely in favour of equipping KMOS with a Ground-Layer Adaptive Optics (GLAO) system to significantly improve the sensitivity, thanks to the AO correction, while still preserving the spatial sampling and hence the current field of view of each IFU. Another possibility considered (albeit not shown in Figure 3), is related to the deterioration of the arms — by far the most delicate optomechanical component in KMOS. In the unfortunate event that we run short on spares for the arms and are not able to build new ones, the solution could indeed be to reduce the number of arms, while increasing the field of view.

Regarding synergies between KMOS and other facilities, the community is divided on whether or not all of the major current and future facilities (for example, the Atacama Large Millimeter/submillimetre Array [ALMA], the Extremely Large Telescope [ELT], and the James Webb Space Telescope [JWST]) are considered crucial to fully exploiting the multiplex capabilities of infrared IFUs like KMOS. These themes also emerged during the sessions, for example, in the talks by Jan Scholz, Chian-Chou Chen, Michele Cirasuolo, Charlotte Mason and Dominika Wylezalek.

During a round table session the discussion turned to which approach would be more effective to increase demand for KMOS — whether it would be better to issue a call for Public Surveys[3] or for more Large Programmes. The community was in favour of the second option.

Data reduction tutorial

In the afternoon of the last workshop day, about 25 participants attended practical tutorials with hands-on sessions dedicated to KMOS data reduction, followed by a final *Glühwein* and *Spekulatius* farewell reception. The aim of the tutorial was to introduce the instrument, the design of the data reduction pipeline and the data reduction cascade, and to present the KMOS ESOReflex (Freudling et al., 2013) workflow as data reduction tool[4,5].

Special emphasis was given to the explanation of different data reduction strategies, including removal of telluric features and sky subtraction. Because KMOS data reduction can be complex, and the optimisation of the results can require different strategies and algorithms, members of the astronomical community have come up with their own solutions for specific datasets over the years, some of which were included in the KMOS pipeline and workflow.

Therefore, one aspect that was covered in the tutorial session was how to modify the KMOS workflow to include external Python scripts within the data reduction cascade.

Main conclusions & ways forward

The workshop brought together the KMOS community to celebrate the fifth anniversary of the first second-generation VLT instrument. All GTO and Large programmes as well as some dedicated studies produced great scientific results, leading to a steadily rising publication and citation record.

The interaction between the community and the KMOS IOT has been fruitful and has led to the implementation of new strategies to broaden the number of users and plan the future of KMOS and its operations. Bruno Leibundgut's warning regarding a decline in the demand of KMOS had a very positive effect on the KMOS community. In Period 104, the requested KMOS time significantly increased, to a level comparable to the first time the instrument was offered (see Figure 3). This can be seen as a great success of the KMOS@5 workshop.

Demographics

The Science Organising Committee sought fair representation from the KMOS science community in terms of gender, seniority and institutes. The committee invited 11 speakers to cover all scientific topics and major KMOS programmes, with a 6:5 ratio of male to female speakers and 5:6 ratio of senior (staff) to junior (postdoc level) speakers. The total number of participants was 60 (with a female fraction of 42%), which allowed a focused and interactive workshop with relaxed time constraints. We therefore had the luxury of accepting all requested talks (25) and posters (6), with the exception of three submissions that were out of the scope of the conference. The gender balance for different groups in the conference can be seen in Figure 4. The female representation was between 33% to 50% in all categories.

The level of participation from young researchers was very high, with the following breakdown according to seniority: ~ 33% students, ~ 35% postdoctoral

researchers, and ~ 30% tenure-track or tenured faculty. In particular, the junior researchers were well-represented in the talks (see Figure 4). Given the nature of the KMOS science community, most of the attendees (excluding the LOC members) came from European institutes (~ 90%), and the rest (~ 8%) from the United States and Australia (~ 2%). The conference picture (Figure 5) shows the majority of the participants in front of the ESO headquarters.

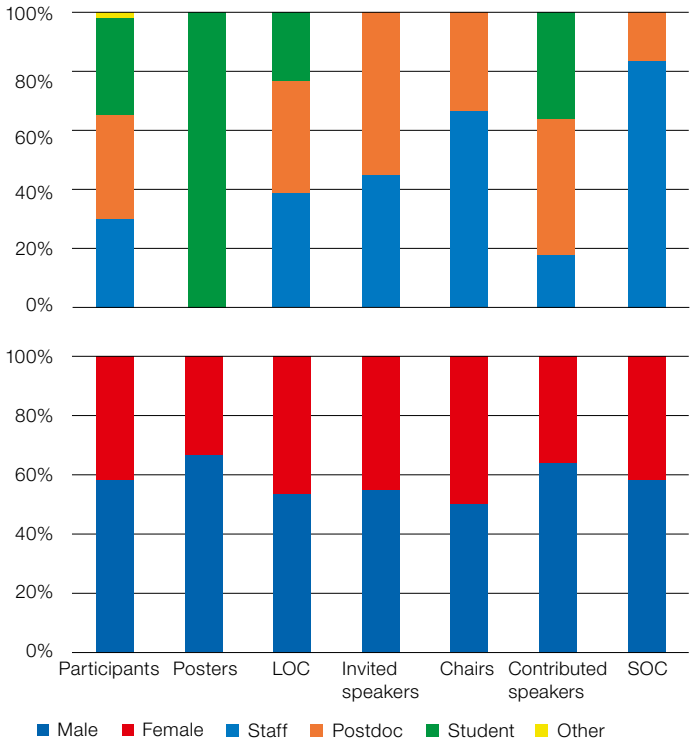

Figure 4. Gender balance and career stage statistics for the KMOS 2018 workshop.

Acknowledgements

We thank all the participants in the KMOS 2018 workshop for their enthusiasm, and the speakers for their outstanding scientific contributions. We are grateful to the Directorate of Science, the Science Operations Department, the Instrument Science Department and the User Support Department for their financial support of this workshop.

References

Beifiori, A. et al. 2017, ApJ, 846, 120
Feldmeier-Krauser, A. et al. 2015, A&A, 584, 2
Feldmeier-Krauser, A. et al. 2017, MNRAS, 464, 194
Ferraro, F. et al. 2018, ApJ, 860, 50
Freudling, W. et al. 2013, A&A, 559, 96
Förster-Schreiber, N. et al. 2019, ApJ, 875, 21
Harrison, C. et al. 2016, MNRAS, 456, 1195
Lang, P. et al. 2017, ApJ, 840, 92
Lanzoni, B. et al. 2018, ApJ, 856, 11
Madau, P. & Dickinson, M. 2014, ARA&A, 52, 415
Mason, C. et al. 2017, ApJ, 838, 14
Mason, C. et al. 2019, MNRAS, 485, 3947
Mendel, J. T. et al. 2015, ApJ, 804, 4
Stott, J. P. et al. 2016, MNRAS, 457, 1888
Swinbank, M. et al. 2017, Nature, 543, 318
Übler, H. et al. 2018, ApJ, 854, 24
Tiley, A. et al. 2019, MNRAS, 485, 934

Links

[1] Link to workshop programme and presentations: https://www.eso.org/sci/meetings/2018/KMOS2018/program.html

[2] The ESO Archive Science Portal: http://archive.eso.org/scienceportal/home

[3] ESO Public Survey Policies: https://www.eso.org/sci/observing/PublicSurveys/policies.html

[4] ESO Reflex: https://www.eso.org/sci/software/esoreflex/

[5] KMOS Tutorial Session at the workshop: https://www.eso.org/sci/meetings/2018/KMOS2018/tutorial.html

Figure 5. The KMOS@5 participants.

ESO/L. Calçada

DOI: 10.18727/0722-6691/5156

Report on the ESO Workshop

Preparing for 4MOST — A Community Workshop Introducing ESO's Next-Generation Spectroscopic Survey Facility

held at ESO Headquarters, Garching, Germany, 6–8 May 2019

Joe Liske[1]
Vincenzo Mainieri[2]

[1] Universität Hamburg, Germany
[2] ESO

The 4-metre Multi-Object Spectroscopic Telescope (4MOST) is a state-of-the-art, high-multiplex, fibre-fed, optical spectroscopic survey facility currently under construction for ESO's 4-metre Visible and Infrared Survey Telescope for Astronomy (VISTA). During the first five years of operation 4MOST will be used to execute a comprehensive programme of both Galactic and extragalactic Public Surveys, and 30% of the observing time during this period will be available to the community. The purpose of this workshop was to prepare the ESO community for this exciting scientific opportunity.

ESO has a long history in survey astronomy, dating all the way back to its original mission. A new chapter will be added to this history by the advent of 4MOST, a spectroscopic survey facility featuring a field of view large enough to survey a large fraction of the southern sky in a few years, and a multiplex of 2400 fibres enabling surveys of tens of millions of objects (de Jong et al., 2019). 4MOST will spectroscopically complement a number of current and future facilities, including Gaia, eROSITA and Euclid, and will address a wide range of science areas, from the structure of the Milky Way to cosmology.

To enable its science goals, 4MOST was specifically designed as a facility for executing large surveys. Hence, for a period of at least five years, VISTA will be dedicated exclusively to observations with 4MOST, and the 4MOST facility will in turn be dedicated entirely to a comprehensive, five-year programme of both Galactic and extragalactic surveys. 70% of the observing time during this five-year period will be awarded to the 4MOST Consortium in return for delivering and operating the facility. This time will be spent on a set of 10 distinct yet interlocking surveys, collectively known as Consortium Surveys. The other 30% of the observing time will be available to the ESO community to conduct additional surveys. Regardless of their provenance, however, all 4MOST surveys will be ESO Public Surveys.

The process of selecting the Community Surveys will be initiated by a Call for Letters of Intent for Public Spectroscopic Surveys, to be issued by ESO by the end of 2019. The workshop reported on here was jointly organised by ESO and the 4MOST Consortium to prepare the broader ESO community for this exciting scientific opportunity, to help potential Principal Investigators (PIs) respond successfully to the Call, and to foster scientific collaborations between the community and the 4MOST Consortium.

Specifically, the goals of the workshop were: (i) to provide the ESO community with up-to-date information regarding the 4MOST facility, its capabilities, survey strategy, data reduction and science pipelines, the 4MOST Consortium's scientific plans, and the application and selection processes for 4MOST Community Surveys; (ii) to provide the ESO community with an opportunity to present their scientific ideas for 4MOST Community Surveys; and (iii) to provide a platform for discussion, networking and collaboration between potential Community Survey PIs and the 4MOST Consortium, and to explore complementarities between Consortium Surveys and potential Community Surveys.

To prime the workshop, the 4MOST Consortium had published a series of 13 articles in the March 2019 issue of The Messenger[1] (i.e., two months before the workshop), describing the facility, its operations, the survey strategy, and each of the 10 Consortium Surveys.

Broadly speaking, the presentations at the workshop fell into three categories, which are described in the following sections.

Providing information about 4MOST to the community

The seven presentations in the first category essentially provided the community participants in the workshop with "technical" information about 4MOST. These presentations largely corresponded to the articles by de Jong et al. (2019), Walcher et al. (2019) and Guiglion et al. (2019) in the above-mentioned 4MOST issue of The Messenger, and all of the information presented is also available on the 4MOST website[2]. The 4MOST PI, Roelof de Jong, presented an overview of the 4MOST project and the technical characteristics and capabilities of the facility. In a separate presentation he also laid out the constraints and principles of the survey strategy.

Jakob Walcher provided a very lucid, high-level account of the complex 4MOST operations scheme. This was a particularly important talk because several aspects of this scheme, including the role of the 4MOST Consortium in operations, and the concepts of a shared focal plane and participating and non-participating Community Surveys, are new to the world of ESO operations and were thus unfamiliar even to experienced ESO users. This talk was further complemented by Nic Walton's presentation on 4MOST data reduction and scientific analysis pipelines, and data products. Sofia Feltzing and Joe Liske explained the concept of the 4MOST Science Team in some depth, i.e., the organisational entity within which all of the Consortium and participating Community Surveys work together to plan, execute and exploit the 4MOST survey programme. Finally, Vincenzo Mainieri, the ESO 4MOST Project Scientist, detailed the process by which ESO will select the Community Surveys.

The second category comprised 10 presentations, one for each Consortium Survey, in which the 4MOST Consortium laid out its scientific plans. Briefly, the Consortium Surveys consist of: four surveys complementing Gaia and targeting the bulge/disc and halo components of the Milky Way at low and high spectral resolutions, respectively; a survey of the Magellanic Clouds; two surveys following up galaxy clusters and active galactic nuclei (AGN) detected by the X-ray telescope e-ROSITA, respectively; a galaxy evolution survey; a cosmology survey; and, finally, a survey dedicated to the follow-up of extragalactic transients.

ESO/M. Zamani

Figure 1. Participants at the Preparing for 4MOST workshop outside ESO headquarters.

Each of the talks in this category presented the survey’s scientific context, specific goals, currently planned survey area and target selection, and its data quality requirements. The goal of these talks was to provide potential Community Survey PIs with enough information to decide whether the scientific questions they had in mind (i) are already addressed explicitly by the Consortium, (ii) can be addressed with the Consortium Surveys’ data (all of which will be made public), or (iii) require a new survey. Since the Consortium Surveys were already succinctly described in the above-mentioned 4MOST issue of the Messenger we will not discuss these talks further here.

Community proposals: Galactic science

The third category consisted of 16 presentations in which members of the community presented their science cases for Community Surveys. Eight of these were concerned with Galactic science, and a recurring theme among them was that 4MOST’s wide field of view is singularly well suited to studying stellar clusters, associations, star-forming complexes and their larger scale environment. Sara Lucatello and Antonella Vallenari jointly proposed complementing the chemo-dynamical studies of field stars by the Consortium Surveys with a commensurate effort to understand the formation of stellar clusters, their evolution, and their relation with the field population by conducting a comprehensive survey of 120 globular and 1500 open clusters.

Meanwhile, Henri Boffin argued the case specifically for observing young stellar clusters in order to unravel their connected formation histories in large complexes. Similarly, Nicholas Wright outlined a survey of high- and low-mass young stars and ionised nebulae across several massive star-forming complexes to extend our view of star formation and early stellar evolution beyond the most nearby and most clustered stellar systems to the entirety of such star-forming complexes. This limitation on our current view of star formation also motivated Germano Sacco to propose an unbiased survey of all pre-main sequence and upper main sequence stars within 500 pc. Pre-main sequence stars were also on Giacomo Beccari’s mind, but in the context of protoplanetary discs, and he discussed how 4MOST data of such stars in young starburst clusters could add chemical and kinematic information to existing Hα, Gaia and WISE data to comprehensively understand disc fractions and lifetimes.

Moving away from clusters and star formation, Carme Gallart addressed the formation history of the Milky Way by discussing age distributions (derived from Gaia colour-magnitude diagrams) of geometrically defined halo and disc samples and proposed a similar analysis for samples defined by abundances and kinematics using 4MOST. Tommaso Marchetti made an interesting case for a 4MOST survey of thousands of candidate hypervelocity stars identified from Gaia data in order to obtain their radial velocities and chemical compositions. A full characterisation of this high velocity population would allow us to trace the Galactic potential and constrain the environment of the Galactic centre, whence these stars were ejected. Finally, Giampaolo Piotto discussed the crucial role of 4MOST in characterising the target sample of the PLATO mission.

Community proposals: extragalactic science

Kicking off the extragalactic part of the community talks, Hans Böhringer put forward a proposal for a 4MOST redshift survey of candidate members of galaxy clusters in the redshift range 0.4–0.8, selected initially from KiDS and VIKING, and later from Euclid. He argued that this survey would support the main Euclid cluster science by extending the cluster sample below a redshift of 0.8 (where Euclid’s own infrared spectroscopy is ineffective) and calibrating the Euclid cluster selection function and cluster masses with high precision. On the topic of AGN, Gandhi Poshak described his efforts to construct a complete sample of AGN within 250 Mpc, which 4MOST could support by providing spectroscopic follow-up of infrared- and X-ray-selected candidates.

Moving on to the domain of galaxies, Arjen van der Wel summarised some results from the recently completed VLT survey Large Early Galaxy Astrophysics Census (LEGA-C) and shared his thoughts on the possibility of complementing the Consortium’s galaxy redshift survey (Wide-Area VISTA Extragalactic

Survey — WAVES) with an intermediate redshift, high-S/N extension, thus allowing stellar populations, star formation histories and kinematics to be derived with the same precision as in the local Universe. Along the same lines, Amata Mercurio presented her proposal for a southern (i.e., 4MOST) extension of the high-S/N Stellar Populations at intermediate redshifts Survey (StePS) which will be carried out with WEAVE, a wide-field multi-object and multi-IFU facility on the William Herschel Telescope. The distinguishing feature of StePS-South would be its synergy with WAVES, i.e., the combination of deep spectroscopy and detailed environmental information.

Another type of synergy — that between 4MOST and MeerKAT — was discussed by Kenneth Duncan. He described the wealth of information that could be derived from the combination of 4MOST spectroscopy with radio continuum and HI data from the deep extragalactic MeerKAT surveys MeerKAT International GigaHertz Tiered Extragalactic Exploration (MIGHTEE) and Looking at the Distant Universe with the MeerKAT Array (LADUMA). This would include, *inter alia*, the star formation history of the Universe, the evolution of the cosmic HI density, and the fundamental relations between galactic HI content and star formation, stellar mass, and environment. Lingyu Wang then proposed a multi-purpose 110-square-degree redshift survey of 0.5 million intermediate redshift galaxies in Stripe 82, a region covered by a wealth of multi-wavelength data, with the primary aims of constraining the nature of dark matter and dark energy, and tracing galaxy and AGN evolution over the redshift range 0.2–0.6. Turning to the low-redshift Universe, Edward Taylor reported on the forthcoming Taipan survey and proceeded to make the case for a complete hemispheric 4MOST redshift survey of 5.5 million galaxies out to a redshift of 0.1 to study the baryon lifecycle of galaxies as a function of mass and environment, and to map out the large-scale density and velocity fields. Finally, Dominik Bomans highlighted the ability of 4MOST to identify relatively large samples of rare galaxies by focusing on the case of extreme emission-line galaxies.

The presentations from the three categories above were interspersed with one another and spread throughout the programme[3]. Also, each day of the workshop included two question and discussion sessions to provide the opportunity for participants to clarify any remaining issues, and to jointly discuss the connections between the scientific ideas presented by the community and the Consortium's plans.

Conclusions

The workshop was a resounding success. As was expected, the community identified a number of exciting scientific themes, ranging from protoplanetary discs to galaxy evolution and cosmology, that can be addressed with 4MOST in addition to the science cases proposed by the Consortium. Many of the community speakers stressed the complementarity between their science goals and those of the Consortium Surveys, thus reinforcing the vision that the scientific value of the 4MOST survey programme as a whole is larger than the sum of its constituent parts. Furthermore, of the ~ 90 workshop participants in total, about 55 were from the community. Considering that this workshop was mostly aimed at potential PIs of Community Surveys, we believe that the turnout, as well as the wide range of science cases presented, demonstrated the strong interest within the community in the large-scale survey capabilities provided by 4MOST. In turn, the organisers received feedback from community participants indicating that the Consortium and ESO had done a good job of providing relevant information to the participants.

Demographics

Although the Scientific Organising Committee considered gender balance while putting together the programme, this was not easy to achieve owing to the special nature of this workshop. Of the total sample of 33 speakers only 8 (24%) were women. This was due to only 1 out of 7 speakers in the first category above being female, reflecting a dearth of women in leadership positions in the 4MOST project, and only 4 out of 16 (25%) talks contributed by the community being delivered by women. The latter ratio was unfortunately slightly lower than the ratio of 7:24 (29%) among the requested talks, but the SOC agreed that the three submissions by women that were not selected did not sufficiently address the goals of the workshop. In the second category (i.e., science presentations by the Consortium) the gender balance was slightly better; while the female fraction should have been 40% in this category according to the initial planning, it became 30% owing to the late arrival of one of the female speakers. This percentage is still representative of the 31% of Consortium Survey PIs who are women. Full gender parity was achieved among the session chairs.

In terms of academic age, the speaker roster was heavily biased towards senior people, with only three postdocs and one PhD student among the speakers. We attribute this again to the special nature of this workshop, where the Consortium was represented by senior figures of the 4MOST project and the Consortium Surveys; similarly, the community was represented by potential leaders of Community Surveys. Such positions tend to require long-term employment stability, i.e., permanently employed staff.

Acknowledgements

The organisers would like to thank ESO for providing the financial, administrative and logistical support for this workshop. Special thanks goes to Stella Chasiotis-Klingner and the rest of the LOC for the smooth and flawless organisation, to Tania Johnston — the ESO Supernova coordinator — for a very enjoyable planetarium show, and to the librarians for their support in publishing the talks using Zenodo.

References

de Jong, R. S. et al. 2019, The Messenger, 175, 3
Guiglion, G. et al. 2019, The Messenger, 175, 17
Walcher, C. J. et al. 2019, The Messenger, 175, 12

Links

[1] Link to 4MOST Messenger issue: https://www.eso.org/sci/publications/messenger/toc.html?v=175&m=Mar&y=19
[2] Link to 4MOST website: https://www.4most.eu
[3] Link to workshop programme: https://www.eso.org/sci/meetings/2019/4MOST/program.html The workshop programme contains links to videos and PDFs of all presentations, as well as videos of the discussion sessions.

DOI: 10.18727/0722-6691/5157

Report on the ESO Workshop

ALMA Development Workshop

held at ESO Headquarters, Garching, Germany, 3–5 June 2019

Tony Mroczkowski[1]
Carlos De Breuck[1]
Ciska Kemper[1,2]

[1] ESO
[2] Academia Sinica, Institute of Astronomy & Astrophysics (ASIAA), Taipei, Taiwan

The Atacama Large Millimeter/Submillimeter Array (ALMA) is the most sensitive observatory spanning millimetre and submillimetre wavelengths. To maintain this position, however, a vibrant and concerted development programme is necessary. Since each partner region in ALMA conducts its own development programme, we hosted an international workshop at ESO to promote further cross-regional discussion of our parallel development efforts. As we describe here, an overriding goal for this was to align our development activities with the goals of the 2030 ALMA development roadmap — a report recently produced by ALMA to provide guidance on what directions we want the ALMA observatory to go in, and how to get there.

Motivations

ALMA[1] is the world's most sensitive facility for millimetre/submillimetre astronomical observations, and will soon be fully operational in all of the originally planned bands (35–950 GHz). Over the last seven years, ALMA has continuously delivered exciting and often surprising results in all areas of astronomy[2], from observations of the first galaxies to the multiphase gas in large-scale structures, and from forming protoplanetary discs to observations of the Sun.

ALMA is a collaboration among three partner regions — Europe (through ESO), North America (USA, Canada and Taiwan), and East Asia (Japan, Korea and Taiwan) — with Chile. In order to keep ALMA at the forefront of technology, each ALMA partner has a continuous development programme. Within Europe, ALMA activities are coordinated through ESO. Since each region conducts and funds its activities differently, we focus here on the EU-ALMA development programme. ESO strives to closely involve the Member State institutes in this programme by issuing calls for EU-ALMA development studies every three years.

In 2016, we decided to coordinate a workshop on ALMA development with that year's call for studies, and found the workshop to be an overwhelming success (Laing, Mroczkowski & Testi, 2016). The result was that proposals submitted to that call were well focused on ALMA's development goals at the time. Following this success, we chose to host the 2019 ALMA Development Workshop at ESO's headquarters in Garching, and timed the meeting to fall just after the announcement of the 2019 call for development studies.

Figure 1. Key science drivers for ALMA, from the ALMA Development Roadmap.

The Working Group proposes the following fundamental science drivers for ALMA developments over the next decade:

ORIGINS OF GALAXIES

Trace the cosmic evolution of key elements from the first galaxies ($z > 10$) through the peak of star formation ($z = 2$–4) by detecting their cooling lines, both atomic ([C II], [O III]) and molecular (CO), and dust continuum, at a rate of 1–2 galaxies per hour.

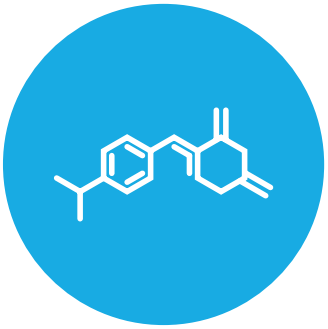

ORIGINS OF CHEMICAL COMPLEXITY

Trace the evolution from simple to complex organic molecules through the process of star and planet formation down to solar system scales (~ 10–100 au) by performing full-band frequency scans at a rate of 2–4 protostars per day.

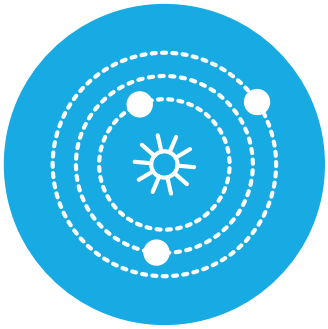

ORIGINS OF PLANETS

Image protoplanetary disks in nearby (150 pc) star formation regions to resolve the Earth forming zone (~ 1 au) in the dust continuum at wavelengths shorter than 1 mm, enabling detection of the tidal gaps and inner holes created by planets undergoing formation.

J. Pinto & N. Lira – ALMA (ESO/NAOJ/NRAO)

Achieving these ambitious goals is currently impossible even with the outstanding capabilities of the current ALMA array. These science goals can be achieved with the upgrades proposed in this document, upgrades that would make ALMA even more powerful and keep it at the forefront of astronomy by continuing to produce transformational science and enabling fundamental advances in our understanding of the universe for the decades to come.

A major theme of the meeting was where ALMA should be by the year 2030. Since 2016, the landscape for ALMA development has changed. Band 1 (35–50 GHz) production is fully under way in East Asia, while the final Band 2 (officially 67–90 GHz, though efforts towards a much wider bandwidth design are ongoing) is now entering Phase 1, which sees the construction of six pre-production cartridges. With a clear path in place to complete the original suite of ALMA bands, ALMA leadership has begun formalising the requirements for the next decade of operations. This effort is known as the 2030 ALMA Development Roadmap[3] and it was released in June 2018.

The 2030 roadmap outlines three new key science drivers for ALMA (see Figure 1), and provides four recommendations. These are as follows (quoting directly from the roadmap)[3]:

1. Origins of Galaxies: Trace the cosmic evolution of key elements from the first galaxies ($z > 10$) through the peak of star formation ($z = 2–4$) by detecting their cooling lines, both atomic ([C II], [O III]) and molecular (CO), and dust continuum, at a rate of 1–2 galaxies per hour.
2. Origins of Chemical Complexity: Trace the evolution from simple to complex organic molecules through the process of star and planet formation down to Solar System scales (~ 10–100 au) by performing full-band frequency scans at a rate of 2–3 protostars per day.
3. Origins of Planets: Image protoplanetary discs in nearby (150 pc) star formation regions to resolve the Earth-forming zone (~ 1 au) in the dust continuum at wavelengths shorter than 1 mm, enabling detection of the tidal gaps and inner holes created by planets in the process of forming.

The specific development priorities set out in the ALMA Roadmap, ranked in order of priority, are as follows:

– Broadening the receiver bandwidth by at least a factor of two, and upgrading the associated electronics and correlator.
– Upgrading the existing receiver bands, where the highest priority is given to receivers operating in the 200–425 GHz region, followed by receivers covering frequencies lower than 200 GHz, and, finally, higher than 425 GHz.
– Enhancing the long-term capabilities of the ALMA archive.
– Performing exploratory studies on potential future development paths, where ESO specifically prioritises feasibility studies into the extension of the maximum baseline length by a factor of 2–3, as well as the applicability of focal plane arrays.

We note that the first two items have the principal aim of increasing the observing speed of ALMA, while the latter two increase the scientific capabilities of ALMA.

Summaries of talks and highlights from sessions

Here we summarise the invited talks and highlight discussions from dedicated sessions and contributed talks. All talks and posters are hosted on Zenodo[4] and are linked to the workshop programme[5].

The opening talks were delivered by the ESO Director General, Xavier Barcons, and the ALMA Director, Sean Dougherty. These overviews were followed by a summary of the ongoing work to update the ALMA receiver and backend electronics specifications, originally defined two decades ago, and by regional overviews from each of the ALMA partners. Overall, there was broad agreement with our vision for ALMA's future.

First and foremost, everyone agrees that lower receiver noise temperature is in ALMA's interest, particularly in the so-called workhorse bands — Bands 3, 6 and 7. However, as we approach the limits of technology (current receivers have 4–10 times the quantum noise limit, which is the ultimate limit for standard receiver technologies), the noise in a fixed bandwidth is dominated by the atmospheric contribution. The largest gains to be had in imaging speed might be easiest to obtain by expanding ALMA's bandwidth (currently < 8 GHz). For example, doubling the bandwidth would result in a factor of two increase in imaging speed for any observation requiring broad bandwidth or needing continuum sensitivity. Any expansion of the receiver bandwidth entails expansion of the backend electronics — digitisers, data transport, and correlator. This implies that a significant number of the most compelling hardware upgrades must be coordinated amongst several development groups, and therefore the exact parameters of any potential bandwidth improvement must be carefully defined.

Frédéric Gueth and Christophe Risacher from the Institut de Radioastronomie Millimétrique (IRAM) and Keith Grainge from the Square Kilometre Array reported on ongoing and planned development and construction activities at their respective observatories. We also heard about the ongoing ALMA Band 1 (35–51 GHz) production, and the prototype development for ALMA Band 2 (67–116 GHz), both of which had been mentioned earlier in the context of completing the original suite of ALMA bands. On the second day, the programme included presentations on the higher-frequency technologies being developed, which are especially applicable to Bands 6–10, and receiver control software that will find more optimal operational parameters for the existing ALMA receivers.

Next, the topics moved to the backend electronics that will take advantage of the upgraded receivers. Crystal Brogan introduced the project to upgrade the current correlator — currently functioning with decades-old hardware — to have higher spectral resolution and a doubling of the existing bandwidth, followed by much discussion of more ambitious projects to build an entirely new correlator.

On the final day, we heard about improvements to ALMA's software and observing capabilities, including improved proposal generation tools, improved observing modes (for example, solar high-cadence and extended baselines), and more sophisticated and rigorous imaging and analysis techniques. Notably, the ALMA Science Archive project called "Additional Representative Images for Legacy" (ARI-L) is now underway to bring the Cycle 2–4 data in the ALMA archive up to the level of Cycle 5 and later, directly addressing one of the ALMA Development Roadmap priorities. We are in an era of data-driven science, and ARI-L will make the ALMA archive much more conducive to such work. Also, a web-based replacement for the

Figure 2. Workshop photo outside the ESO Supernova, showing that we chose a week of lovely weather in Garching.

current Java-based ALMA Observing Tool (ALMA-OT) is in the works and will improve compatibility going forward. Most users will welcome this, as the vast majority of user tickets related to the ALMA-OT are essentially Java support issues, not issues with the tool itself.

Main conclusions & ways forward

Throughout the workshop, it was clear that ALMA is not a project that will be neatly completed — which is the impression one sometimes gets as we race to build the final bands in the original ALMA band definition. Rather, ALMA is an ongoing and vibrantly active project. Only through continued development can ALMA remain a competitive, groundbreaking observatory. The breadth of work presented in the talks showed that the next decade will continue to be as exciting for ALMA as the first has been. To achieve this ambitious goal, the ALMA executives showed a clear willingness to collaborate.

Demographics

The workshop was attended by 79 registered participants, only 12 of whom were female (15%). The Science Organising Committee sought fair representation from the community, but sadly the gender balance within the applications was particularly poor. We feel this reflects much of the skewed gender ratio in teams working on ALMA-related technology development, which we are striving to improve. In future, groups within ALMA should be encouraged to increase the visibility of women within their groups, rather than consistently choosing only male group members to present group efforts.

The balance for regional representation was better, with attendees coming from all three regions defined in the ALMA collaboration and Chile in the following percentages:
– 66% Europe;
– 14% North America;
– 11% East Asia;
– 9% Chile (South America).

Since this was a small workshop, all abstracts submitted by the deadline were accepted. Submissions coming after this deadline were given posters.

Acknowledgements

We thank Elena Zuffanelli for all her hard work in coordinating the workshop logistics, Sandor Horvath for technical support, Herbert Zodet for taking the group photo, Rein Warmels for help with the workshop website and Evanthia Hatziminaoglou and Luca Di Mascolo for help with the registration desk. This conference was supported by EASC.

References

Laing, R., Mroczkowski, T. & Testi, L. 2016, The Messenger, 165, 47

Links

[1] ALMA observatory: https://www.almaobservatory.org/en/home/
[2] ALMA Press Releases: https://www.almaobservatory.org/en/category/press-release/
[3] The ALMA Development Roadmap (Carpenter et al., 2018): https://www.almaobservatory.org/en/publications/the-alma-development-roadmap/
[4] Zenodo link to the workshop presentations: http://doi.eso.org/10.18727/0722-6691/5058, https://zenodo.org/communities/almadevel2019/search?page=1&size=50
[6] The workshop programme: http://www.eso.org/sci/meetings/2019/ALMADevel2019/program.html

DOI: 10.18727/0722-6691/5158

Report on the ESO Workshop

The VLT in 2030

held at ESO Headquarters, Garching, Germany, 17–21 June 2019

Antoine Mérand[1]
Bruno Leibundgut[1]

[1] ESO

This four-day workshop offered a forum to discuss the scientific future of the VLT and VLTI. Overview talks of some of the main scientific topics for the next decade were followed by presentations on the most important facilities operating in 2030. Several instrument concepts and ideas were presented which would signifantly enhance the current VLT and VLTI capabilities. The workshop discussions are the basis for the plans for the VLT after 2025.

Introduction

The VLT/I ranks amongst the most productive and most visible astronomical facilities worldwide. As the world's premier ground-based facility, it provides a powerful suite of visible and infrared instruments, including unique capabilities like coherent and incoherent combinations of the four 8-metre Unit Telescopes (UTs) and a multi-laser-guided adaptive optics (AO) system. In combination with the Atacama Large Millimeter/submillimeter Array (ALMA), VLT/I provides comprehensive coverage of the electromagnetic spectrum from the ultraviolet and visible through the infrared to submillimetre wavelengths for the European astronomical community and its partners.

With the advent of ESO's Extremely Large Telescope (ELT), the VLT and VLTI will take on a new role. They will continue to serve a large community and provide unique data. The VLT's and VLTI's unique capabilities are due to the versatile instrumentation on the four 8-metre telescopes, the spatial resolution achievable by interferometry with baselines of over 100 metres, access to ultraviolet/blue and optical wavelengths (including support from adaptive optics) and the flexible operations model. The telescopes and instruments have been maintained at peak performance and new capabilities continuously developed over the past two decades. An ongoing programme to avoid hardware and software obsolescence ensures that the facility can be operated for many years to come. A dedicated instrumentation programme is in place for the coming decade.

Workshop structure

How do we make sure that the future of the VLT and VLTI remains science driven? The workshop was designed to address this question by charting some of the most exciting current research topics into the next decade and deriving the necessary capabilities based on discussions throughout the workshop programme. The workshop was attended by about 130 participants. Two approaches were followed. First, the workshop participants heard reviews of five central research topics: cosmology, galaxy and black hole evolution, resolved stellar populations, star and planet formation, and the Solar System. In the second part, facilities that are due to be operating in the second half of the next decade were presented. These include ALMA, the next generation of ELTs, European Space Agency (ESA) space-based observatories, the James Webb Space Telescope (JWST), the Large Synoptic Survey Telescope (LSST), the Cherenkov Telescope Array (CTA) and the Square Kilometre Array (SKA). The ESO status, in particular the current VLT and VLTI setup (instrumentation, operations, calibrations, surveys) was also laid out. This was followed by contributed presentations on science cases and potential new VLT instruments. All sessions had ample time set aside for discussions. The workshop programme is available online[1].

ESO Director General Xavier Barcons opened the workshop and gave an overview of the current ESO situation and plans. He stressed that ESO's ELT is central to the organisation's efforts in the coming years and cautioned the audience that VLT developments would need to proceed within the available resources. Within that envelope there is stable funding for Paranal instrumentation developments and Paranal operations (the ELT will eventually be integrated into this operational paradigm). This implies that there will not be a new generation of VLT and VLTI instruments, rather a steady, albeit limited, flow of new instruments in the coming decade.

Five major topics were chosen for broad summaries and forward looks into the next decade. It is always difficult to predict the future, but the five reviewers did an excellent job. Matthew Colless (Australian National University, Canberra) reviewed the current and future plans in cosmology. He restricted himself to the determination of cosmological parameters and astrophysical contributions to fundamental physics but excluded topics like galaxy formation and evolution. In the realm of multi-object spectroscopic facilities he acknowledged the significant potential of the 4-metre Multi-Object Spectroscopic Telescope (4MOST); he also pointed out that other projects, for example, the Dark Energy Spectroscopic Instrument (DESI) at the National Optical Astronomy Observatory (NOAO), are more advanced and will begin observations sooner. Versatile facilities like the VLT will become very important, should a deviation from the currently favoured Λ-Cold Dark Matter (ΛCDM) model be discovered. He noted the important contributions to the study of strong gravity by the VLT and the VLTI. It was pointed out during the discussion that the VLT has played critical roles in addressing some of the most fundamental cosmological problems, for example, providing crucial spectroscopy for supernova cosmology projects and to probe the variation in fundamental constants such as the fine-structure constant. Looking to 2030, he felt that other facilities such as Euclid would become significantly more important for cosmology than the VLT.

Linda Tacconi (Max Planck Institute for Extraterrestrial Physics [MPE], Garching) presented the current status of the very wide field of galaxies and black holes. Resolved properties, like rotation curves or velocity dispersions, will gain in importance to the understanding of the dynamics of early galaxies. She emphasised the strength of integral-field spectroscopy for such studies and how well the VLT already caters to this type of research (for example, the Spectrograph for INtegral Field Observations in the Near Infrared [SINFONI], the Multi Unit Spectroscopic Explorer [MUSE], and the *K*-band Multi Object Spectrograph [KMOS]). Several of

the planned instrument developments will be extremely helpful for this field (the Enhanced Resolution Imager and Spectrograph [ERIS], and the MCAO-Assisted Visible Imager and Spectrograph [MAVIS]), and for some other studies presented during the workshop. Of course, a better understanding of individual supermassive black holes is critical and GRAVITY, the AO-assisted, two-object, multiple beam-combiner on the VLTI, represents a breakthrough in this respect. Linda Tacconi emphasised the importance of very high angular resolution observations of active galactic nuclei (AGN) as probes of galaxy evolution over cosmological times.

The ESA space observatory Gaia has fundamentally changed our view of the Milky Way, its various components and the dynamics of Local Group galaxies. Eline Tolstoy (Kapteyn Institute Groningen) presented the many open questions stemming from the analysis of Gaia data. Follow-up spectroscopy will be extremely important to complementing the positional information with radial velocities and abundances of the stars to be provided by massive surveys with ground-based facilities. A most important aspect is covering the ultraviolet for the study of the nucleosynthesis of heavy elements. 4MOST already dedicates a large fraction of its observing time to Gaia follow-up. Other instruments of interest are the Fibre Large Array Multi Element Spectrograph (FLAMES) and the Multi-Object Optical and Near-infrared Spectrograph (MOONS). But there remains a gap in respect of fainter stars and the need for higher spectral resolution to better constrain the stellar parameters and abundances with a potential future VLT multi-object high-resolution spectrograph.

Our knowledge of planet formation continues to develop rapidly. Anne-Marie Lagrange (Institut de planétologie et d’astrophysique de Grenoble, IPAG) reviewed the current situation; many protoplanetary disks are known but the number of directly imaged planets remains small. Clearly, sensitivity and higher angular resolution are key for this field. The ELTs (and JWST) will be major players, but there remain various capabilities which the VLT and VLTI can offer. An upgraded Spectro-Polarimetric High-contrast Exoplanet REsearch instrument (SPHERE) and an optical AO system, like MAVIS, would be beneficial. The importance of coronagraphy was stressed. The VLTI with GRAVITY and the Multi AperTure mid-Infrared SpectroScopic Experiment (MATISSE) is just beginning to tackle exoplanets, and better characterisations of planetary atmospheres can be expected. Transit measurements and follow-up observations of PLATO targets clearly represent another exciting research theme waiting to be explored.

The importance of the VLT for Solar System objects was described by Heike Rauer (DLR, Berlin). The VLT provides both the versatility and stability needed for regular and continuous observations of Solar System objects. While space missions will always provide more detailed views, they are mostly limited to short periods (of the order of years). Ground-based observatories can provide steady observations and long-term coverage. They can also yield larger statistical samples for asteroids, comets and trans-Neptunian objects. Special and unforeseen events on timescales that prevent satellite missions, for example the Shoemaker-Levy 9 impact on Jupiter, will heavily rely on ground-based observations. Synergetic observations to complement future planetary missions, like the JUpiter ICy moons Explorer (JUICE) or Europa Clipper, will enhance the science return of these space missions. The best angular resolution is clearly an asset for observations of Solar System bodies.

Summary talks on existing and future facilities set the stage for synergies and complementarity. Ciska Kemper (ESO) presented some science results based on the synergy between ALMA and VLT data and described the ALMA2030 Development Roadmap. The ELTs will be the flagship ground-based near-infrared observatories and their strengths were outlined by Michele Cirasuolo (ESO). The exciting ESA programme for the coming decade was detailed by Fabio Favata (ESA). The JWST launch is planned in early 2021 and Gillian Wright (UK Astronomy Technology Centre [UKATC], Edinburgh) described its scientific plans and capabilities. With a 10-year planned lifetime, the JWST and VLT will complement each other for many projects.

Starting in 2022, the LSST will provide many variable objects, which will need dedicated follow-up observations. The VLT and many 4-metre telescopes will be prime facilities for the required spectroscopy, as outlined by Pierre Astier (Laboratoire de physique nucléaire et de hautes énergies [LPNHE], Paris). The planning for the best usage of the various telescopes has already begun. Pierre also presented an interesting connection with gravitational wave observations, suggesting that the LSST could find many optical counterparts. The Cherenkov Telescope Array (CTA) is under construction and its status and plans were presented by Werner Hofmann (Max-Planck-Institut für Kernphysik [MPIK], Heidelberg). It will be exciting to search for optical counterparts of the many ultra-high-energy sources CTA will discover. Anna Bonaldi (Square Kilometre Array Organisation) introduced the SKA. It will be interesting to combine the radio detections with optical sources. Sofia Randich (Istituto Nazionale di Astrofisica [INAF], Arcetri) summarised the Gaia-ESO survey. She underscored the importance of high spectral resolution and blue efficiency for stellar abundance work. A summary of the findings of the Public Survey Panel after its scientific review of the completed and ongoing ESO public surveys in May 2019 was delivered by Bruno Leibundgut (ESO).

Several talks provided background information on the current VLT/I situation. The instrumentation planning for the VLTI (Antoine Mérand, ESO) and the VLT (Bruno Leibundgut, ESO) were followed by presentations on data flow operations (Michael Sterzik, ESO), Paranal operations (Steffen Mieske, ESO) and calibration plans and issues (Alain Smette, ESO). New ideas include atmospheric forecasting to allow planning of observations in more detail, or at least implementing “now-casting” to obtain a full understanding of the current status for real-time scheduling. A move away from standard stars to physical atmosphere models for calibration of the atmosphere was also presented.

Lively discussions followed these sessions. The importance of adequate preparation for LSST transient follow-up was stressed several times. The complementarity of JWST infrared imaging and

Figure 1. Workshop participants enjoy a break in front of the ESO Supernova Planetarium & Visitor Centre.

low-resolution spectroscopy with ground-based infrared high-resolution spectroscopy was highlighted, although this will probably be more in synergy with the ELTs than with the VLT. In general, better coordination between ground- and space-based observatories was urged. The programmatic aspects of VLT and VLTI instrumentation were presented by Luca Pasquini (ESO) setting the framework for the 21 contributed talks outlining science cases and concepts of new instruments. Individual presentations on the science plans of MOONS (Michele Cirasuolo, ESO), MAVIS (Richard McDermid, Macquarie University Sydney) and an ultraviolet spectrograph (Chris Evans, UKATC Edinburgh) started off this part of the programme. Several new and exciting instrument ideas on different scales were presented, which will further enhance the VLT and VLTI capabilities.

The workshop programme provides an overview of the newly proposed projects and their science cases and we refer the reader to that list for a summary. There were also 16 posters[2] on display, as not all requested talks could be accommodated in the workshop programme. It is too early to discuss any of these proposals, suggestions and ideas in detail. However, some trends can already be discerned. There are a few concepts for instruments with a wide range of astrophysical applications. Others cater to more specific science cases or have a relatively narrow science focus. The workshop finished with an extensive discussion. Because of the different levels of detail in the science cases and instrument concepts, a wide range of opinions and positions was voiced. The workshop closed with a summary by Denis Mourard (chair of the Scientific Technical Committee [STC], Observatoire de la Côte d'Azur [OCA]); he outlined a first categorisation of the different topics, which will be the basis for future discussions.

Demographics

The Science Organising Committee was composed of one Council and four STC members as well as relevant ESO staff. Its gender distribution was 4 female and 7 male members. Among the invited speakers 8 out of 20 were women (4 out of the 5 reviews). However, among the 45 submitted contributions only one was by a woman and there were 24 women among the 130 participants. While this gender ratio reflects that of the instrumentation community, we hope that these stark statistics act as a wake-up call to ESO instrument builders. On the timescales explored by this meeting, positive action to ensure more inclusion in our community can and should be undertaken.

Outlook

The workshop successfully laid out the scientific landscape and explored the interests of the community regarding VLT/I developments. The enthusiasm displayed by the community presentations on the scientific potential and the ideas for new instrumentation was obvious. It has become clear that the VLT/I will remain a facility that can serve many different interests and science applications. This versatility should be maintained as far as possible. At the same time, VLT/I operations may open up to more specific experiments or projects, for example through visiting instruments. The planning of the future VLT instrumentation complement needs to account for the existing (and aging) instrumentation; some instruments may not be maintainable at reasonable cost for another decade. A summary of the concepts presented at the workshop together with a first scientific assessment will be prepared for the next STC meeting in October for further discussion. A concrete plan for VLT and VLTI after 2025 will be prepared by the Programme Scientists and presented for recommendation to the STC in April 2020. With the long-term planning in hand, the next instrumentation studies can start to be fully operational some time during the second half of the coming decade.

Acknowledgements

We would like to thank the SOC members for their help in preparing the scientific programme and during the workshop. The logistics were handled superbly by Svea Teupke.

Links

[1] Workshop programme: https://www.eso.org/sci/meetings/2019/VLT2030/program.html
[2] Workshop poster papers: https://www.eso.org/sci/meetings/2019/VLT2030/posters.html

DOI: 10.18727/0722-6691/5159

Fellows at ESO

Chentao Yang

Chentao Yang

Growing up in one of the most remote cities from the sea, Urumqi, deep in northwestern China, I was fascinated by astronomy since my early childhood, just like hundreds of millions of other boys on this planet. I can still remember one night more than 20 years ago, at nine-years old, I was copying a table of the temperatures and fluxes of the brightest stars in the sky from a book with my friend. I would come to consider that moment the beginning of my scientific career in astronomy. My love of astronomy just kept growing over my childhood, partially because of my stubbornness and persistence.

Four years later, in junior high school, I started to write letters to the author of that same book — the then director of Yunnan Observatory — asking astronomy questions. I was incredibly grateful that he responded to all my mails carefully. Among those letters, I asked how I could get prepared to be a professional astronomer. He replied with detailed and insightful suggestions covering two pages that have impacted my life ever since. Later, in high school, my passion for astronomy helped me join the astronomy club. The teacher responsible for the club was Gao Xing — one of the most famous amateur astronomers in China. With him, we learned a lot about basic concepts in astronomy and had many unforgettable experiences of observations such as eclipses, meteor showers, the transit of Venus and Messier marathons (during which amateur astronomers try to find as many Messier objects as possible in one night).

Naturally, after high school, I chose one of the few universities in China that has an astronomy department to pursue my passion for a career in astronomy. I was very serious about becoming an astronomer. During the last year of my undergraduate life, I started to study the cold dust emission in galaxies with data from the Submillimetre Common-User Bolometer Array (SCUBA) on the James Clerk Maxwell Telescope, under the mentorship of Gao Yu from Purple Mountain Observatory in Nanjing. It was also then that I learned about the Atacama Large Millimeter/submillimeter Array (ALMA) and that it would become the most powerful telescope in the near future. I dreamed of using it one day. After I graduated, I entered the masters programme at the same university.

By coincidence Gao Yu happened to meet Alain Omont from Paris during that time. Alain was working on a new project that could lead to a masters student project. So I was fortunately introduced to Alain and started a research programme co-supervised by Yu and Alain. Around that time, submillimetre water vapour lines were coming back to people's attention because of the launch of the Herschel Space Observatory. Its instruments the Spectral and Photometric Imaging Receiver (SPIRE) and the Heterodyne Instrument for the Far Infrared (HIFI) enable us to detect a massive number of submillimetre H_2O lines in our Galaxy and in nearby galaxies. These H_2O lines are a unique and essential diagnostic tool that helps us understand better the conditions in the interstellar medium. So I started to investigate those H_2O lines using Herschel Science Archive data, by collecting data from all of the galaxies that had been observed. At the same time, with Alain, we also started to target those bright H_2O lines in the high-redshift Universe, by picking up strongly lensed starbursts from large-area Herschel SPIRE maps. We quickly built the largest sample of the H_2O-line-detected sources across cosmic time.

After obtaining my masters degree, I entered Purple Mountain Observatory for a PhD programme with Yu. And to continue our study of the sample of strongly lensed high-redshift starbursts, I started a co-tutelle (joint) PhD programme between Université Paris-Sud and University of Chinese Academy of Sciences from 2014. I moved to Paris from Nanjing that year and started my research projects under the supervision of Alain Omont and Alexandre Beelen. Université Paris-Sud is in Orsay, the beautiful southern urban area of Paris. I started a systematic investigation of the physical conditions of the cool interstellar medium in the high-redshift strongly lensed starburst galaxies using different telescopes. With the 30-metre telescope of the Institut de Radioastronomie Millimétrique (IRAM), one of my favorite telescopes, I had several observing runs lasting weeks to study the CO ladder of those galaxies. We also obtained a massive amount of data from the Plateau de Bure Interferometer, from which I gained most of my knowledge of interferometry. Unfortunately, I never had a chance to see the

antennas on the plateau. However, on my 28th birthday I observed with the James Clerk Maxwell Telescope and finally saw world-famous telescopes like Keck with my own eyes. It was an unforgettable experience. With the Karl G. Jansky Very Large Array (VLA), we studied the properties of dense gas in those lensed starbursts and, little by little, I realised that my passion is for astronomy observations, including the joy when the proposal is accepted, and the excitement of checking freshly acquired data.

During the last year of my PhD, when I received an offer from ESO for a fellowship in Chile in January 2017, I was thrilled that I would be working with ALMA, the most powerful (sub)millimetre telescope that I dreamt about back in 2010. My dream came true and I moved to Chile in November 2017.

At ESO, I spend 50% of my time at ALMA performing functional duties. I still remember my first trip to the 5000-metre-high array operations site of ALMA. The landscape is simply Martian. I have enjoyed participating in the science operations at ALMA a lot, where I keep learning every day and work to contribute to ALMA. During the other half of my time, I continue my research into molecular gas and dust in galaxies. Using ALMA, I acquired images of dust and gas emission at scales of 100 pc for dusty galaxies when the Universe was about two billion years old. I am also using the NOrthern Extended Millimeter Array (NOEMA) of IRAM and ALMA conducting spectral line surveys of high-redshift galaxies, pushing the limit of astrochemistry studies to the early Universe. Besides, the submillimetre H_2O emission from galaxies has been one of my areas of interest. With the Atacama Pathfinder Experiment telescope (APEX), we achieved the first detection of the 752-GHz H_2O line in extragalactic systems from the ground.

DOI: 10.18727/0722-6691/5160

External Fellows at ESO

In addition to the ESO fellowships, a number of external fellows are hosted at ESO. Profiles of two of these fellows are presented here.

Prashin Jethwa

It could so easily not have happened at all! My two-year stint at ESO has been a fortunate coincidence. Sidestepping the usual route taken by fellows, my voyage through the seas of ESO has been at the command of a brave captain: Glenn van de Ven. I joined Glenn's group, funded through a European Research Council grant, for a position which was originally intended to be hosted at the Max Planck Institute for Astronomy in Heidelberg. However, along with Glenn, my position moved to ESO Garching, where I have been based since October 2017. No sooner have I learnt to navigate through the ESO headquarter buildings, however, than my time here has come to an end. I will soon move to re-join the newly appointed Professor van de Ven, this time at the Institute for Astrophysics in Vienna. Despite, then, my time at ESO having been largely unplanned, it has been an immense pleasure, and I leave as a more enriched and fulfilled person than when I arrived.

I was born and raised in London, where I spent my childhood enjoying football (Liverpool), Pokémon (Charizard), and ice cream (all varieties). Notably absent from this list is astronomy. Perhaps I can blame urban light pollution, but I cannot claim to have been especially awestruck by the Universe in my formative years. Rather than looking up through a telescope, I kept my head down, often in a mathematics textbook. This is what really absorbed the academic side of my youthful brain: maths problems, puzzles and... polynomials? This led me to the University of Cambridge, where I completed an undergraduate degree in mathematics. It was a broad curriculum, spanning aspects of pure and applied maths as well as theoretical physics. The latter topic dominated my choice of courses in the final year, reflecting my evolving interest in mathematics: not just as an abstract puzzle, but a tool for modelling real phenomena and solving real problems.

My transition then began in earnest. I chose to continue at Cambridge with a master's degree in astronomy, learning the fundamentals of the subject from a mostly theoretical perspective. I then spent a year as a European Space Agency (ESA) Young Graduate Trainee in Madrid, where I got to experience a more "hands-on" side to astronomy. My project at ESA consisted of modelling overexposures on the cameras of XMM-Newton, a space-based X-ray telescope. During this time, I also enjoyed my first look through a telescope. After an impromptu 100-kilometre drive south of Madrid with a friend's 20-inch Dobsonian telescope, I saw Saturn's rings, Jupiter's moons and made amends for my youthful oversight. Having ticked this box, gained some substantial research experience, and seen part of the wider astronomy community, I felt ready to move on to the next step.

For my doctoral studies, I returned to the Institute of Astronomy in Cambridge. Under the supervision of Vasily Belokurov and Denis Erkal, I completed a thesis about the Milky Way halo. The halo refers to the region out to distances of a few

hundred kiloparsecs from the Galaxy. It is filled with satellite galaxies, star clusters, and diffuse clouds and streams of stars, all orbiting around the Milky Way. Structures in the halo are remnants of smaller galaxies merging with the Milky Way over timescales of billions of years. By disentangling and characterising these structures we can see into the Galaxy's past evolution and growth.

One main result from my thesis concerns newly discovered dwarf galaxies. Early in my PhD, two teams raced to report the discovery of dozens of dwarf galaxies in the Dark Energy Survey (DES), a photometric survey in the southern hemisphere. The number of dwarfs discovered in DES far exceeded expectations from previous, similar surveys in the north. One possible explanation for this overabundance was that the new dwarfs were associated with the Magellanic Clouds, the largest of the Milky Way satellites, which lay close the boundary of the DES footprint. I tested this hypothesis by building a dynamical model of the Magellanic Clouds, Milky Way and dwarf galaxies, and devising a statistical framework to compare this model to observations. The results confirmed that most of the DES dwarfs were likely to be associated to the Clouds, and furthermore predicted their velocities, several of which have since been corroborated with follow up observations. This work encapsulates the main tools used in my research, which are mainly theoretical, with plenty of dynamics, and using statistical modelling techniques.

Moving to ESO, my scientific focus has shifted slightly. Whilst still interested in the evolution and growth of galaxies, I now focus on those outside of our local neighborhood. The type of data available for studying more distant galaxies is very different from data we have in the Milky Way. Some of the richest datasets come from Integral Field Units (IFUs). These observe not just 1D spectra, or 2D images, but 3D data-cubes: images where every pixel of the image contains a spectrum. A powerful method to study galaxies using IFUs is decomposition, i.e., breaking the data-cube down into parts that represent physical components. This can reveal the history of when stars were formed, how the chemistry of gas and stars evolves, and uncover the remnants

Prashin Jethwa

of past galactic mergers. Decomposition is therefore very powerful, but it can be computationally challenging and will become increasingly challenging as data quality improves. Some of the highest quality IFU data currently come from the MUSE instrument on the VLT and, looking to the future, the High Angular Resolution Monolithic Optical and Near-infrared Integral-field spectrograph (HARMONI) on the Extremely Large Telescope (ELT) will improve spectra and spatial resolution yet again by orders of magnitude. To prepare for this increase in the size and quality of data, I have been investigating dimensionality-reduction techniques to allow us to perform decomposition for large datasets. Alongside many other examples, this project has expanded my scientific horizons.

In addition to being scientifically eye-opening, in my two years at ESO I have grown in several other ways. The students and fellows I have met in Garching are an exceptionally proactive and engaged group of people. We take excellent advantage of opportunities provided to us and take the initiative to create further opportunities for ourselves and future ESO scientists. Seizing these opportunities has been a key part in my personal development. I leave with teaching experience, having co-supervised an undergraduate summer student in the inaugural ESO Summer Research Programme, and PhD student Meghan Hughes who is enrolled in the ESO studentship programme. I leave with enhanced organised skills, having organised the ESO Garching Science Day, group meetings and one of several seminar series. I leave with an unexpected friendship with the owner of the local *Getränkemarkt* (bottle shop) having bought hundreds of crates for our weekly after-work Beer Fridays. On display here, every Friday, is the warm atmosphere and friendly, interesting people who really make ESO a pleasure to be part of. Above all, I leave ESO with countless good memories and friends.

Foteini Oikonomou

I was born and grew up in Athens, Greece. I cannot remember a fascination with the night sky, perhaps because of the light-pollution in Athens, until at an age of around nine I visited the observatory of Penteli during one of the open evenings. That evening we observed the Hercules globular cluster. Hearing the astronomers there describe the system we were looking at and explain the time it had taken the light to reach us made me, for the first time, very aware of the vastness of the Universe and filled me with a sense of wonder.

During my teenage years, my interest in the Universe grew, mostly from reading popular science books and occasional visits to the observatory. Those were the days without internet, and I can remember that I got into the habit of scanning the local press for information about the next open evening at the observatory, and the frustration I felt when I couldn't find anything scheduled. In high school, I decided to take mostly science courses so that I could apply for a university degree in astrophysics. I chose my high

school diploma thesis to be on black holes because they captured my curiosity the most. I think that Stephen Hawking's popular science books were what sparked this interest. I have since confirmed that this was the case for many of the fellow astrophysics students of my generation at university.

I went to England to study astrophysics at University College London (UCL). I made the decision because there was no bachelor's degree in astrophysics in Greece. It seemed to me at the time that studying physics instead wouldn't be as much fun. It was in London that I truly got acquainted with astronomy. The degree I took involved many astrophysics courses, but also lots of time using telescopes and analysing astronomical data at the University of London Observatory. I am still fascinated by the dedication and excitement of all the astronomers there, for the great research they manage to do, just next to the A1 motorway in the suburbs of the often cloudy London!

In my final years at university, I became most interested in extragalactic astrophysics and elementary particle physics. I decided that I'd like to pursue a PhD on a topic which combined elements of both. At the time, UCL launched an initiative called the Institute of Origins, designed to foster collaboration between the Particle Physics and Astrophysics groups at UCL. In this platform, I found a PhD topic that greatly interested me: an investigation on the origin of ultra-high-energy cosmic rays. These fascinating messengers of the extreme Universe, which are most likely extragalactic, are the most energetic particles known. They possess energies ten million times higher than the particles that can be accelerated at the Large Hadron Collider. We do not know by what astrophysical objects they are accelerated, and to this day, this question has been the backbone of my research endeavours.

I was fortunate enough to be offered a PhD position at UCL. I still remember the offer email I received as one of the happiest moments of my life. I worked alongside Ofer Lahav, Amy Connolly, and Kumiko Kotera on the signatures of plausible astrophysical sources of ultra-high-energy cosmic rays. Towards the end of my PhD, I was offered a postdoctoral position at the Pennsylvania State University (Penn State). There, I was able to work alongside Miguel Mostafa and Stephane Coutu on the Pierre Auger Observatory. This is the largest ultra-high-energy cosmic ray detector ever built. Distributed particle counters cover an area of 3000 square kilometres in the pampa, in the Mendoza region of Argentina. I was lucky to be able to visit the experiment several times and to operate the fluorescence telescopes during shifts. During my time at Penn State, I also worked alongside Kohta Murase on jetted active galaxies, called blazars. These objects are powered by the Universe's most massive black holes and have long been thought to be sources of ultra-high-energy cosmic rays.

I next moved to ESO, to my current position, to work alongside Paolo Padovani and Elisa Resconi on blazars, and on high-energy neutrinos, expanding my multi-messenger expertise so as to tackle the ultra-high-energy cosmic ray problem from additional directions. The time of my arrival in Munich was very opportune because, within a week of the start of my position at ESO, the IceCube neutrino detector registered an alert for a high-energy neutrino coincident with a flare from the powerful blazar, TXS 0506+056. This event probed in-depth investigations on neutrino emission from this and other blazars, and I was very lucky to be able to research this topic in the midst of world experts on blazars and on high-energy neutrinos.

At ESO and the surrounding institutes in Garching, the opportunities to grow as a scientist seem endless. I heard somewhere that Munich is the city with the largest number of astrophysicists in the world. I do not know if this is true, but it certainly feels that way. At ESO and in Garching I enjoy the very rich variety of excellent weekly talks, and other regular events, the Joint Astronomy Colloquium, Active Galactic Nuclei (AGN) Club, Journal Club, and the various weekly seminars of the many institutes in Garching. My position is funded by the DFG (German Research Foundation) collaborative research centre SFB1258: Neutrinos and Dark Matter in Astro- and Particle Physics. Within this programme, I am able to participate in additional regular cross-institute colloquia, lectures, and workshops, collaborative gatherings with artists, and outreach activities. While writing these lines I realised that not much has changed in my main astrophysics interests since as a teenager I got excited by the mysteries of the high-energy Universe, and the mysteries of black holes. I feel very fortunate to be able to nourish this curiosity every day.

Foteini Oikonomou

DOI: 10.18727/0722-6691/5161

Lodewijk Woltjer (1930–2019)

Daniel Hofstadt[1]

[1] ESO

"Lo" Woltjer (b. Noordwijk 1930, d. 2019) was ESO Director General from 1975 to 1987. Despite originally studying geology, Lo was to become one of the youngest professors of astronomy in the Netherlands. From there he went to the USA to chair the department of astronomy at Columbia University from 1964 to 1974. He related to ESO early on and realised the potential an international organisation had for European astronomy, in keeping with the spirit of its founders.

Lo Woltjer's scientific interests were initially focused on the Crab Nebula supernova remnant. He also made extensive contributions to the study of quasars and magnetic fields in stars and galaxies.

When he was appointed ESO Director General in 1975 he reshaped the Organisation in line with a unique ambition, emphasising in-house technical developments initiated with the support of CERN. He later engaged ESO in collaborations with industry and astronomy institutions across Europe. In his proposal for the ESO directorship he conditioned his acceptance on the creation of a scientific department at ESO in order to anchor the role of Organisation in the European community.

During his thirteen years as Director General ESO became the world-class institution it is today. The financial contribution of its Member States increased vastly over his tenure. Italy and Switzerland joined the Organisation, followed by other European countries. The Max-Planck-Gesellschaft (MPG)/ESO 2.2-metre telescope and the Swedish–ESO Submillimetre Telescope (SEST) antenna saw their first light at La Silla observatory as well as an ever-larger set of advanced instrumentation during his tenure at ESO. The New Technology Telescope (NTT) was designed thanks to the joining fees provided by Italy and Switzerland when they joined ESO. Lo Woltjer also established an interface with the European Space Agency (ESA) through the Space Telescope European Coordinating Facility, which he decided should be hosted at the ESO Headquarters in Garching.

However, clearly his leading achievement remains the Very Large Telescope (VLT) conceptual design outlined in his blue book and subsequently approved by ESO Council in 1987. The new observatory site was selected on the Paranal mountain. In the VLT design, Lo included an interferometric mode, an option which was not met with universal enthusiasm in the scientific community at the time but has subsequently proved to be visionary.

Lo Woltjer became President of the International Astronomical Union and later served as Chair of the ESA Space Science Advisory Committee. He was instrumental in the development of the European Astronomical Society (EAS), whose annual lectures carry his name. He was honoured with the Karl Schwarzschild medal of the Astronomische Gesellschaft (German Astronomical Society) and was a member of several national science academies.

Who was Lo Woltjer?

Lo was an enigmatic personality with a strong determination to promote European astronomy and raise ESO to the status of a world class Institution. He was a natural leader with outstanding managerial skills. If intelligence is defined as the ability to convert raw information into practical and challenging developments, he must be portrayed as an exceptional masterminding individual. He fully identified with his mission. Everybody connected to the Organisation was aware of that simple equation: Woltjer was ESO and ESO was Woltjer. Some of his struggles and achievements are summarised in his book "Europe Conquest of the Universe". With Roger Bonnet, ESA's Director of Scientific Programmes, he wrote "Surviving 1000 centuries. Can we do it?" – a perfect illustration of his extended range of interests.

He was not an easy guest on planet Earth. The suitcase in his hand was as much a symbol as a travel outfit. He hated public exposure and confrontations, maintaining a formal distance behind an elegant style. It was not always easy to guess what he had in mind, often hiding behind nonchalant gestures and leaving to others the challenge of interpreting his purpose. Highly respected, at times very much admired for his courage, he could be very stubborn in imposing his will. In his function as ESO Director General he also had to make diplomatic compromises, but most of the time he managed to impose his own views. For those who had the privilege to interact with him, whether under his leadership or privately, he was a beacon and a reference point.

Lo was also a lover of the Sun with a passion for the outdoors, whether in Saint Michel l'Observatoire, on canoeing trips with his daughter Eleonore, or hiking and swimming at Lago Rupanco in the south of Chile. Six months ago, his wife Ulla died. She was of outstanding assistance to him and provided an enjoyable link to his social environment both in Europe and Chile. His health failed over the last few months of his life, his legs gave way and he broke a shoulder. With Ulla gone he lost interest in life and slowly faded away. He was 89 years old.

Figure 1. Lodewijk Woltjer welcoming guests at the inauguration of the headquarters at ESO Garching.

Personnel Movements

Arrivals (1 July–30 September 2019)

Europe

Adams, Henning (DE)	Mechanical Engineer
Bazin, Gurvan (FR)	Web & Advanced Projects Coordinator
Beuchert, Tobias (DE)	ESO Supernova Presenter
Calistro Rivera, Gabriela (PE)	Fellow
Caseiro de Almeida, Álvaro José (PT)	ESO Supernova Technical Assistant
Chaturvedi, Avinash (IN)	Student IMPRS
Hayden-Pawson, Connor (UK)	Student
Hofer, Josef (AT)	Software Engineer
Hoffstadt Urrutia, Arturo (CL)	Software Engineer
Huber, Florian (DE)	Logistics Officer
Kabátová, Anežka (CZ)	Student
Lamperti, Isabella (CH)	Student
Miles Páez, Paulo Alberto (ES)	Fellow
Pfuhl, Oliver (DE)	Optical Engineer
Popping, Gergely (NL)	ALMA Regional Centre Astronomer
Ramírez Molina, Andrés (CL)	Software Engineer
Richerzhagen, Mathias (DE)	Optical Engineer
Szostak, Artur (PL)	Software Engineer
Zsidi, Gabriella (HU)	Student

Chile

Anania, Andres (CL)	Software Engineer
Cea, Victor (CL)	Electronics Group Leader
Gran, Felipe (CL)	Student
Herenz, Edmund Christian (DE)	Fellow
Kravchenko, Kateryna (UA)	Fellow
Macías, Enrique (ES)	Fellow
Olguin, Rodrigo (CL)	Head of Engineering Department
Ribas, Alvaro (ES)	Fellow
Solarz, Aleksandra (PL)	Fellow
Vial, Sofia (CL)	Procurement Officer

Departures (1 July–30 September 2019)

Europe

Avila, Gerardo (MX)	Engineer/Physicist
Chen, Chian-Chou (TW)	Fellow
Circosta, Chiara (IT)	Student
Cosentino, Giuliana (IT)	Student
Fensch, Jérémy (FR)	Fellow
Jeřábková, Tereza (CZ)	Student
Käufl, Hans-Ulrich (DE)	Infrared Instrument Scientist
Klitsch, Anne (DE)	Student
Querejeta, Miguel (ES)	Fellow
Sagatowski, Jakob (SE)	Software Engineer
Whitehouse, Lewis James (UK)	Student

Chile

Dias, Bruno (BR)	Fellow
Gallenne, Alexandre (FR)	Fellow
Hau, George (UK)	Operation Staff Astronomer
Hüdepohl, Gerhard (DE)	Electronics Group Leader
Lillo Box, Jorge (ES)	Fellow
Messias, Hugo (PT)	Fellow
Minniti, Javier (AR)	Student
Razza, Alessandro (IT)	Student
Rojas, Alejandra (CL)	Student
Toledo, Pedro (CL)	Software Engineer
Villenave, Marion (FR)	Student

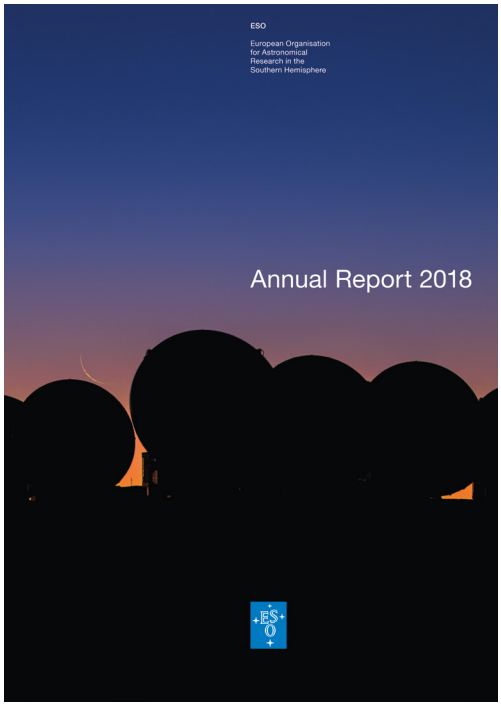

The ESO Annual Report 2018 is available online now at www.eso.org/public/products/annual-reports/ar_2018/.

Road to the stars

A unique opportunity to conduct part of your PhD research at the European Southern Observatory

#ESOJOBS

eso.org/studentship

ESO Headquarters, Garching near Munich, Germany
ESO Vitacura, Santiago, Chile

Application deadline: 31 May and 15 November, each year